

CHIMERIC ANTIGEN RECEPTOR (CAR) T CELL IMMUNOTHERAPY FOR
MUCIN 1 (MUC1)-POSITIVE PANCREATIC DUCTAL ADENOCARCINOMA

by

Mahboubeh Yazdanifar

A dissertation submitted to the faculty of
The University of North Carolina at Charlotte
in partial fulfillment of the requirements
for the degree of Doctor of Philosophy in
Biology

Charlotte

2019

Approved by:

Dr. Pinku Mukherjee

Dr. Kenneth Bost

Dr. Kausik Chakrabarti

Dr. Richard Chi

Dr. Didier Dreau

©2019
Mahboubeh Yazdanifar
ALL RIGHTS RESERVED

ABSTRACT

MAHBOUBEH YAZDANIFAR. Chimeric Antigen Receptor (CAR) T Cell Immunotherapy for Mucin 1 (MUC1)-positive Pancreatic Ductal Adenocarcinoma (Under the direction of Dr. PINKU MUKHERJEE)

Chimeric antigen receptor engineered (CAR) T cells have shown remarkable success in the treatment of hematologic cancers. However, this efficacy has yet to translate to treatment in solid tumors. Pancreatic ductal adenocarcinoma (PDA) is a fatal malignancy with poor prognosis. Treatment options are limited and commonly associated with severe side effects. We have developed and characterized a second generation CAR using the light and heavy chain sequence derived from a novel monoclonal antibody, TAB004, that specifically binds tumor-associated MUC1 (tMUC1) antigen. tMUC1 is overexpressed in >85% of all human PDA. We present data showing that the TAB004 derived CAR engineered T cells (tMUC1-CAR T cells) specifically binds tMUC1 on PDA cells and is cytotoxic against the majority of PDA cell lines *in vitro*. Importantly, the tMUC1-CAR T cells do not bind or kill normal epithelial cells. We further demonstrate that the tMUC1-CAR T cells control the growth of orthotopic pancreatic tumors *in vivo*. PDAs are immunologically cold tumors with resistance to many standard treatment modalities, thus, it was not surprising that some of the PDA cell lines were refractory to CAR T cell treatment. qPCR analysis of several genes known to be associated with immune resistance revealed overexpression of indoleamine 2, 3-dioxygenases-1 (IDO1), Cyclooxygenase 1 and 2 (COX1 and COX2), Adenosine deaminases acting on RNA (ADAR1) and galectin-9 (Gal-9). We treated resistant PDA cells with a combination of CAR T cells and biological inhibitors of IDO1, COX1/2, ADAR1, and Gal-9. Results showed a significant

enhancement of CAR T cell cytotoxicity against resistant PDA cells when inhibiting IDO1, COX1/2, and Gal-9 but not ADAR1 or COX2. In addition, we show that pre-treatment of resistant PDA cells with sub-optimal doses of standard chemotherapeutic drugs (paclitaxel, gemcitabine, or 5FU) significantly increased CAR T cell cytotoxic efficacy against resistant PDA cells. Overcoming CAR T cell resistance in PDA is a significant advancement in the field and may lead to future combination therapies that may be less toxic and more efficient against this lethal disease.

DEDICATION

To my best friend, my life partner and my husband, Saeed, for believing in me more than I believed in myself, and for selflessly supporting the pursuit of my career. I could not have done this without you. You always inspired me to push through and look for the better coming days. I am so lucky to have you by my side.

To my beloved parents, Sedighe Ghezelbash and Ebrahim Yazdanifar for their faith, love and endless support and sacrifices. Thanks to my brothers and sisters (Maryam, Hamzeh, Hamid, Fatemeh and Reza Yazdanifar) for believing in me and always encouraging me.

To my friends, specially Golabia, who have been patiently listening to my everyday struggles and supporting me through this long journey.

ACKNOWLEDGEMENTS

This accomplishment would not have been possible without helps of many people including my mentor, my family, colleagues, and friends. I am thankful for the financial support from NIH with two grants, R01 CA135650-05A1 and NIH 1 R15 CA173668-01. I express my sincere and whole-hearted thanks to my advisor Dr. Pinku Mukherjee for her endless support and guidance through every small and big steps throughout the course of my research. She has been an amazing mentor and given me the chance to learn to be an independent scientist who is committed to critical thinking and hard work. I thank her for giving me the freedom to pursue various projects and explore the field, which gave me invaluable insight and experience. I would like to extend a special thanks to Dr. Ru Zhou who has been my close mentor and friend at every step of this journey. I am truly thankful to her for her dedicated support throughout my research and providing crucial remarks and insightful suggestions. I learned a lot from our everyday work discussions. I like to sincerely thank Dr. Didier Dréau for being available and supportive any time I needed support and for providing his expert advice in troubleshooting my experiments. I like to thank Dr. Richard Chi for his help in conducting the imaging experiments and providing invaluable advice. I would also sincerely thank the rest of my dissertation committee members; Dr. Bost and Dr. Chakrabarti for their valuable constructive criticism that have helped me present my research with great confidence. I am truly thankful to our vivarium staff members for their assistance with training and animal care. I would also like to thank the amazing faculty and staff of the Biology department for providing excellent education program that allowed me to conduct my research.

TABLE OF CONTENTS

LIST OF FIGURES.....	ix
LIST OF ABBREVIATIONS.....	x
CHAPTER 1: INTRODUCTION.....	1
1.1 PANCREAS.....	1
1.2 PANCREATIC CANCER.....	2
1.3 PANCREATIC DUCTAL ADENOCARCINOMA.....	4
1.4 MUC1.....	6
1.5 TAB004 ANTIBODY.....	9
1.6 CANCER IMMUNOTHERAPY.....	12
1.6.1 Overview.....	12
1.6.2 Immune Checkpoint Blockade.....	13
1.6.3 Adoptive T cell Therapy.....	14
1.6.5 Immune Resistance.....	32
1.6.6 Combination Immunotherapy.....	33
1.7 RATIONAL AND AIMS.....	34
1.7.1 Rationale.....	34
1.7.2 Aims.....	35
CHAPTER 2: IN VITRO CHARACTERIZATION OF TMUC1-CAR T CELLS.....	36
2.1 MATERIALS AND METHODS.....	36
2.1.1 Cells Cultures.....	36
2.1.2 CAR Constructs and Cloning.....	37
2.1.3 Retroviral Packaging System.....	37
2.1.4 Viral Transfection of T Cells.....	39
2.1.5 Flow Cytometry.....	40
2.1.6 Binding Assay.....	41
2.1.7 Imaging.....	41
2.1.8 T Cell Cytotoxicity.....	42
2.1.9 ELISA.....	44
2.1.10 Statistical Analysis.....	44
2.2 RESULTS.....	44
2.2.1 CAR Architecture.....	44
2.2.2 CAR Expression on Engineered T Cells.....	45
2.2.3 tMUC1-CAR T Cells Binding to Target PDA Cells.....	49
2.2.4 tMUC1-CAR T Cells Show Robust Cytotoxicity Against PDA Cells.....	50
2.2.5 tMUC1-CAR T Cells Do Not Harm Normal Cells.....	54
2.2.6 tMUC1-CAR T Cells Produce IFN- γ and Granzyme B upon Activation and Antigen Recognition.....	57
2.3 DISCUSSION.....	58

CHAPTER 3: IN VIVO EFFICACY OF TMUC1-CAR T CELLS.....	60
3.1 MATERIALS AND METHODS.....	60
3.1.1 Cell Culture.....	60
3.1.2 Animal Study.....	60
3.1.3 In vivo Imaging.....	61
3.1.4 CAR T Cells Tracking.....	61
3.1.5 Immunohistochemistry (IHC).....	61
3.1.6 Statistical Analysis.....	62
3.2 RESULTS.....	63
3.2.1 tMUC1-CAR T Cells Control Pancreatic Tumor Growth in vivo.....	63
3.2.2 tMUC1-CAR T Cells Traffic to the Tumor Site.....	64
3.2.3 Immunohistochemistry Analysis of Tumor Tissues.....	65
3.3 DISCUSSION.....	66
CHAPTER 4. PDA RESISTANCE TO CAR T CELL THERAPY.....	70
4.1 MATERIALS AND METHODS.....	70
4.1.1 Flow Cytometry.....	70
4.1.2 Apoptosis Assay.....	71
4.1.3 Proliferation Assay.....	71
4.1.4 RT-PCR, qPCR.....	71
4.1.5 Combination Therapy with Drugs and Blocking Antibody.....	73
4.1.6 Statistical Analysis.....	73
4.2.1 Deciphering the Intrinsic Resistance Mechanism Utilized by PDA Cells to CAR T Cell Therapy: Role of IDO1 and Gal-9.....	73
4.2.2 Battling the Resistance of PDA Cells with Combination Therapy.....	77
4.3 DISCUSSION.....	82
CHAPTER 5: SUPPLEMENTAL DATA.....	86
CHAPTER 6: CONCLUSIONS AND FUTURE DIRECTION.....	90
6.1 CONCLUSIONS AND FUTURE DIRECTION.....	90
6.2 APPENDIX.....	93
6.2.1 DNA Sequences of CAR Constructs.....	93
6.3 REFERENCES.....	100

LIST OF FIGURES

Figure 1. Anatomy of the pancreas.....	2
Figure 2. Progression of normal pancreatic ductal epithelial cells to PanIN lesions and to PDA. ..	6
Figure 3. Schematic of the MUC1 structure on the cell membrane.....	8
Figure 4. Normal MUC1 vs. tumor associated MUC	9
Figure 5. TAB004 antibody.....	11
Figure 6. MUC1 detection by TAB004	12
Figure 7. CAR architecture.....	18
Figure 8. Different CAR designs	19
Figure 9. CAR manufacturing.....	20
Figure 10. Hurdles of CAR-T cell therapy in epithelial tumors.	28
Figure 11. Life cycle of retrovirus.....	39
Figure 12. Different CAR constructs used in this study	45
Figure 13. CAR structure on the engineered T cells membrane.....	46
Figure 14. RT-PCR on mRNA isolated from CAR viral particles.. ..	47
Figure 15. CAR expression on human primary T cells detected by flowcytometry.....	48
Figure 16. Fluorescent tagged-CAR (CAR-mKate) expression on T cells.....	49
Figure 17. Light and fluorescent image of CAR-mKate T cells binding to MUC1 expressing cancer cell.....	51
Figure 18. MUC1 level in PDA cells.....	52
Figure 19. tMUC1-CAR T cells show robust cytotoxicity against PDA cells.....	55
Figure 20. tMUC1-CAR T cells do not harm normal cells.....	56
Figure 21. tMUC1-CAR-T cells produce IFN- γ and granzyme B upon activation and antigen recognition.....	58
Figure 22. tMUC1-CAR T cells control pancreatic tumor growth in vivo.....	64
Figure 23. Visual representation of CAR T cells trafficking in the pancreatic tumors.....	65
Figure 24. Immunohistochemistry staining of CD3 and MUC1 in tumor tissues harvested at day 68 post tumor inoculation.....	66
Figure 25. Deciphering the resistance mechanism utilized by PDA cells against CAR T cell therapy.....	76
Figure 26. Targeting resistance related genes with small molecule inhibitors.....	79
Figure 27. Targeting resistance related genes with anti-Gal-9 blocking antibody.....	80
Figure 28. tMUC1-CAR T cells work synergistically with common chemotherapy drugs to kill resistant PDA cells.....	81
Figure S1. In vitro characterization of T cells.....	87
Figure S2. Immune resistance related mechanisms.....	88
Figure S3. CAR T cell therapy in combination with anti-PD1 blocking antibody.....	89

LIST OF ABBREVIATIONS

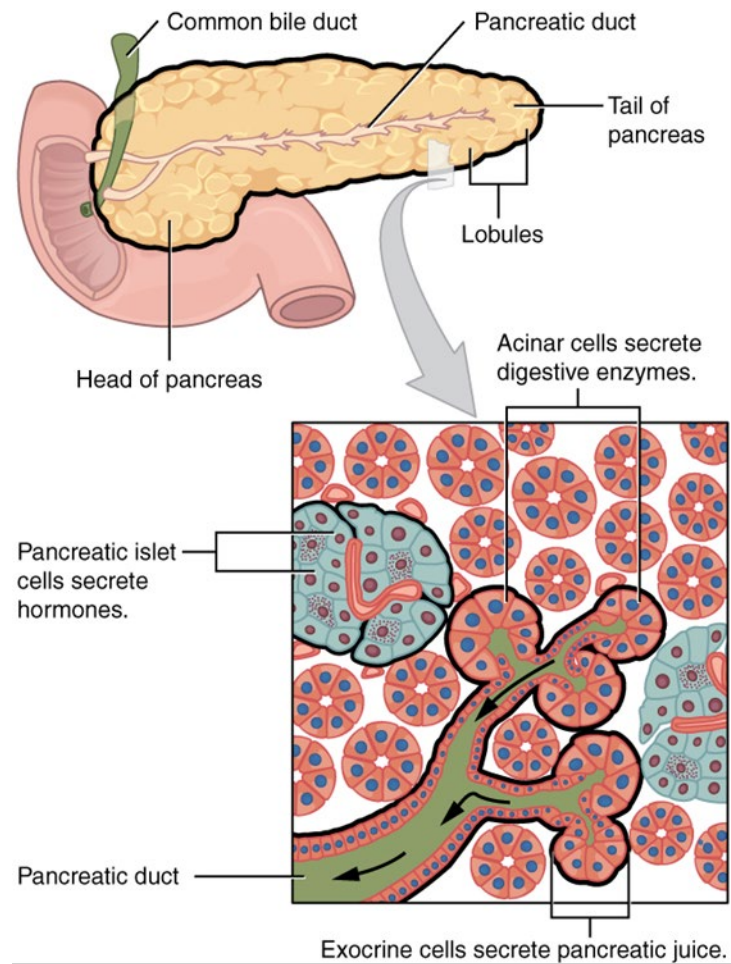
ADAR1	Adenosine Deaminase Acting on RNA
ANOVA	Analysis of Variance
BxPC3-MUC1	BxPC3 cell line overexpressing human MUC1 protein
BxPC3-Neo	BxPC3 cell line overexpressing only neomycin resistant gene
CAR T cells	Chimeric Antigen Receptor T cell
COX1/2	Cyclooxygenase ½
Gal-9	Galectin-9
GEM	Gemcitabine
IDO1	Indoleamine Dioxygenase 1
IFN-γ	Interferon gamma
IHC	Immunohistochemistry
IL-2	Interleukine-2
IL-7	Interleukine-7
IL-15	Interleukine-15
LDH	Lactate Dehydrogenase
mAb	Monoclonal Antibody
mRNA	messenger RNA
MTT	3-(4,5-dimethylthiazol-2-yl)-2,5-diphenyltetrazolium bromide
MUC1	Mucin 1
PanIN	Pancreatic Intraepithelial Neoplasia
PBMC	Peripheral Blood Mononuclear Cells
PC	Pancreatic Cancer
PDA	Pancreatic Ductal Adenocarcinoma

PDGF	Platelet Derived Growth Factor
PD1	Program Death 1
PI	Propidium Iodide
PDL1	Program Death Ligand 1
PTX	Paclitaxel
scFv	single chain variable fragment (of the antibody)
TAB004	anti-MUC1 antibody clone 004
Tim-3	T-cell immunoglobulin and mucin domain-3
tMUC1	Tumor associated MUC1
5-FU	5-Fluorouracil

CHAPTER 1: INTRODUCTION

1.1 Pancreas

Pancreas is a glandular organ located in the abdomen behind the stomach. Pancreas is anatomically separated into the head, body, and tail [1]. In the pancreas, there are main and accessory pancreatic ducts that run through the body and ultimately join with the common bile duct. Pancreas plays a role in the digestive system by secreting hormones and peptides into the descending part of the duodenum. It also releases hormones into the bloodstream for its role in the endocrine system [2]. The pancreas is consisted of exocrine and endocrine cells, which have distinctive morphologies and serve different functions (schematically represented in figure 1). The exocrine part of the pancreas is made up of acinar cells, which produce digestive enzymes. These enzymes include trypsin and chymotrypsin to digest proteins, amylase to break down carbohydrates, and lipase to digest fats [3]. The endocrine pancreas is consist of the islets of Langerhans, which constitute 1-2% of the total pancreatic volume [4]. The islet cells including alpha, beta, delta, epsilon, and gamma cells [5], release hormones directly into the bloodstream. Alpha cells release glucagon which regulates the concentration of glucose and fatty acids in the bloodstream [6]. Beta cells, the prominent group in the islets of Langerhans, release insulin and amylin. Dysfunction of beta cells can lead to type 1 or type 2 diabetes [7]. Delta cells produce somatostatin, which can regulate stomach acid production [8]. Epsilon cells release ghrelin, a neuropeptide which increases hunger and gastric acid secretion [9]. Lastly, gamma cells produce pancreatic polypeptide, which self-regulate endocrine and exocrine secretions of pancreas [10].



Anatomy and physiology. Chapter 23. The Digestive System

Figure 1. Anatomy of the pancreas. The pancreas is located in the abdomen behind the stomach and is anatomically separated into the head, body, and tail. The pancreas is consisted of exocrine, endocrine and duct cells. The islets of Langerhans secrete hormones and peptides, which are transferred to the bloodstream. The exocrine pancreas (acinar cells) produces regulatory hormones and peptides. They are secreted via ducts that are lined with pancreatic ductal cells [11].

1.2 Pancreatic Cancer

Pancreatic cancer (PC) is one of the worst cancer diagnoses with 5-year overall survival rate of 9%. [12]. It is the third leading cause of cancer-related deaths in the United States, with its mortality rate nearly matching its incidence rate [12] [13]. By 2020, PC is estimated to become the second leading cause of cancer-related deaths by overtaking colorectal cancers [14]. There are

several risk factors for PC such as familial history, cigarette smoking, chronic pancreatitis, diabetes mellitus and nutritional status [15, 16].

PC is commonly differentiated based on the anatomical location of the tumor. The tumor could be in the tail, neck, and head of the pancreas, however the pancreatic head is the most common site where tumors arise [16]. Similar to many cancer types, common health ailments, i.e. pain, weight loss, and appetite-related problems, are used in diagnosis, and patients are usually asymptomatic until metastases have already developed [17]. Diabetes is also a common diagnostic tool and is one of many risk factors [16].

Treatment of PC generally includes surgery, chemotherapy, and radiotherapy and the treatment options are usually dependent on the stage and spread of the disease upon diagnosis. Tumor resection dramatically improves outcome, but unfortunately only 20% of the cases are eligible for surgery [18] and most cases involve metastases (liver and lymph nodes commonly) that are very difficult to control and treat with standard care [19].

Currently, the standard of care for metastatic PC is combination cytotoxic therapy, folinic acid-fluorouracil-irinotecan-oxaliplatin namely FOLFIRINOX or gemcitabine plus nab-paclitaxel [20]. FOLFIRINOX has shown better response than gemcitabine plus nab-paclitaxel and increased overall survival in patients with metastatic PC [21]. However, it has been associated with physiological complications, such as sensory neuropathy [22]. The emerging field of immunotherapy has provided new treatment opportunities. Perhaps the most promising results that have been generated so far are with vaccines (peptide, tumor lysate, or dendritic cells (DCs) to boost resident immune responses to PC [23, 24]. Clinical records support that PC is sensitive to T cell reactions and suggests that direct adoptive transfer of PC-reactive T cells could result in robust clinical responses. New strategies within the immunotherapy field such as chimeric antigen receptor T cell therapy and antibody guided nanoparticles might be the future of PC treatment [25, 26], however, they are still early in the research and development phase. Like other cancers, PC is

very resistant to any therapy including immunotherapy. Therefore, it is imperative to develop and evaluate novel targeted therapeutics to improve outcome of this deadly disease.

1.3 Pancreatic Ductal Adenocarcinoma

Pancreatic ductal adenocarcinoma (PDA) is the most frequent type of PC (>95% of all PCs), and one of the most aggressive solid malignancies [27, 28]. Despite low incidence, it remains the third leading cause of cancer-related deaths in the modern world, mainly because of dismal diagnosis [29]. Significant improvements have been achieved in the screening and therapy of different solid cancers in the last decades, highly incrementing patients chance for cure. Nevertheless, the mortality to incidence ratio in pancreatic cancer has not experienced significant revision over the last few decades. The five-year survival rate remains just around 9% and one-year survival is achieved in less than 20% of cases [30]. This grim prognosis is primarily because of lack of visible and distinctive symptoms and reliable biomarkers for early diagnosis as well as aggressive metastatic spread leading to meager response to therapy [31]. In fact, around 50% of diagnosed patients present with metastatic disease. Furthermore, tumor heterogeneity and plasticity in PDA cause chemoresistance.

Progression of the disease through consecutive stages is accompanied by accumulating morphological and genetic alterations. Subsequently, signaling pathways undergo alterations in PDA progression. Over-activation of several signaling pathways involved in growth and proliferation, as well as altered expression of tumor suppressor genes are frequently detected in PDA, influencing cell proliferation, survival and invasion.

Primarily, PDA arises from epithelial cells that experience certain genetic mutations. 95% of PDA are initiated by KRAS point mutations [32]. Other mutations such as CDKN2A, TP53, and SMAD4/DPC4 also have been identified to play a role in the PDA development [33]. These mutations seem to occur in a temporal sequence in progressive pancreatic intraepithelial neoplasia

stages (PanIN). Full blown PDA arise from these PanINs lesions that are categorized as PanIN-1A, PanIN-1B, PanIN-2, and PanIN-3 according to the histological atypia after pathology [34] (Schematically represented in figure 2). In the pancreas, normal ductal epithelial cells typically are cuboidal in shape with an apical surface, which faces the duct and is covered with mucins that protect the cell from bacterial invasion or mechanical damage. These cells also have a basement membrane near the blood supply where growth factors accumulate. In PanIN-1 lesions, the epithelial cells start to lose their cuboidal shape and become elongated. Here, they start to overexpress mucins. In PanIN-2 lesions, the cells start to lose their polarity and detach from the basement membrane. PanIN-3 lesions lead to invagination of the cells, which then bud off. This is sometimes termed as carcinoma-in-situ. PanIN-4 is considered full onset invasive carcinoma. Progressing from the initiating gene mutation in KRAS in a pancreatic ductal epithelial cell to a full blown PDA can take about twenty years [35] (figure 2).

Due to broad repertoire of genetic and metabolic remodeling, PDA can survive under severe conditions and increase proliferative ability. Furthermore, recent analysis of gene expression and activity allowed for classification of detected mutations into four distinct phenotypic subtypes defined as squamous, pancreatic progenitor, immunogenic and aberrantly differentiated endocrine exocrine (ADEX) [36]. Each subtype is characterized by different mutational landscape, tumor histopathological characteristics and correlates with different prognosis. Classification of diagnosed patients into one of these four subtypes may provide substantial prognostic value and be of great therapeutic relevance, allowing for more personalized treatments. Additionally, a dense, diffuse stroma called desmoplasia, is formed around the tumor, contributing to its resistance and influencing tumor progression and invasion [37, 38]. The mentioned events make pancreatic cancer resistant to currently applied therapies, demanding for novel, broader approaches to improve PDA patients' perspectives. Conventional cytotoxic treatments, such as chemotherapy and radiotherapy, have been rather unsuccessful in improving patient's survival, offering marginal benefits. Single

agent gemcitabine, as well as its combinations, prolonged life expectancy only moderately and failed to provide expected results. Similarly, multidrug regimens (e.g. FOLFIRINOX) and targeted therapies yield disappointing effects. Therefore, there is a pivotal need for development of novel and effective strategies aiming to advance current therapeutic possibilities.

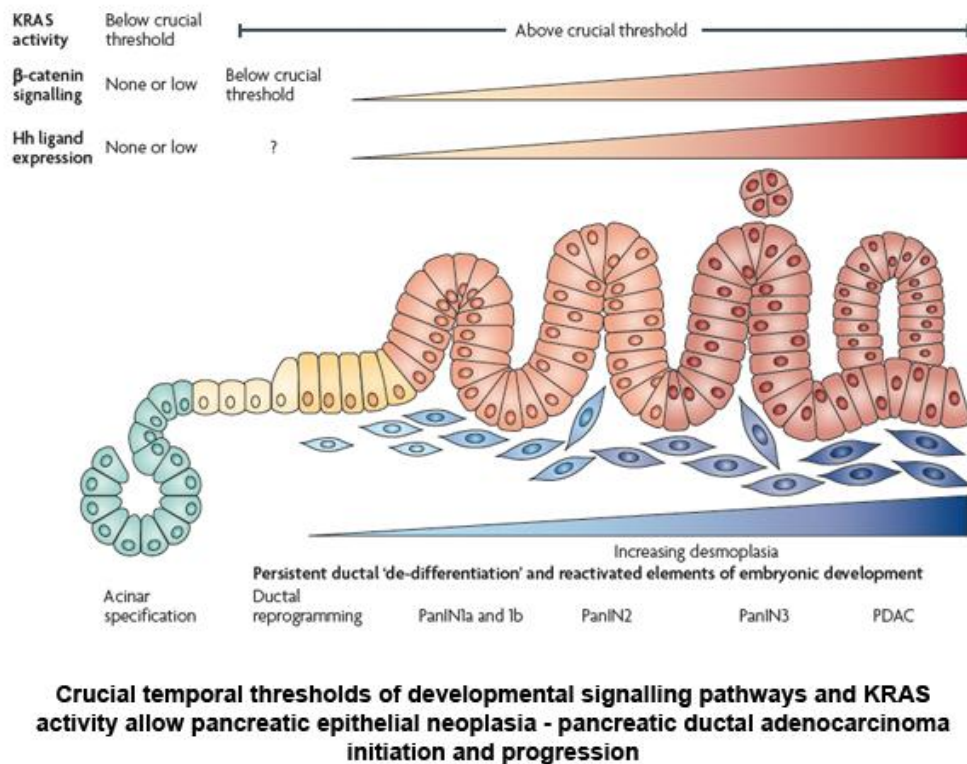


Figure 2. Progression of normal pancreatic ductal epithelial cells to PanIN lesions and to PDA. Initiating mutations in genes such as KRAS drives emergence of early pancreatic neoplasia, which lead to the development of PanIN lesions and full-blown PDA [39].

1.4 MUC1

Mucin 1 (MUC1) protein is a membrane-associated glycoprotein overexpressed in the majority of human malignancies and considered as a predominant protein biomarker in cancers.

MUC1 has been targeted by many therapies and it is recognized as the second most targetable antigen by the National Cancer Institute [40].

MUC1, is a single pass type I transmembrane protein with a heavily glycosylated extracellular domain that extends up to 200-500 nm from the cell membrane [41]. MUC1 is normally expressed on the glandular or luminal epithelial cells [42, 43] which line the digestive, respiratory, and reproductive tracts, such as esophagus, stomach, duodenum, pancreas, uterus, prostate, mammary glands, and lungs [44]. MUC1 creates a protective physical barrier on the apical surface that prevents bacteria from entering the cells. Over 50% of the mucins mass are carbohydrates that are O-linked to the protein core via serine and threonine residues [45]. The hydrophilic, negatively charged sugar branches of the mucins oligomerize and form a mucinous gel that lubricates and protects the underlying epithelia from dehydration, pH changes, pollutants, and microbes [46]. MUC1 has a N-terminal domain, followed by a sequence called the variable number of tandem repeats (VNTR), a transmembrane section, and finally a cytoplasmic tail. The larger extracellular portion comprises of the N-terminus (104 amino acids) and the VNTR sequence (20 amino acids) that is repeated 25-125 times because of polymorphism. The VNTR segment contains 5 prolines and up to 5 O-linked glycans owing to serine and threonine residues. The C-terminus consists of 170 amino acids. The MUC1-C consists of an extracellular domain (58 amino acids), a transmembrane domain (28 amino acids), and a cytoplasmic tail (72 amino acids) [47]. The cytoplasmic tail (also known as CT) is highly conserved through various species, however the rest of the molecule is not. The extracellular region adjacent to the transmembrane domain which is called Sea Urchin Sperm protein enterokinase and agrin (SEA) domain, anchors the N-terminus to the C-terminus through stable hydrogen bonds [48]. The SEA domain contains cleavage sites that can release the extracellular N-terminus (Schematically represented in figure 3).

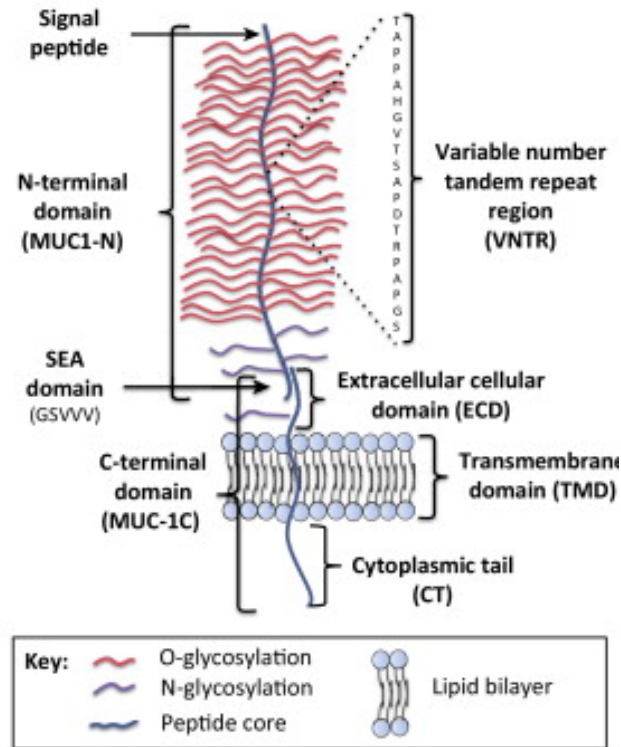


Figure 3. Schematic of the MUC1 structure on the cell membrane. MUC1 on the normal cells is heavily glycosylated on the T-terminal domain. It has O- and N- glycosylation, protecting the VNTR region of the N-terminus. N terminus is bound via hydrogen bonds to extracellular SEA domain of the C-terminus. Adapted from Nath et al 2014 [41].

MUC1 in normal epithelial cells is localized on the apical surface and functions as a protective barrier. However, when normal cells transform to malignant cells and lose their polarity, MUC1 expression is no longer restricted to the apical surface; it becomes hypo-glycosylated and comes in contact with multiple growth factor receptors [49] (Schematically represented in figure 4). This allows tumor associated MUC1 (tMUC1) to play a significant role in oncogenic signaling [50-53]. Many studies have confirmed that the oncogenic signaling happens via the cytoplasmic tail of MUC1 (tMUC1-CT) [54, 55]. It has been established that overexpression of tMUC1 in tumors is linked to enhanced epithelial to mesenchymal transition (EMT) leading to increased

invasiveness, metastasis, and drug resistance [41, 56, 57]. tMUC1 is not only overexpressed in PDA but is aberrantly glycosylated in over 80% of human PDA cases [41, 46, 50, 58, 59]. tMUC1 plays a critical role in tumor progression and metastasis in PDA [41] [60] [61]. tMUC1 overexpression occurs at the early stages of the disease [62] and high expression is associated with poor prognosis in PDA patients [53].

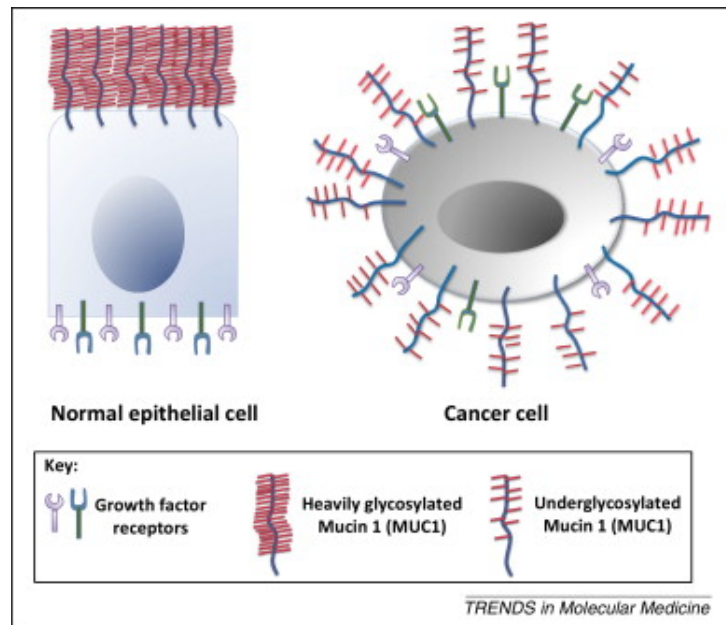


Figure 4. Normal MUC1 vs. tumor associated MUC1. tMUC1 is overexpressed and aberrantly glycosylated. In a transformed cell that has lost its polarity, tMUC1 expression is not restricted to the apical surface. It comes in close proximity to growth factor and plays a role in oncogenic signaling. Adapted from [41].

1.5 TAB004 Antibody

Our lab has developed a mAb named TAB004 (patent US 8518405 B2 and US 9090698 B2 and US20160130357 A1) [63] that detects tMUC1 on human PDA tumor tissues. While other anti-MUC1 antibodies such as Pentumomab (HMFG1) was developed using human milk fat globule, TAB 004 was developed using tumors expressing the altered form of MUC1 [59, 64]. It has been

generated by immunising Balb/c mice with MUC1-positive pancreatic tumors, previously generated in MUC1 transgenic mice. TAB004 has been reported to detect MUC1 in tumors isolated from stage 2-4 pancreatic cancer (figure 5) [65]. TAB004 does not bind to normal MUC1 on normal pancreatic cells. Aberrant glycosylation in tMUC1 provides new motifs that are hidden in normal MUC1. TAB 004 recognizes the altered glycosylated epitope (Tn) within the MUC1 tandem repeat sequence (schematically presented in figure 5) [65].[66] Importantly, this is different from the epitopes recognized by the other MUC1 antibody and has unique complementary determinant regions (CDRs) of the heavy and light chains. The antibody binds the target antigen with high binding affinity at 20 pM and does not bind unrelated antigens [65].

Further, immunohistochemistry (IHC) staining data with TAB 004 was compared to the protein atlas data for other normal epithelial tissues (e.g.: normal colon, small intestine, stomach, heart, spleen, lung, liver, pancreas) and, show that TAB 004 does not bind normal MUC1 (figure 5) while other MUC1 antibodies recognize the antigen expressed on normal tissues. Immunohistochemistry staining with TAB004 on human tissue sections from liver, heart, lung, esophagus, small intestine, spleen, pancreas, stomach, and colon revealed minimal staining, confirming that TAB004 does not detect normal MUC1 on normal epithelial cells (figure 6B). Moreover, in an orthotopic model of murine PDA (bioluminescent KCM-luciferase cells injected in the pancreas of C57BL/6 mice), TAB004 – conjugated to indocyanine green (TAB-ICG) accumulated only in the tumor, confirming the high tumor specificity of TAB004 (figure 6 C).

Moreover, we have shown that TAB004 could bind to MUC1 in cancer stem cells (CSCs) isolated from pancreatic cancer patients [65]. Furthermore, the specificity of TAB004 was investigated in a breast cancer mouse model, where it showed detection of early and metastatic breast cancer [67].

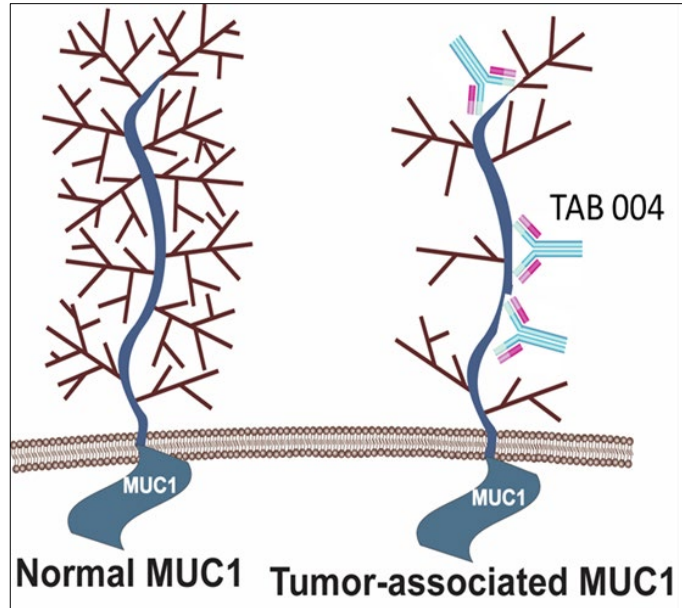


Figure 5. TAB004 antibody. TAB004 binds to newly formed epitope in tumor associated MUC1, which is aberrantly glycosylated, but it does not bind to normal MUC1.

Currently, TAB004 antibody is being commercially developed by OncoTAB Inc., a start-up company established by Professor Pinku Mukherjee [68]. The company has generated their first commercially-available product, named as Agkura™ Personal score. Agkura™ is a non-invasive blood test which is being offered for breast cancer detection, in supplementation to mammogram, for women with dense breast tissue. Its technology is based on detecting circulating MUC1 with the use of TAB004 antibody [68].

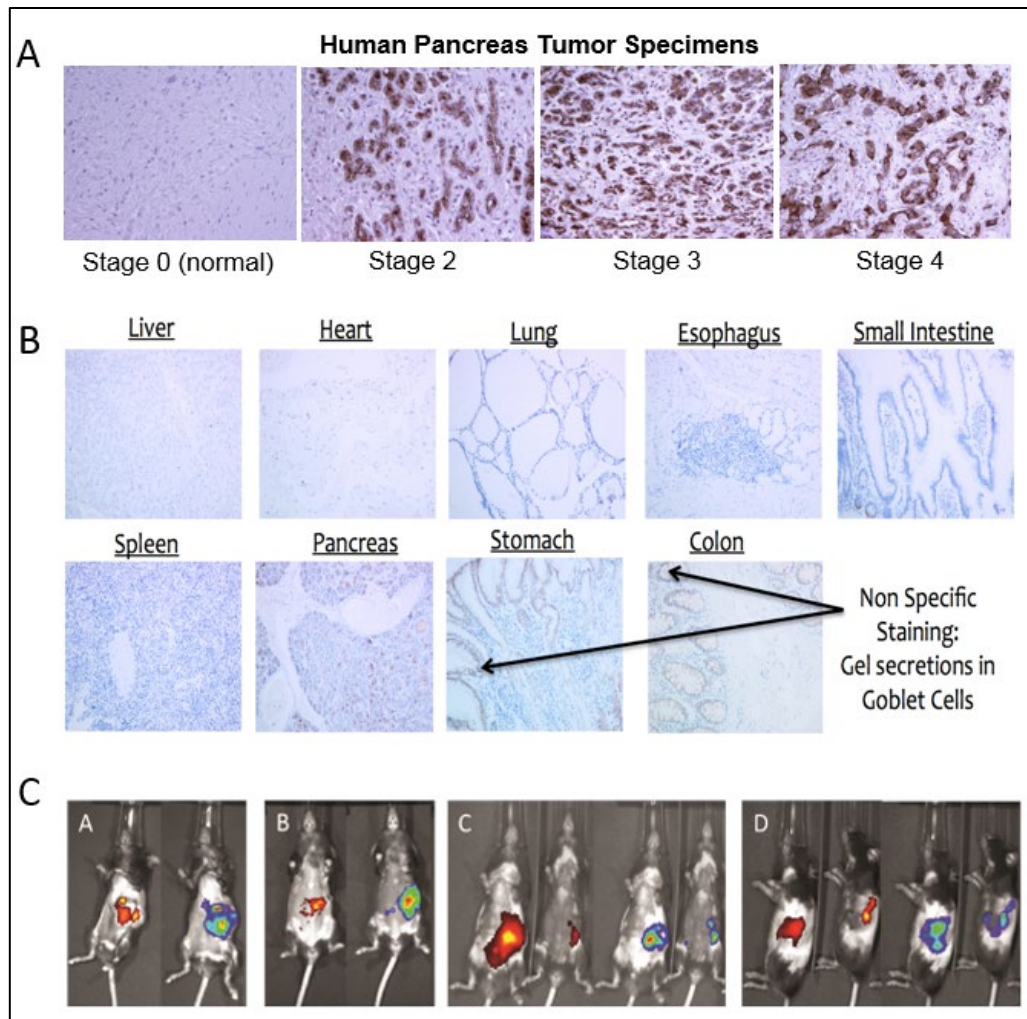


Figure 6. MUC1 detection by TAB004. A. Immunohistochemistry images of human pancreatic tumors stained with TAB004. Brown stain indicates tMUC1. B. IHC of a panel of normal epithelial tissue stained with TAB 004. TAB 004 does not stain normal epithelial tissues. C. In vivo imaging using TAB004-ICG in orthotopically injected tumor cells in the pancreas - bioluminescent KCM tumor bearing mice (rainbow); TAB-ICG: (red/yellow).

1.6 Cancer Immunotherapy

1.6.1 Overview

The immune system is body's fundamental defense system against infectious organisms and other invaders. In recent decades, there has been great advancement in our understanding of the

immune system and its close inter-relationship to cancer. Although there are substantial evidence supporting the existence of the immune surveillance of cancer; it is apparent that T cells generally do not create immune responses potent enough to eradicate established tumors. Different mechanisms have been proposed which are responsible for this incapability. For instance, it has been suggested that cancer cells can “hide” from immune cells by down-regulating their tumor-specific antigens or Major Histocompatibility Complex (MHC) molecules [69]. In addition, in the tumor microenvironment, there is an increase in the level of immunosuppressive cytokines (e.g. IL-10 and transforming growth factor (TGF)- β) as well as concentration of suppressive cell populations such as regulatory T- cells (Tregs), M2 polarised macrophages (TAM) and myeloid derived suppressor cells (MDSC) (reviewed by Hanahan and Weinberg [70-75]).

There are three fundamentally different immunotherapeutic approaches that harness the immune system against cancer. The first category involves the administration of cancer vaccines that intent to boost the immune responses against an immunogenic tumor specific antigen (e.g. MUC1 vaccines). The second category includes the development and use of monoclonal antibodies (mAbs) which block overexpressed proteins such as ErbB dimers. A major antibody application includes immune checkpoint blockade. The third category consists of different adoptive T cell immunotherapeutic strategies.

1.6.2 Immune Checkpoint Blockade

The concept of immune checkpoint blockade is based on the idea of counteracting tumor-mediated suppression of immune responses. T cell stimulation is regulated positively or negatively through the interaction of co-stimulatory or co-inhibitory ligands with their receptors. Co-inhibitory ligands are usually expressed on tumor cells or immunosuppressive subtypes of macrophages or dendritic cells. A variety of mAbs have been developed to inhibit the effect of these negative regulatory signals. Most clinically relevant immune checkpoint inhibitors are targeted against

CTLA-4 and PD-1, which are expressed on T cells, and PD-L1 which is expressed on tumor cells. Ipilimumab (Yervoy), an anti-CTLA-4 antibody has shown promising results in treatment of patients with metastatic melanoma [76]. Due to its positive results, Ipilimumab was approved by the FDA for the treatment of melanoma patients with metastatic or unresectable disease in 2011 [77]. In 2015, ipilimumab was FDA approved for the treatment of patients post-surgery that are in high-risk for disease recurrence [78]. Furthermore, two anti- PD-1 antibodies, namely pembrolizumab (Keytruda) and nivolumab (Opdivo), have been FDA approved for the treatment of different advanced malignancies, including melanoma, head and neck squamous cell carcinoma, non-small cell lung cancer, classical Hodgkin's lymphoma, non-squamous non-small lung cancer and urothelial carcinoma [79, 80]. In May 2017, pembrolizumab was also approved for the treatment of patients with any type of metastatic or unresectable solid malignancy which is defined by microsatellite instability-high (MSI-H) or mismatch repair deficiency (dMMR) [81].

1.6.3 Adoptive T cell Therapy

Adoptive T cell therapy (ACT) is the most recently advanced immunotherapeutic strategy that involves the adoptive transfer of either autologous or allogeneic T cells into cancer patients. The pioneer of adoptive T cell therapy is Steven Rosenberg who developed T cell immunotherapy using tumor-infiltrating lymphocytes (TILs). In this approach, patient's TIL cells are isolated from an excised tumor mass, expanded ex-vivo in culture with IL-2 and then re-injected back to the patient after conditioning with either chemotherapy or radiotherapy. The first promising results came in 1988 when 60% of melanoma patients achieved tumor regression after TILs injection [82]. However, this approach is not applicable in many other tumor types as it is very difficult to detect or expand tumor-specific T cells.

To broaden the application of ACT for different tumor types, other strategies were developed which became feasible with improved efficiency of gene transfer technology. In these derivative

approaches, patient-derived T cells are re-directed against tumor cells by introduction of genetically encoded receptors. The redirection is achieved by expressing on the T cell surface either an antigen specific T cell receptor (TCR) or chimeric antigen receptor (CAR). Conventional $\alpha\beta$ T cell receptors recognize processed peptide antigen, presented in a HLA-dependent manner. By contrast, chimeric antigen receptors are artificial fusion molecules that recognize native cell surface targets in an antibody-like manner.

Regarding the former approach, a variety of TCRs with different antigenic specificities have been developed and examined in numerous clinical trials [83]. The efficacy results derived from some early-phase clinical trials are promising. In 2015, it was reported that NY-ESO-specific TCR engineered T cells demonstrated promiscuous clinical responses, including 50% response rate in multiple myeloma patients and 91% in synovial sarcoma [84].

Although the results were promising, this approach may be problematical by occurrence of “on target, off tumor” toxicity. These toxicities result from the fact that the expression of the targeted antigen is not restricted to tumor cells but is also present in some normal tissues. In a trial for metastatic melanoma, patients were treated either with engineered TCR T cells specific for either the melanoma-associated antigen recognized by T cells (MART-1) or the glycoprotein 100 (gp100) [85]. Objective tumor regressions were witnessed in 30% and 19% of patients respectively. Unfortunately, responses were accompanied by on target off tumor toxicity to skin, ears and eyes, due to the presence of melanocytes in these tissues [85]. In another clinical trial, anti- MAGE (melanoma associated antigen) A3/A9/A12 TCR-engineered T cells were administered to nine patients with melanoma, synovial sarcoma or oesophageal cancer [86]. Five patients achieved tumor regression. However, three of the patients developed altered mental status, which proved fatal in two cases. These neurological toxicities were linked to physiological expression of MAGE A12 in the brain which was recognized by the TCR engineered T cells, leading to neuronal cell destruction [86].

1.6.4 Chimeric Antigen Receptors

Chimeric antigen receptor T cell (CAR T cell) therapy is an exciting approach that arm T cells with a chimeric receptor that can recognize a surface antigen on tumor cells [87]. In the last decade, CAR engineered T cells have shown exceptional promise in the treatment of hematologic malignancies [88, 89] such as refractory B-cell malignancy [90-93] and metastatic melanoma [94]; however, this success has not been extended to adenocarcinomas [95].

Chimeric antigen receptors was first introduced in 1989 by Eshhar and colleagues who created chimeric T cell receptors [93, 96, 97]. These fusion molecules were combining the cytolytic activity of T cells with the specificity of mAbs. In this concept, they have replaced the TCR's antigen binding domain by that of a mAb; thus the T cells attacked and destroyed the tumor cells as a result of recognition of surface antigens in an HLA independent manner [96, 97]. The fact that the CAR T cells can recognize tumor-antigen in non-HLA restricted manner is an important advantage over TCR engineered T cells, since most tumors down regulate their HLA expression.1.6.4.1 CAR Structure

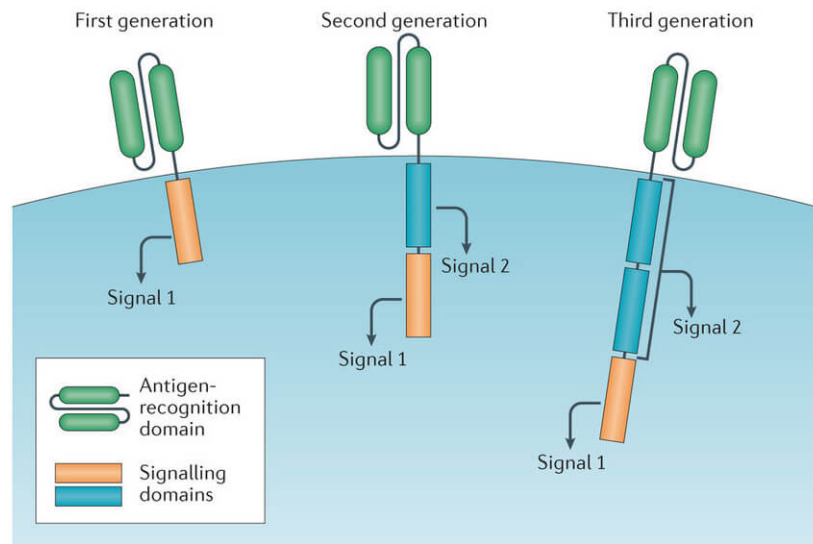
A CAR molecule consist of three domains: the extracellular antigen-specific domain, a transmembrane domain and the intracellular signaling element (figure 7). The extracellular domain is responsible for the recognition and binding to the target antigen of interest. This binder can be of different types; the most commonly used is a single chain variable fragment (scFv) derived from an antibody. Alternatively, target binding may be achieved using a ligand specific for a receptor or an antigen-binding fragment (Fab). Compared to engineered TCR, CARs have the advantage of recognizing not only peptides but also any type of macromolecules. However, a significant drawback of CARs, which is not characteristic of TCRs, is that they can only bind to cell surface antigens. The antigen-binding moiety is followed by the spacer which is connected with the transmembrane domain. The spacer should be flexible and of optimal length in order to allow the binder to reach the target of interest [98]. The CAR intracellular domain contains the signaling motifs essential for the activation of the receptor and is connected with the extracellular domain

via a transmembrane element. The simplest CAR signaling domain consists of the CD3 ζ chain, adapted from the CD3 signaling complex (normally associated with the TCR). The CD3 ζ chain contains of three immune-receptor tyrosine-based activation motifs (ITAMs) which are phosphorylated upon the attachment of the binder to the antigen of interest. The phosphorylation events are followed by the activation of downstream signaling pathways which are responsible for the triggering the antigen-specific immune response.

The first in vitro experiments with CAR T cells, incorporating the CD3 ζ signaling domain (1st generation CARs), showed that the CAR T cells were able to mediate cytotoxic responses against antigen expressing cancer cells; however, these responses were not highly potent [99]. Further studies were focused on the improvement of the signaling domain in order to enhance the immune responses. This was achieved by the addition of either one (2nd generation CAR) or two co-stimulatory motifs (3rd generation CAR) in the intracellular domain, such as CD28, OX40, 4-1BB etc. figure 7 and 8) [100, 101]. Recently, modern CAR structures containing suicide or cytokines gene have been designed that may be dubbed as fourth generation CAR [102] [103] (figure 8).

One subtype of fourth generation CAR-T cells is also known as T cells redirected for universal cytokine-mediated killing (TRUCKs) [102, 104]. This approach is based on the fact that T cell functions and those of cooperating anti-tumor immune cells can be modulated by several cytokines. Since some of these cytokines may cause systemic toxicity, localized delivery of potentially dangerous cytokines by the inherent CAR-T cell mechanism is plausible. Cytokine expression is designed to occurs via NFAT signaling upon antigen recognition by the CAR. In their earlier work, Abken et al demonstrated increased anti-tumor efficiency using TRUCKs to deliver IL-12 to the tumor niche. Improved tumor control was achieved through recruitment of anti-tumor macrophages via IL-12 expression [102, 104]. Other cytokines were also tested with TRUCK strategy. Interestingly, IL-18 was found to increase human T cell engraftment and persistence in

murine xenograft models, while negatively affecting Treg engraftment and suppressive effects [105]. A CD19 CAR-T cell designed to constitutively co-express IL-18 improved tumor control in murine models of leukemia and melanoma [106]. Additionally, using the TRUCK strategy to deliver IL-18 resulted in superior anti-tumor activity of CAR-T cells directed against the carcinoembryonic antigen in a pancreatic tumor model [107].



Nature Reviews | Clinical Oncology

Figure 7. CAR architecture. Chimeric antigen receptors consist of three different parts: the extracellular domain, the transmembrane element and the endodomain. The simplest CAR endodomain generally contains the CD3 ζ chain; however, most CARs that are being tested in clinical trials additionally include one or two co-stimulatory modules (e.g. CD28, 4-1BB, OX40). First generation CARs have incorporated the CD3 ζ signaling chain (or another module that signals similarly), which provides signal 1 and thus results in T cell activation upon antigen ligation to the CAR's binding domain. Second generation CARs utilize CD3 ζ to provide signal 1 but they also have incorporated a co-stimulatory molecule upstream of CD3 ζ , which provides signal 2. Delivery of both signal 1 and signal 2 is required for optimal T cell activation. The signaling domain of third generation CARs contains the CD3 ζ chain and two co-stimulatory modules. Adapted from [108].

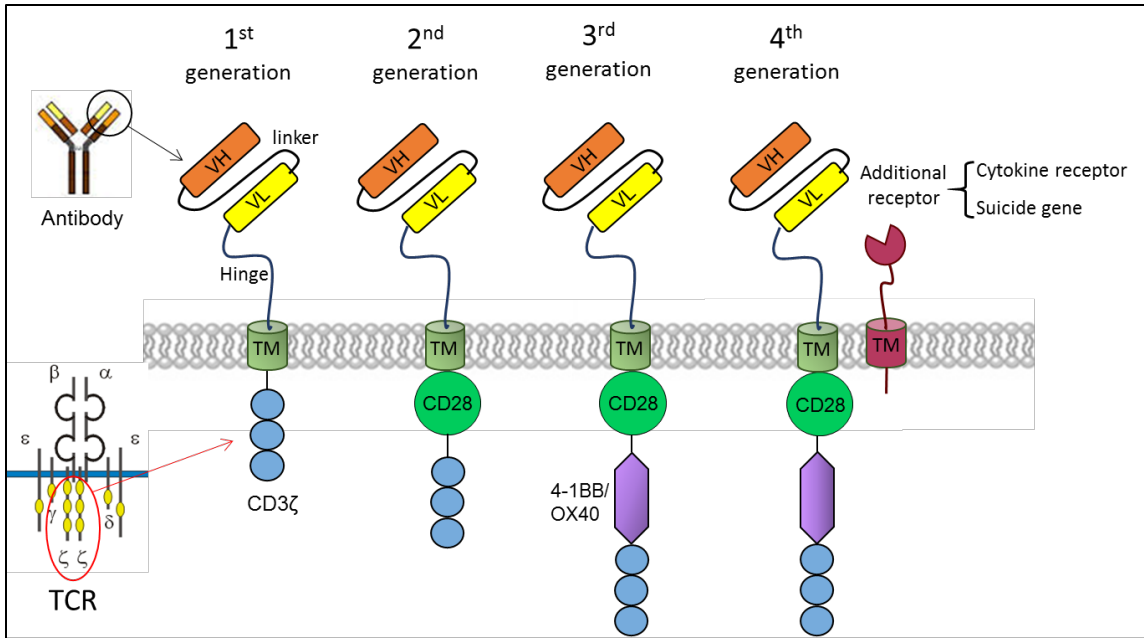


Figure 8. Different CAR designs. In a CAR molecule, the extracellular region consists of the binding domain (which can be a scFv derived from a mA, a peptide or a receptor ligand) and a spacer of optimal length and flexibility called hinge (e.g. CD8, CD28). A transmembrane domain follows (e.g. CD28, CD4) and serves to connect the extracellular regions with the endodomain. The endodomain contains the CAR signaling domain. The simplest design of CAR consists of a scFv, transmembrane and CD3 ζ domain. The 2nd, 3rd and 4th generation CARs have additional costimulatory genes incorporated in the C-terminal end of the molecule. A cytokine or inhibitory receptor is co-expressed with the CAR in 4th generation design to increase the stimulatory signal or stop over activation of the T cells respectively. Adapted from [95].

Although CAR-T cells have numerous designs and utilize various tumor-specific scFvs, their manufacturing procedure remains the same. Briefly, T lymphocytes are isolated from peripheral blood mononuclear cells (PBMC) of patient using apheresis or blood sampling. Next, T lymphocytes are expanded *ex vivo* via activation with beads covered with activating antibodies or different cytokines. Subsequently T cells become genetically modified to express CAR cDNA using electroporation, Lipofectamine or viral vectors. It is then followed by large-scale expansion, final formulation, and lastly infusing back to the patients. Generally, both CD4⁺ and CD8⁺ T cells

are injected as a mixed population, since CD4⁺ cells support CD8⁺ cells and activate other immune cells by producing cytokines such as IFN- γ and IL-2. However, CD4⁺ or CD8⁺ T cells may further be sorted depending on the application [109] (figure 9).

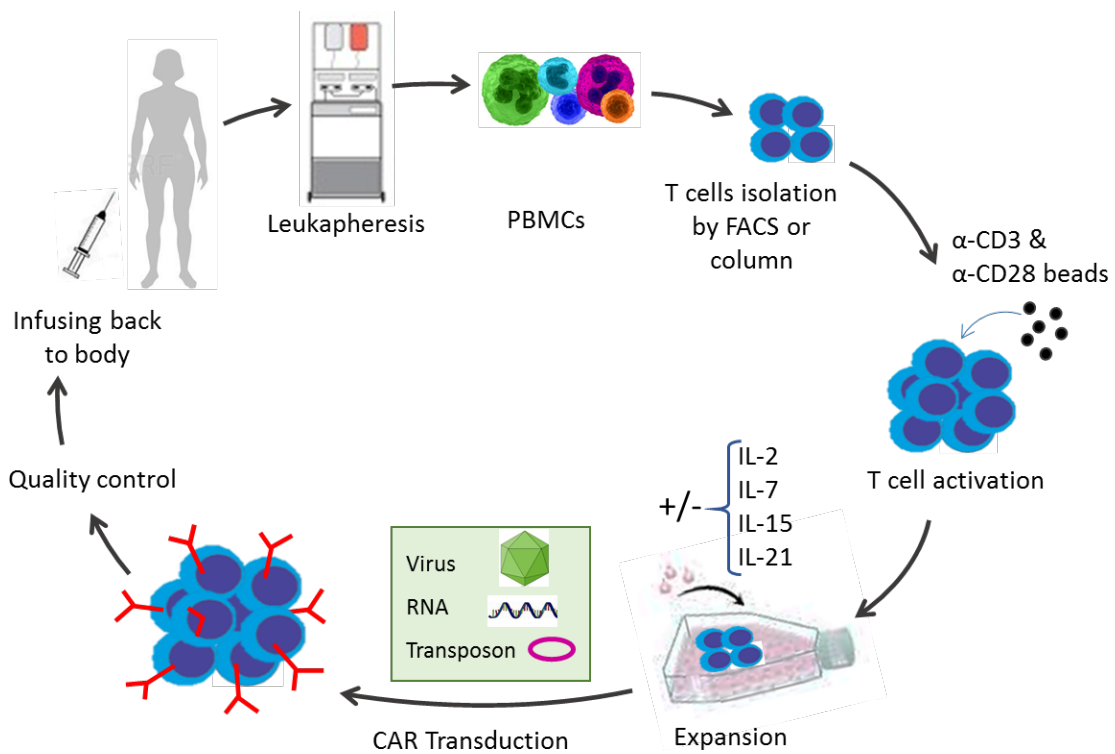


Figure 9. CAR manufacturing. Manufacturing workflow of gene engineered T cells. Patient-derived T lymphocytes are harvested from the patients' blood *via* Leukapheresis or blood sampling and further activated by beads. The CAR gene is delivered to T cells by retroviral or lentiviral vectors, electroporation (RNA) or transposons. Subsequently, the transduced T cells are expanded ex-vivo and undergo quality control before injecting back into patient. Adapted from [95].

1.6.4.2 CAR T cells from bench to clinic

As mentioned, CAR T cells have shown remarkable responses in haematological malignancies in which CD19 proved to be a very attractive target. This success has been based upon the use of second generation CARs in which either CD28 or 4-1BB have been incorporated

upstream of CD3 ζ . In a historic moment, the first CAR T cell therapy was recently approved by the FDA for the treatment of children and young adults with refractory acute lymphoblastic leukaemia (ALL) [81].

Several studies demonstrate the clinical efficacy of CD19-targeted CAR T- cell immunotherapy of B-cell malignancy. In a trial conducted by Porter and colleagues in the University of Pennsylvania, 14 adults with refractory, relapsed chronic lymphocytic leukaemia (CLL) were treated with anti-CD19 CAR T cells (CTL019- comprising a 4-1BB based second generation CAR) [90]. Three patients achieved a complete response (CR), 5 patients had a partial response (PR) while 6 had no response. The overall response rate was 53%²⁰⁸. The same group has also treated 10 CLL patients in a Phase II dose optimisation trial, again using the CTL019 CAR approach. The results of this study indicated that 2 of the patients had CR and 2 of them PR with an overall response rate 40% [91].

Kochenderfer et al. in another trial, used anti-CD19 CAR T cells for the treatment of 15 patients with either diffuse large B-cell lymphoma (DLBCL, n=9), indolent lymphoma (n=2) or CLL (n=4)²¹⁰. Complete remissions were observed in eight patients. Four patients were partial responders, one had stable lymphoma and, in two cases, the results were not evaluable. Noticeably, four of the complete responders were DLBCL patients. Unfortunately, acute toxicities were observed, including neurological toxicities, while one patient died 16 days after injection for unknown reasons. Despite these toxicities, this was first study that showed complete responses in DLBCL patients and importantly the most durable CR was still ongoing at 23 months after treatment [92].

Outstanding results were achieved by a trial where 25 patients aged 5-22 years old and five older patients with refractory or relapsed acute lymphoblastic leukaemia (ALL) were treated with CTL019 CAR T cells [93]. Remarkably, CR were seen in 90% of patients (27/30 patients) while sustained remissions were observed in 15 out of 22 evaluable individuals (7 months average follow-

up) [93]. Additionally, it has been reported that 63 ALL patients were treated with CTL019, with 83.2% overall response rate [101]. These impressive results led to the approval of the first CAR T cell therapy (tisagenlecleucel, marketed by Novartis as Kymriah) in the USA and its release to the market. The product is administered in a single dose and is designated for patients with refractory and/or refractory ALL. According to the manufacturer's dosing instructions, patients with body weight equal or less than 50kg will receive a single dose of $0.2-0.5 \times 10^6$ CAR-positive viable T cells per kg while patients with body weight higher than 50kg will receive $0.1-2.5 \times 10^6$ CAR-positive viable T cells. Tocilizumab, a mAb directed against the receptor of interleukin-6 (IL6-R), was also approved along with Kymriah for the management of cytokine release syndrome [110, 111].

1.6.4.3 Challenges of CAR-T Cell Therapy in Adenocarcinomas

1.6.4.3.1 Trafficking & Tumor Microenvironment

Despite enormous success of CAR-T cell therapy for hematopoietic cancers, unfortunately, less encouraging results have been shown for epithelial tumors. This is due to several factors. The mechanical barrier in epithelial tumors, which is absent in liquid tumors, impede successful infiltrating of T cells to tumor sites. Unlike the “liquid tumor” setting of hematologic malignancies, CAR-T cells must pass multiple barriers in order to reach the tumor site. Potential mismatches of T cell chemokine receptors and their ligands on tumor cells and the presence of the dense stroma in most epithelial tumors makes T cell trafficking truly cumbersome. Numerous pre-clinical studies have shown that combining CAR-T cells with chemokine receptors improves migration and infiltration of T cells, once they are inside the tumor bed [112]. Moreover, antigen loss and heterogeneity of epithelial tumors contribute to the ineffectiveness of CAR-T cell [113]. Even after reaching the tumor sites, T cells must overcome various challenges in order to exert their anti-tumor effect. These challenges include: a hostile tumor microenvironment enriched by oxidative stress,

nutritional depletion, acidic pH, hypoxia, existence of numerous suppressive soluble factors and cytokines, suppressor immune cells such as Tregs, myeloid derived suppressor cells (MDSC), tumor-associated macrophages (TAM) or neutrophils (TAN), intrinsic negative regulatory mechanisms of T cells (expression of inhibitory receptors), and over-expression of inhibitory molecules and immune checkpoints [113]. To reduce these inhibitory effects, coupling pro-inflammatory cytokines, such as IL-12, with CAR-T cells, also combinations of CAR-T cells with immune-checkpoint inhibitors, are currently being tested [114].

A possible down side of CAR-T cell therapy is the fact that these T cells recognize antigen independently of MHC molecules. Although this independency is considered a strength of CAR-T cells, it also limits the pool of antigens targetable by CAR, as a majority of tumor associated antigens (TAAs) are intracellular neoantigens being solely expressed in the context of MHC [115]. This hurdle is not exclusive to epithelial solid tumors.

1.6.4.3.2 Toxicity

A disadvantage of CAR-T cell therapy is that CAR-T cells are “living drugs”, therefore, failure in treatment may not be easily managed. Over activation or cross reactivity with antigen on healthy tissue may result in fatal outcome. Thus, effective strategies must be devised toward managing the safety issues [116]. As said by Robert Tepper, Chief Medical Officer at Jounce Therapeutics, “The good news - and the bad news - is that the immune system is incredibly powerful”.

Much of the toxicity data, exists for the CAR-T cells against hematopoietic tumors, but not as much in epithelial solid tumors. The toxicities include cytokine release syndrome (CRS, systemic inflammatory response following CAR-T cells activation), B cell aplasia (specific for CD19 CAR-T cells), neurological toxicity, “on-target, off-tumor” toxicity (reactivity to target antigen on

healthy tissues), anaphylaxis or allergy (host immune reaction to foreign antigen on CAR-T cell), and insertional oncogenesis (mutagenesis by viral genes) [117].

The most prominent cytotoxicity seen in CD19 CAR-T cell trials is CRS which is associated with rapid T cell proliferation [118]. The main reason for this effect is not clearly explained yet; however, it is likely due to infused CAR-T cells secreting products that can trigger a toxic release of pro-inflammatory cytokines, such as IL-6, IFN- γ , and TNF α [119]. CRS symptoms range from high fever and myalgia to unstable hypotension and respiratory failure. This effect was not observed in pre-clinical animal models, so it was unexpected [120].

Other types of toxicity which have been profoundly described in recent CD19 CAR-T cell trials are B cell aplasia and a diverse array of neurological toxicities [121]. B cell aplasia, which is an on-target/off-tumor consequence, is associated with hypogammaglobulinemia which is easily managed by γ -globulin replacement therapy [92]. Neurologic toxicities seem to be exclusive to CD19-targeted therapies and have been reported in almost all CD19 CAR constructs as well as the CD19 BiTE[®] blinotumumab [114].

It is said that CRS has not yet been reported for solid tumors trials. This could be due to low level of T cell engraftment and proliferation in solid tumors compared to leukemia. However, with development of enhanced CAR and utilizing stronger lymphodepletion regimens, this kind of toxicity may become a problem [113]. In one case, CRS in solid tumors has occurred due to “on-target, off-tumor” toxicity. To avoid T cells reacting to normal tissues, the most suitable tumor antigens need to be targeted. In addition, we need to develop tumor-specific antibody that does not recognize and bind normal tissue. Unlike CD19 which is exclusively expressed on B lymphocytes, majority of solid tumor antigens are also present at low levels on normal cells [114]. In contrast to the ease of management of B-cell aplasia, off-tumor toxicities that may occur in solid tumors are not easily controlled. A prominent example is targeting ERBB2 (HER2/neo), a marker overexpressed on both breast and colon cancers. A patient with metastatic colon cancer was treated

with 3rd generation ERBB2-CD28-41BB ζ CAR (based on Trastuzumab mAb), in 2010, and experienced a severe respiratory distress associated with development of new lung infiltrates. Infiltrates were also found at low levels in several normal organs including heart and the pulmonary vasculature. The patient died 5 days after from CRS, despite intensive medical management. CRS was attributed to CAR-T cell targeting ERBB2 on lung epithelium [122]. On the contrary, this unexpected toxicity has not been reported repeatedly in solid tumors. It may have been stimulated by high dose of infused CAR-T cells (10 million cells) and precondition therapy in the patient, since subsequent studies using a different ERBB2-specific CAR with considerably lower doses of CAR-T cells have proven safe in treating patients without preconditioning chemotherapy [123].

Anaphylaxis, allergy, or graft versus host disease (GVHD) has not been a major concern with CAR-T cell therapy, since autologous T cells are used, and infused cells are the donor's own cells. Also, no reaction has been recorded to exogenous viral genes following CAR-T treatment [124] [125]. Despite this proven safety to reduce the time and cost of treatment, establishment of an "off-the-shelf" or "third-party" cell bank, wherein universal CAR-T cells are available to anyone, seems like an attractive solution. In this case, immune reactivity to graft is of higher concern. To manage this, two strategies have been suggested so far, including using specific cells for CAR expression and silencing the immunogenic molecule, TCR, on T cells [126]. These approaches are in process and can broaden application of CAR-T cells in the future.

Lastly, insertional oncogenesis may occur by engineered T cells. Viral vectors or plasmid DNAs used to transfer gene into T cells might carry the risk of malignant transformation in clinical setting. Despite copious studies demonstrating safety of viral vectors, it is too early to decide if this approach is safe for larger patient populations [127].

1.6.4.3.3 Mechanisms to combat toxicity

Despite impressive clinical efficacy of CAR-T cells, severe treatment-related toxicities have restricted universal use of CAR-T cells [128]. To address CAR-T cell toxicity, numerous strategies prominently involving CAR design have recently been devised (schematically represented in figure 10):

1) Dual targeting strategy to increase specificity and safety. For example, a modified T cell expresses two CARs, wherein T cell activation signal 1 (via CD3 ζ) is physically separated from the costimulatory signal 2 (via CD28) and each CAR recognizes a separate tumor antigen. This CAR-T cell exhibit full activation and function only if both CARs are engaged [129] [130, 131]. This approach provides a path for controlling CAR-T cell selectivity and activity in a way that retains both effectiveness and safety.

2) Suicide genes. These specific genes have been introduced into the CAR vector [132] and CAR-T cells get permanently eradicated upon activation of these suicide genes. So far, use of herpes simplex virus thymidine kinase (HSV-TK) and an inducible caspase 9 (iCasp9) genes have shown success in clinical trials [129].

3) Co-expression of a depletable receptor. A polypeptide on cell surface can be targeted by depleting antibodies in order to eliminate engineered T cells. This strategy is already in clinical use, for example, EGFR and CD20 [133].

4) Inhibitory CARs (iCAR). When target antigen is shared between tumor and normal cells, off-tumor toxicity may occur. If normal tissues express another antigen which is not expressed by tumor cells, it could be targeted by CAR-T via a receptor which triggers an inhibitory response. This receptor which comprises intracellular domain of T cell inhibitory receptors (PD-1 and CTLA-4) is co-expressed by CAR-T cells. Fedorov *et al.* have shown that iCAR protects normal tissues in preclinical mouse model [134]. Significantly, primary regulatory effect of iCARs was selective

and transitory, allowing for future activation of T cells upon later encounter with target cells that exclusively express the antigen [135].

5) Switchable CARs (sCAR) and multi-chain CARs (mcCARs). These CAR-T cells need an intermediate switch molecule to get fully activated [136] [137]. In sCAR design, an antibody based switch molecule is co-infused, and it bridges the target cell and the sCAR expressing T cell, while mcCARs are only activated in the existence of the small-molecules, such as rapamycin. Switchable CARs have been designed to reversibly control CAR-T cell activity and specificity in immunocompetent mouse model of CD19 and CD22 expressing cancers.

Moreover, multiple antigens could be targeted using the same CAR simply by infusing various or bispecific switch molecules. For instance, two or more switch molecules such as anti-CD19 and -CD22 fused to FITC could be targeted by same anti-FITC CAR-T cells (“universal CAR”) [128].

6) Masked CARs. In this design, the antigen-recognition domain of CAR is sterically blocked by a substrate peptide which is cleaved in the presence of matrix metalloproteinases. When T cells enter the tumor microenvironment, which is enriched by these enzymes, substrate will be cleaved, and binding capacity of T cells will be unmasked. Once the receptor is unblocked, T cells mainly localize to the tumor area. Use of masked CARs provides a way to focus CAR-T activity toward targets shared with healthy tissues [138].

7) Self-limited CAR. This strategy uses mRNA rather than retro/lenti-virus to transiently express CAR receptor [139] [111]. In this method, CAR expression level will diminish after a period of time as mRNA start to vanish in the cell.

8) Pharmacologic therapy. IL-6 receptor blockade with tocilizumab is used to control CRS. Corticosteroids are used for neurologic toxicities and for CRS not responsive to tocilizumab. However, pharmacologic management of these therapies remains challenging, since it entails the

risk of suppressing anti-tumor immune response by CAR-T cells [140]. Hurdles in CAR-T cell therapy of epithelial tumors and the ways to combat them are illustrated in Figure 10.

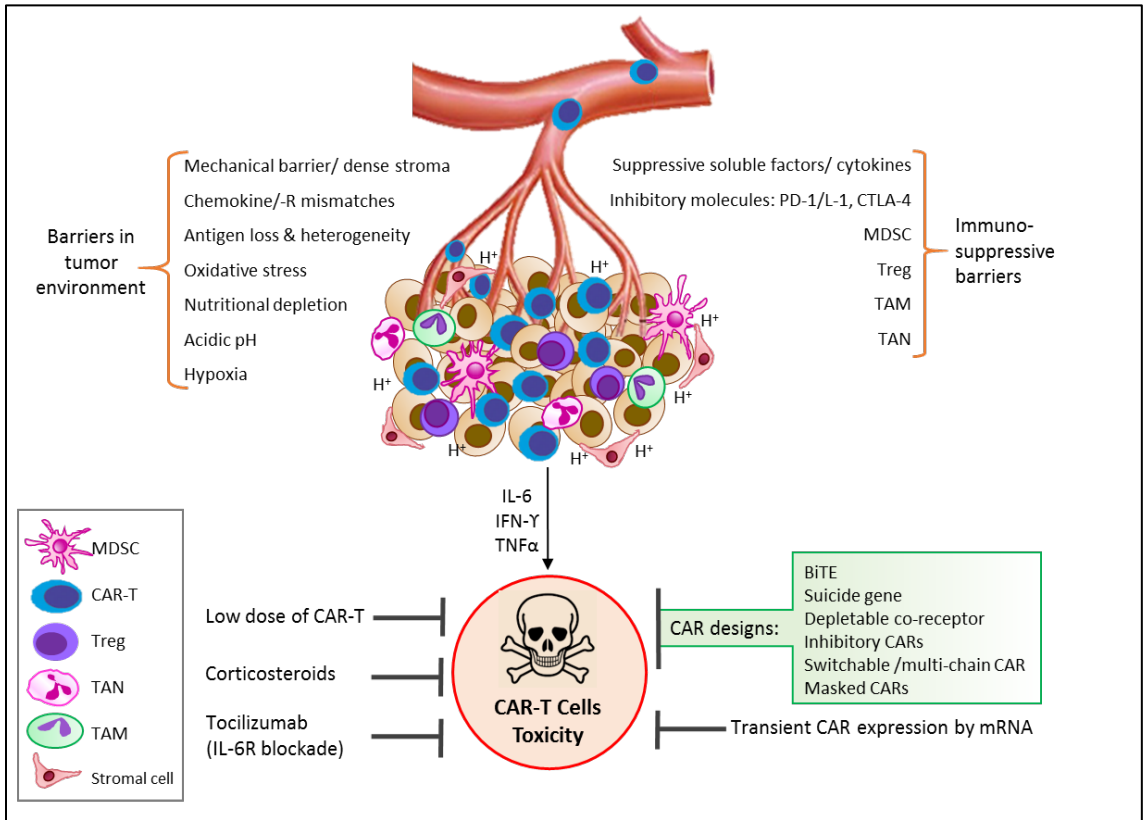


Figure 10. Hurdles of CAR-T cell therapy in epithelial tumors. T cells face multiple barriers in solid epithelial tumors which negatively affect T cell trafficking and function within the tumor microenvironment. These barriers are acting either mechanically, biochemically (metabolically) or immunologically. CAR-T cell therapy may result in toxicity that could be managed via different suggested mechanisms. Adapted from [95].

Despite challenges associated with CAR-T cell treatment, immunotherapy remains the most promising therapy that is revolutionizing how we treat cancer. This is exemplified with FDA’s approval of anti-tumor antibodies, immune checkpoint inhibitors, cellular and peptide tumor vaccines, antibody drug conjugates (ADCs), and adoptive T cell therapies for various epithelial

malignancies. No cancer treatment is devoid of toxicity, and we have learnt over the years how to manage it. Therefore, much still needs to be learnt about how to mitigate the risks associated with immunotherapy. For targeted CAR-T cell therapy, most critical is the selection of the tumor antigen, and even more critical, is the generation of antibodies that bind tumor cells but spares normal tissue.

1.6.4.4 MUC1-Adoptive T cell therapy

In adoptive T cell therapy, patient-derived PBMCs are isolated and different cell populations, such as T cells or dendritic cells, are expanded. These can be further manipulated in distinct ways. One strategy includes the activation of CTLs or DCs by presenting to them tumor-associated peptides, such as those derived from MUC1 [141]. The activated cell populations are expanded *ex vivo* and are then adoptively transferred back to the patient. These activated cells can either specifically eliminate tumor cells, in the case of CTLs, or enhance anti-tumor immune responses, in the case of antigen-loaded DCs [142].

Numerous clinical trials have been performed in which the effectiveness of CTLs or pulsed dendritic cells has been explored. In some cases, the combination of both approaches was shown to have some benefit in the patients' outcome [143]. In one combinatorial study, Kondo et al. treated 20 patients with unresectable or recurrent pancreatic cancer with both MUC1- pulsed dendritic cells and activated CTLs. Based on the results, one patient with metastatic disease showed complete response and four patients presented stable disease [143].

In another approach, patient-derived T cells are isolated and engineered to express MUC1-specific CARs on their surface. Few research groups have engineered MUC1-specific CAR T cells and have investigated their anti-tumor activity using pre-clinical *in vitro* and *in vivo* models. Wilkie et al. developed various versions of a MUC1-specific CAR, as published in a study in 2008 [144]. In this paper, a 3rd generation MUC1-specific CAR named HOX showed the most promising

efficacy. This CAR consists of a binding domain based on the HMFG2 antibody and it signals via CD3 ζ , CD28 and OX-40. Additionally, this CAR has incorporated a longer hinge (IgD), which provides enhanced flexibility to the binding domain of the CAR. Mice bearing MUC1- positive tumors showed delayed tumor growth after treatment with HOX- engineered CAR T cells [144, 145]. In a novel subsequent approach, Wilkie et al. co-expressed an anti-ErbB2 CAR (signals via CD3 ζ alone) together with a MUC1-specific chimeric co-stimulatory receptor (containing CD28 alone). Their results showed that both antigens were required in order to achieve maximal tumor cell cytotoxicity and T cell activation [131]. More recently, Posey et al. showed control of tumor growth in leukaemia and pancreatic cell xenograft models using a 2nd generation MUC1-specific CAR. The latter contained an scFv based on 5E5 MUC1-Tn specific antibody [146, 147]. Our group has demonstrated the effectiveness of TAB004 derived anti-MUC1 CAR T cells in treating triple negative breast cancer [148]. A 2nd generation CAR construct was used in this study and its combination with anti-PD1 antibody was examined.

Clinical trials of MUC1 specific CAR T cells has been limited to date. The efficacy of two different SM3-based MUC1-specific CAR T cells has been investigated in a Phase I clinical trial, although data from only a single patient has been reported as yet [149]. One set of CAR T cells contained an SM3-based CAR co-expressed with IL-12. The second set contained a CAR with a modified SM3 scFv to achieve increased binding of the CAR to MUC1. The latter lacked co-expression of IL-12. In this trial, these two types of MUC1- specific CAR T cells were injected using the intratumoral route in two different lesions in a patient with metastatic seminal vesicle malignancy. Based on a published case report, the lesion treated with the modified-SM3 CAR T cells showed significant tumor necrosis while no difference was observed in the lesion treated with the SM3-IL12 CAR [149].

Four other clinical trials are currently recruiting patients in order to test MUC1-specific CARs in patients with different types of malignancy. Distinct strategies are being evaluated. In two

Phase I/II clinical trials (NCT02617134 and NCT02587689), the effectiveness and safety of MUC1-redirectioned CAR T- cells is being investigated in patients with solid malignancies. In the NCT02839954 trial, the efficacy and safety of NK cells transduced with a MUC1 CAR is being evaluated. Lastly, in a Phase I/II clinical trial (NCT03179007) patients with an advanced solid tumor burden are being treated with MUC1 CAR T cells that are engineered to secrete PD-1 and CTLA-4 checkpoint inhibitors [150].

1.6.4.5 CAR T Cell Therapy for PDA

Researchers have shown MUC1-CAR-T cells as a potential candidate for PDA therapy [151] [146], including our lab [152]. A clinical trial has investigated the role of anti-MUC1 CAR-T cells in treating patients with MUC1 positive advanced refractory solid tumors (NCT02587689). Anti-MSLN CAR T cells have been developed for treatment of PDA. MSLN is a cell surface antigen present on normal mesothelial cells and overexpressed in several human tumors, such as mesothelioma, lung, pancreas, breast, ovarian, and other solid cancers [153]. MSLN-CAR-T cell therapy in a phase I study (NCT01355965) has demonstrated antitumor response for the first time in PDA and has shown the development of new antibodies [111]. A second generation of CAR T cells against mesothelin (CARTmeso) using patients' own T cells to express anti-mesothelin receptors linked to TCR ζ and 4-1BB as a co-stimulator for metastatic PDA is being investigated in clinical trials (NCT03638193, NCT02465983). Ongoing trials are testing genetically engineered T cells to target the immunogenic peptide derived from the cancer-testis antigen (NY-ESO-1), an antigen usually found in normal testis and in a variety of tumors (NCT01967823). Preclinical and phase I trials have studied CAR T cells targeting HER2, CEA, and mesothelin (NCT02713984, NCT02850536, NCT02349724, NCT02706782, NCT02580747, NCT03323944), but limited data has been presented. The orphan tyrosine kinase receptor, ROR1, is expressed by many tissues during embryogenesis but is absent in many organs after maturation, except for B cell precursor

and in low levels in the pancreas, lung, and adipose tissue. ROR1 targeting CAR-T cells have also been evaluated in preclinical trials and it showed effectiveness in leukemia and some solid tumors, including pancreatic cancer [154]. ROR1-CAR-T safety was confirmed in nonhuman primates [155]. Additional tumor specific antigen targeted CAR T cells are under investigation and include an ongoing phase I/II trial testing an “off-the-shelf” anti-KRAS G12V and G12D murine TCR–transduced peripheral blood lymphocyte therapy in patients with PDA who harbor the mutant RAS variants presented on HLA-A*1101 (NCT03190941, NCT03745326). Although these approaches have the potential to overcome the challenge of a lack of effective PDA–specific T cells, CAR T cells might still have difficulty trafficking into the tumors and sustaining their activity.

1.6.5 Immune Resistance

Cancer cells evade from a cytotoxic or proinflammatory immune response by changing their phenotype. This process is called Adaptive immune resistance. This adaptive process is elicited by the specific recognition of cancer cells by T cells, which result in the production of immune-activating cytokines. Cancers protect themselves from the T cell attack by hijacking mechanisms developed to limit inflammatory and immune responses. Hindering adaptive immune resistance is the mechanistic basis of responses to PD-1 or PD-L1–blocking antibodies, and may be of relevance for the development of other cancer immunotherapy strategies.

Various new immunotherapy strategies have been developed based on impeding processes thereby cancer adapts and evades from an immune response. Recognizing the specific adaptive resistance mechanisms in each case is likely to allow the personalized development of immunotherapies tailored to block how a particular cancer protects itself from the immune system [156].

1.6.6 Combination Immunotherapy

Even though single agent immunotherapy has demonstrated clear anti-tumor activity across multiple tumor types, the response rates are still low. In order to achieve better treatment efficacy, large dosages are usually utilized, which subsequently lead to drug resistances or toxicity. For example, the objective response rate (ORR) of ipilimumab (anti-CTLA-4 antibody) alone in advanced melanoma is only 10.9%, and the ORR of nivolumab (anti-PD-1 antibody) alone in advanced melanoma is 40%. However, by combining ipilimumab and nivolumab at a much lower dosages for both antibodies, the ORR can achieve 40% [157]. Additionally, in CAR-T cell based therapy, the trafficking of CAR-T cells to the tumor microenvironment is essential for the success of immunotherapy. Researchers found that PD-1 blockade was capable to enhance T cell migration to tumors by elevating IFN- γ inducible chemokines, including CXCL10. Therefore, in order to enhance the homing of CAR-T cells into tumors, researchers are focused on combining PD-1 blockade and CAR-T cell therapy together to achieve better antitumor activity [158, 159].

The traditional notion was that chemotherapy is a contra-event for immunotherapy as it may cause lymphocyte depletion (lymphopenia) and the programmed cell death induced by chemotherapy is tolerogenic. However, more evidence has demonstrated that a number of immune cells killed by the chemotherapy may be beneficial rather than detrimental for the cancer therapy over long-term treatment [160]. For example, the loss of regulatory CD4⁺ T cells caused by chemotherapy may benefit the anti-tumor T cell response induced by immunotherapy [161]. In addition, it has been shown that lymphopenia can trigger a phase of immune system regeneration [160]. In addition, it has been shown that chemotherapy, especially targeted therapies, may also directly regulate immune responses. For example, sunitinib, a multi-targeted receptor tyrosine kinase (RTK) inhibitor, is shown to attenuate the activities of specific immune cell populations that restrain cytotoxic T lymphocytes (CTLs), including FoxP3⁺ regulatory T cells and myeloid derived suppressor cells (MDSCs) [162]. Other studies also show that the inhibition of Jak2/Stat3 augments

the tumor antigen presentation by DCs, thereby enhancing the priming of tumor-specific immune responses of CTLs [163, 164]. Some studies have shown that the general response rate of tumor-specific mAb is 8-10% in patients with advanced cancers or recurrent disease. While it yields an increased response rate of 30% when combined with chemotherapy and/or radiotherapy [165].

1.7 Rational and Aims

1.7.1 Rationale

PC is the 3rd leading cause of cancer-related deaths with a 5-year survival rate of only 9% and a mean life expectancy of ≤ 6 months [166]. Only 20% of the patients are eligible for surgery. Radiotherapy and chemotherapy remain largely ineffective. CAR-T cell technology that can activate and redirect host T cells to kill tumor cells presents an attractive alternative [167]. CARs are fusion receptors comprised of an antibody-derived single-chain variable fragment (scFv) coupled via hinge and transmembrane elements to a T cell signaling and co-stimulatory domain. For CAR-T cells to work, both the target antigen and the scFv recognizing the target have to be highly specific. We have strong preliminary data using a novel tMUC1-specific CAR-T that utilizes the scFv motif of TAB004, a patented antibody [168, 169]. TAB004 specifically recognizes the tMUC1 but spares recognition of normal MUC1. tMUC1 is expressed on ~80% of human PDA [170, 171]. The antigenic isoform recognized by TAB004 is hidden in normal epithelia making it a safe strategy. CAR T cells have recently been developed and showed enormous success against hematopoietic malignancies, but it has not gain momentum in treating solid tumors. Hence, we propose to develop and test novel anti-tMUC1 CAR T cells that contains TAB004 antibody derived scFv domain as the antigen recognition site. Preliminary data suggests that the tMUC1 CAR engineered T cells are capable of recognizing and killing tMUC1 expressing triple negative breast

cancer cells while ignoring the normal cells. Here, we hypothesize that tMUC1-CAR engineered T cells can be effective in treating human PDA model.

PDA is an immunologically cold tumor with known resistance to a variety of therapies including immunotherapy [172]. Thus, it was not surprising that we found that some of PDA cells were refractory to tMUC1-CAR T cell treatment. Gene expression profile of resistant vs. sensitive PDA cells revealed the overexpression of several genes associated with immune tolerance such as IDO1, COX1/2, ADAR1, and Gal-9. Thus, we hypothesized that blocking the above proteins can overcome the immune tolerance of resistant PDA cells to tMUC1-CAR T cell therapy. We suggest combination therapy of tMUC1-CAR T cells with biological inhibitors of resistance inducing genes will result in enhancement of tMUC1-CAR T cell cytotoxicity against resistant PDA cells.

1.7.2 Aims

This PhD thesis was performed in order to achieve the following aims:

- 1) Testing *in vitro* the cytolytic efficacy of CAR-T cells in a panel of human PDA cells.
- 2) Testing the anti-tumor efficacy and toxicity of CAR-T therapy *in vivo* in relevant models of PDA.
- 3) Developing a combinatorial immunotherapeutic strategy to treat resistant PDA and enhance survival.

CHAPTER 2: *IN VITRO* CHARACTERIZATION OF TMUC1-CAR T CELLS

In this chapter CAR T cells characteristics in *in vitro* models will be discussed. Different CAR constructs that were used in this project will be explained. After confirming CAR expression on the T cells, they were tested against PDA cells. For CD8+ CAR T cells to exert their cytotoxicity effect, binding to the target cells is require. Therefore, we investigated CAR T cells binding to the MUC1 expressing PDA cells. Cytotoxicity of CAR T cells against a large panel of PDA cells as well as normal primary cells was examined. Most PDA cells showed reduction in survival after treatment with tMUC1-CAR T cells, however normal cell were intact. We then investigated the mechanism of CAR T cells activation and killing by measuring the important cytokines.

2.1 Materials and Methods

2.1.1 Cells Cultures

All the PDA cell lines used in this study were originally purchased from American Type Culture Collection (ATCC, Manassas, VA 20110, USA) and cultured as instructed. All cells were cultured in a humidified incubator at 37°C containing 5% CO₂ in air. HPAFII cells were cultured in complete MEM media (Gibco). Capan-2, BxPC3-MUC1 and -Neo cells were cultured in complete RPMI (Gibco). All other PDA cell lines were cultures in complete DMEM (Gibco). Primary T cells were derived from human peripheral blood mononuclear cells (PBMCs), which were bought from STEMCELL Technologies (Cambridge, MA #70025.1). Normal human fibroblasts and breast epithelial cells were obtained from Coriell Institute (NJ, USA). The BxPC3-MUC1 cell line was made by retroviral transfection of BxPC3 wild type (ATCC) with the PLNCX.1 plasmid (Mayo Clinic K1060-C), which contains the full-length human MUC1 gene.

BxPC3-Neo was made by retroviral transfection of BxPC3 wild type with the empty vector PLNCX.1 plasmid.

2.1.2 CAR Constructs and Cloning

A second generation anti-MUC1 CAR harboring TAB004 antibody scFv was synthesized by subcloning the scFv from TAB004 [63] into the SFG-based retroviral backbone plasmid encoding the transmembrane and intracellular domains of CD28 and CD3 ζ (synthesized by Dr. John Maher's group [144]). This CAR contains a myc tag for detection. The CAR-mKate construct was made by cloning PCR-amplified tMUC1-CAR sequence into the PLNCX.1 retroviral vector (Mayo Clinic K1060-C) at the MluI site along with the mKate2 sequence fused through a GA linker. The mKate2 gene (pFA6a-mkate-kanmx6) was a gift from Dr. Richard Chi. CTL-CAR was created by PCR cloning of CAR in three fragments missing the majority of the TAB scFv sequence. All cloning was done using NEBuilder® HiFi DNA Assembly Cloning Kit (NEB #E5520). PCRs were done using Q5® High-Fidelity DNA Polymerase (NEB #M0491).

2.1.3 Retroviral Packaging System

A critical step in the generation of CAR T cells is the genetic modification of T-lymphocytes to stably express the CAR construct of interest. This was achieved by delivering a retroviral vector that carries the CAR transgene into pre-activated T cells. The retroviral vector is delivered to the cells by appropriately pseudotyped viral particles produced by retroviral packaging cell lines.

Retroviruses are considered useful tools in the field of gene therapy as they have the ability to integrate their genome into the DNA of a host cell. Retroviral virions include two copies of single-stranded RNA consisting of at least four genes, gag, pol, pro and env 299,300. Each of these genes encode for viral proteins with different function. Gag encodes for the structural proteins necessary for the viral core. Pol encodes for integrase, RNA H and reverse transcriptase. Env directs

expression of the proteins related to the viral envelope and lastly, pro encodes for protease which is responsible for the processing of gag and pol proteins 300.

Infection of the host cell by retroviruses is initiated when the glycoproteins of the viral envelope attach to their receptors on the surface of the host cell. Upon recognition, the viral envelope is fused with the cell membrane and the viral RNA is released to the cytoplasm 301. A viral protein, named reverse transcriptase, converts the viral RNA into double-stranded DNA (dsDNA) which is then transferred inside the host cell nucleus. The next step is the integration of dsDNA to the host cell genome in order to form the provirus. This process occurs in an almost random manner throughout the host cell genome. The integrated provirus is then transcribed to yield mRNA that encodes for viral proteins, a process mediated by RNA polymerase II. The mRNA is exported from the nucleus and is translated by the host T cell translation machinery. These translated proteins are further processed by a viral protease and are encapsulated into viral particles. The newly formed viral particles exit the infected cell through a process known as budding 303 (The retroviral life cycle is summarized in figure 11).

In this project, we used GP2-293 packaging cell line to produce retroviral particles containing CAR genes. GP2-293 is a HEK 293-based retroviral packaging cell line. The essential viral packaging genes gag and pol are stably integrated, the viral envelope must be supplied in trans. High titer retrovirus is produced by transient co-transfection of an MMLV- or MSCV-based retroviral expression vector and a plasmid that expresses a viral envelope, such as pVSV-G.

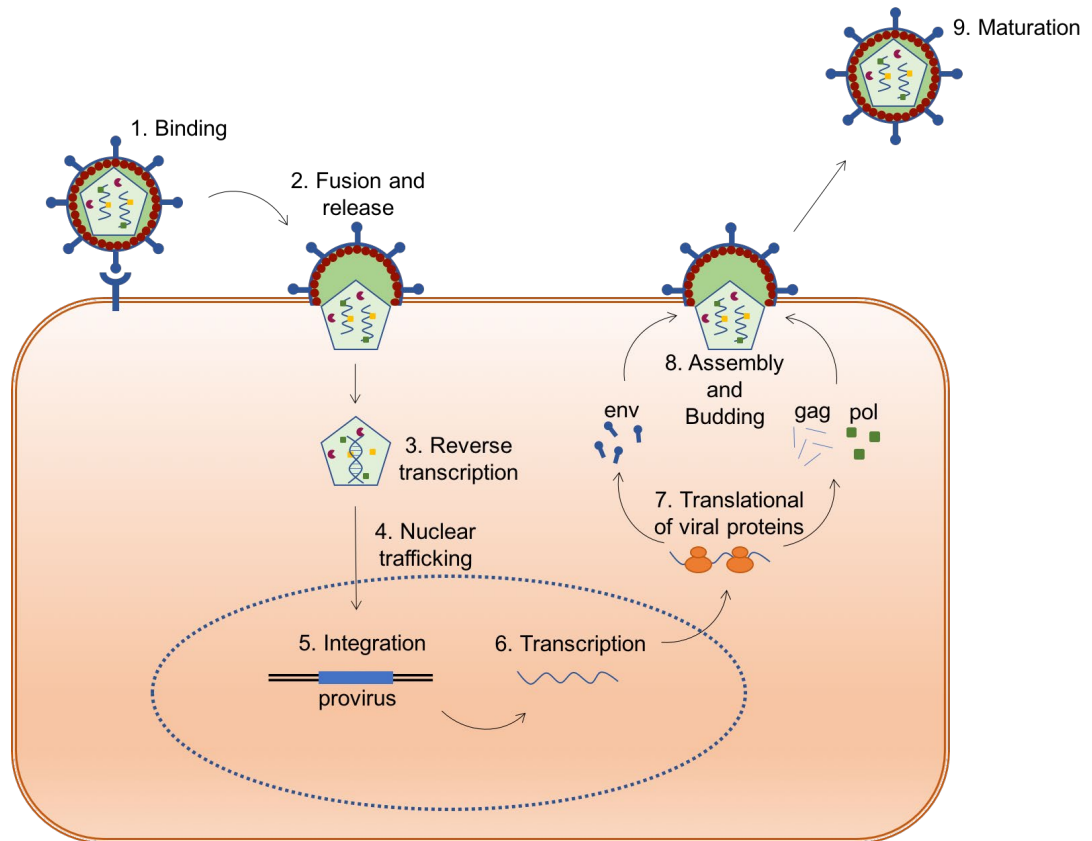


Figure 11. Life cycle of retrovirus. Infection of the host cell by the retrovirus begins when the viral envelope proteins bind to their receptors on the host cell membrane (1). The viral and cell membranes are fused and the capsid including the ssRNA is released into the cytoplasm (2). ssRNA is reverse transcribed to cDNA (3) and is transported to the nucleus upon mitosis (4). Viral cDNA is integrated to the host cell DNA, thus forming the provirus (5). Provirus is transcribed to mRNA by the host cell's transcription machinery (6). The latter is translated, leading to the production of viral proteins (7). The latter are further processed by viral protease and subsequently are encapsulated together with new viral RNA in order to form new viral particles. The newly formed viral particles exit the host cell via budding (8) and they undergo maturation in order to initiate the infection of a host cell (9).

2.1.4 Viral Transfection of T Cells

Retroviruses were generated by transduction of GP2-293 packaging cell line with 10ug CAR DNA and pVSV envelope plasmid. Viral supernatant (48h post transduction) was used to infect T

cells. Human PBMCs were cultured in RPMI supplemented with IL2 (100-300IU/ml), and activated by CD3/CD28 beads (Dynabeads, Gibco #111.61D) 3 days prior to infection. Non-tissue culture plates (Corning #351146) were coated with retronectin (1mg/ml) (Takara, Mountain View, CA) and incubated at 4 °C at least 12 hrs before infection. The following day, retronectin was removed and the plates were blocked with 2% BSA for 30 minutes. Viral supernatant was added to retronectin-coated plates, which were subsequently centrifuged at 2000g for 2 hrs at 32 °C. Viral supernatants were removed and activated T cells were added to the coated plates. IL-2 was added at 100-300 IU/ml concentration. Plates with cells were spun at 1000g, at 32 °C for 10 min and incubated overnight. Cultures were maintained in complete RPMI with 100-300 U/ml human recombinant IL-2 (PeproTech, Rocky Hill, NJ #200-02) and media was refreshed every 3 days. To avoid T cell exhaustion, from day 10 onward cultures were maintained at 50 U/ml IL-7 and IL-15 (PeproTech, Rocky Hill, NJ #200-07). T cells that had been activated but not transduced were used as mock T control. CAR expression level was characterized by flow cytometry using anti-myc tag Ab, and T cells were used between days 11 to 14 days post infection.

2.1.5 Flow Cytometry

The CAR expression level was quantified using myc tag-FITC staining (Cell Signaling Technology, Danvers, MA). T cell subtypes were determined by staining for CD4-PE/Cy7 and CD8-eF450 (BD Biosciences, San Jose, CA). PD1-APC (eBioJ105), IFN- γ -APC (clone 4S.B3) and perforin-PE (clone dG9) Abs were obtained from eBioscience. The human tMUC1 expression on PDA cells was measured by staining with TAB004 primary antibody (provided by OncoTab Inc., Charlotte, NC) and FITC-anti-mouse secondary antibody (Invitrogen #31535). Dead cells were excluded by 7-AAD staining (BD Biosciences #555816). Data were acquired on BD LSR Fortessa flow cytometer (BD Biosciences) and analyzed using the FlowJo software (version 8.8.7, Tree Star Inc).

2.1.6 Binding Assay

HPAFII, a moderate-to-high MUC1-expressing PDA cell line was plated in 6 well plates (150,000 cells/well) and incubated at 37 °C overnight. Next, the cells were stained with nuclei live cell stain Hoechst (Thermo Fisher #33342) for 30 minutes and washed 3X. 1×10^6 CAR T cells or CTL T cells (both expressing CAR constructs fused to mKate fluorescent tag) were added to the respective wells and cocultures were incubated at 37 °C for 4 hrs with occasional rocking. Cells were washed 2X and imaged using the DeltaVision workstation (Applied Precision). Texas Red and DAPI channel were used to detect CAR T cells and cancer cells respectively.

2.1.7 Imaging

1×10^6 CAR T cells expressing CAR-mKate were plated in 35 mm Poly-d-lysine Coated MatTek dish (MatTek #P35GCOL-0-14-C) for 24 hrs. The next day, cells were stained with nuclei live cell stain, Hoechst (Thermo Fisher #33342) for 30 minutes and washed gently once, then imaged by DeltaVision workstation (Applied Precision). Image analysis was done using Softworx 6.1 (Applied Precision Instruments).

Videos of CAR T cells killing BxPC3-MUC1 vs. BxPC3-Neo cells were taken by time lapse imaging using a DeltaVision OMX-SR imaging system (GE #29115476). Cancer cells and CAR T cells were co-cultured in 35 mm MatTek dish and placed in the microscope's 37 °C 5% CO₂ incubator overnight. Images were taken over the course of 8 hrs at 7 min intervals. PI dye was added to the culture at 50 ng/ml [173]. Only apoptotic cells are susceptible to PI infusion, and turn red upon absorption. Pictures were analyzed using ImageJ v1.51f program (Rasband).

2.1.8 T Cell Cytotoxicity

2.1.8.1 MTT Assay

To test T cell cytotoxicity against target cells, 5,000-10,000 cancer cells or normal cells were plated in triplicate in 96 well plates one day prior to co-culture. Mock or CAR T cells were counted and added to cancer cells at the indicated target to effector (T:E) ratio. Cell viability was evaluated by MTT assay (MTT 500 ug/ml, Sigma) 24, 48, and 72 hrs after co-culture according to the product instructions. The MTT assay is a colorimetric assay for assessing cell metabolic activity. It is based on the ability of nicotinamide adenine dinucleotide phosphate (NADPH)-dependent cellular oxidoreductase enzymes to reduce the tetrazolium dye MTT to its insoluble formazan, which has a purple color. NADH-dependent cellular oxidoreductase enzymes may reflect the number of viable cells present. Briefly 100ul MTT (0.5mg/ml) was added per well in a 96w plate. Plates were then incubated for 2-4 hrs in 37' incubator. Next, MTT was removed using aspirator and 200ul DMSO was added to the wells to dissolve the formazan crystal formed by MTT. Then, plates were incubated at 37' for 10 min, and the OD value at 540 nm was read. The percentage survival was calculated as $100 - [(mock\ T\ OD - CAR\ T\ OD) / mock\ T\ OD \times 100]$.

2.1.8.2 CytoTox 96® Non-Radioactive Cytotoxicity Assay

To measure direct cytotoxicity activity of the CAR T cells, a lactate dehydrogenase (LDH)-based technique, CytoTox 96® Non-Radioactive Cytotoxicity Assay (Promega, USA) was used. The CytoTox 96® Non-Radioactive Cytotoxicity Assay is a colorimetric alternative to ⁵¹Cr release cytotoxicity assays. The CytoTox 96® Assay quantitatively measures LDH, a stable cytosolic enzyme that is released upon cell lysis, in much the same way as ⁵¹Cr is released in radioactive assays. The half-life of LDH that has been released from cells into the surrounding medium is approximately 9 hours. Released LDH in culture supernatants is measured with a 30-minute

coupled enzymatic assay, which results in the conversion of a tetrazolium salt (iodonitrotetrazolium violet; INT) into a red formazan product. The amount of color formed is proportional to the number of lysed cells. Visible wavelength absorbance data are collected using a standard 96-well plate reader. BxPC3-Neo and BxPC3-MUC1 cells were plated in 96 well plate (20,000 cells/well) and incubated with 200,000 mock or CAR T cells (T:E 1:10) for 8, 16 and 24 hrs.

The four controls listed below must be performed with CytoTox 96® cell-mediated cytotoxicity assays. Controls #2 and #3 are identical to those in a standard 51Cr release assay (target cell spontaneous release and target cell maximum release). The three additional controls account for LDH activity contributed from other sources.

1. Effector Cell Spontaneous LDH Release: Corrects for spontaneous release of LDH from effector cells.
2. Target Cell Spontaneous LDH Release: Corrects for spontaneous release of LDH from target cells.
3. Target Cell Maximum LDH Release: Required in calculations to determine 100% release of LDH.
4. Culture Medium Background: Corrects for LDH activity contributed by serum in culture medium and the varying amounts of phenol red in the culture medium.

The amount of released LDH and subsequent cytotoxicity was measured and calculated as follow.

$$\% \text{ Cytotoxicity} = \frac{\text{Experimental} - \text{Effector Spontaneous} - \text{Target Spontaneous}}{\text{Target Maximum} - \text{Target Spontaneous}} \times 100$$

2.1.9 ELISA

ELISA (enzyme-linked immunosorbent assay) is a plate-based assay technique designed for detecting and quantifying substances such as peptides, proteins, antibodies and hormones. A capture antibody on the multi-well plate will immobilize the antigen of interest. This antigen will be recognized and bound by a detection antibody conjugated to biotin and streptavidin-HRP. The final HRP mediated reaction results in a colored end product which correlates to the amount of protein present in the sample.

The supernatant of PDA cells co-cultured with T cells was assessed for released IFN- γ and granzyme B after 72 hrs of co-culture, using the human IFN- γ ELISA Kit (Life Technologies 88-7316-22) and human Granzyme B DuoSet ELISA (R&D DY2906-05). Shed MUC1 was measured using human MUC1 ELISA kit (OncoTAb Inc., Charlotte, NC). All of the ELISAs were performed on the supernatant after 72 hrs of co-culture.

2.1.10 Statistical Analysis

All of the data were analyzed by Prism (version 8.0; GraphPad Software) and results presented as mean \pm SEM. Data are representative of two or more independent experiments. The statistical significance was determined using unpaired Student's t-test, two-way ANOVA, or Non-parametric Mann-Whitney U test where indicated (*, $p < 0.05$, **, $p < 0.01$, ***, $p < 0.001$).

2.2 Results

2.2.1 CAR Architecture

The architecture of CAR constructs used in this study is illustrated in figure 12 and 13. TAB004 Ab's variable fragments are cloned into a 2nd generation CAR plasmid (SFG muT4 vector backbone) containing CD28 and CD3 ζ genes (tMUC1-CAR). To test specificity of the tMUC1-

CAR, we generated a control CAR (CTL-CAR), in which TAB004 scFv sequence is removed. T cells expressing CTL CAR construct is referred to as CTL T. Furthermore, to visualize surface expression of CAR constructs on T cells, we generated mKate fluorescent-tagged CARs named CAR-mKate and CTL-mKate, in which mKate2 gene is fused to the C terminus of CD3 ζ in tMUC1-CAR and CTL-CAR respectively. We also used uninfected T cells (designated as mock T cells) as another control.

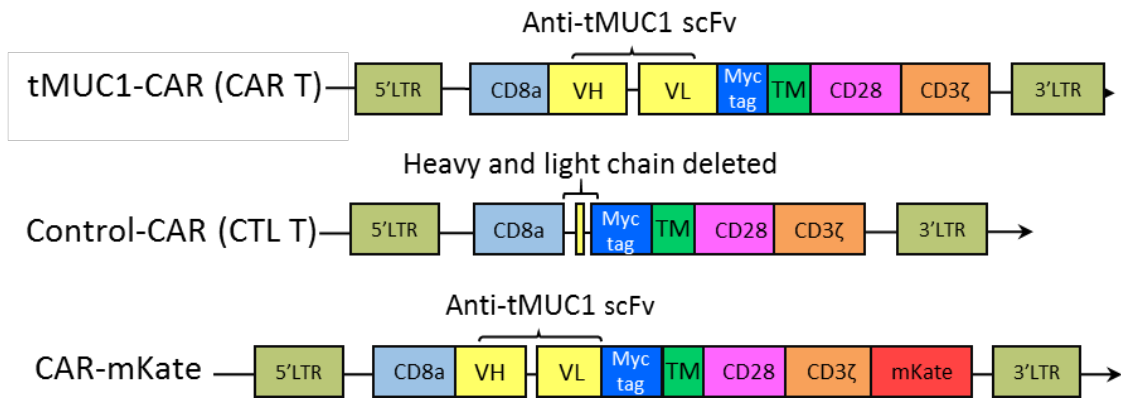


Figure 12. Different CAR constructs used in this study. Their name and gene sequences are shown. tMUC1-CAR construct consists of CD8a leader peptide, TAB004 derives scFv, a myc tag, followed by CD28 transmembrane domain (TM), CD28 and CD3 ζ endodomains. CD8a leader sequence was used as signal peptide for cell membrane expression of the CAR. Myc tag was incorporated for detection purposes. The CAR genes are placed between the two LTRs of retroviral plasmid. The second construct, CTL CAR has the same structure except missing the majority of the VH and VL sequence of TAB004 scFv. The third construct, CAR mKate is similar to the original construct, except having a florescent tag (mKate) fused to C terminus of the CAR molecule for visualizing purposes.

2.2.2 CAR Expression on Engineered T Cells

Initially, the presence of CAR gene in viral particles was confirmed using RT-PCR. Viral supernatant was collected at day 2 and day 6 after transduction and RNA was extracted. Then, RT-PCR was done on mRNA using primers reading the sequence of light and heavy chains in

human CAR plasmid (6667-6893). Product size expected was 226bp. Figure below depicts the results. Bands with size 226 base pair indicates amplification of the CAR genes at scFv domain (figure 14).

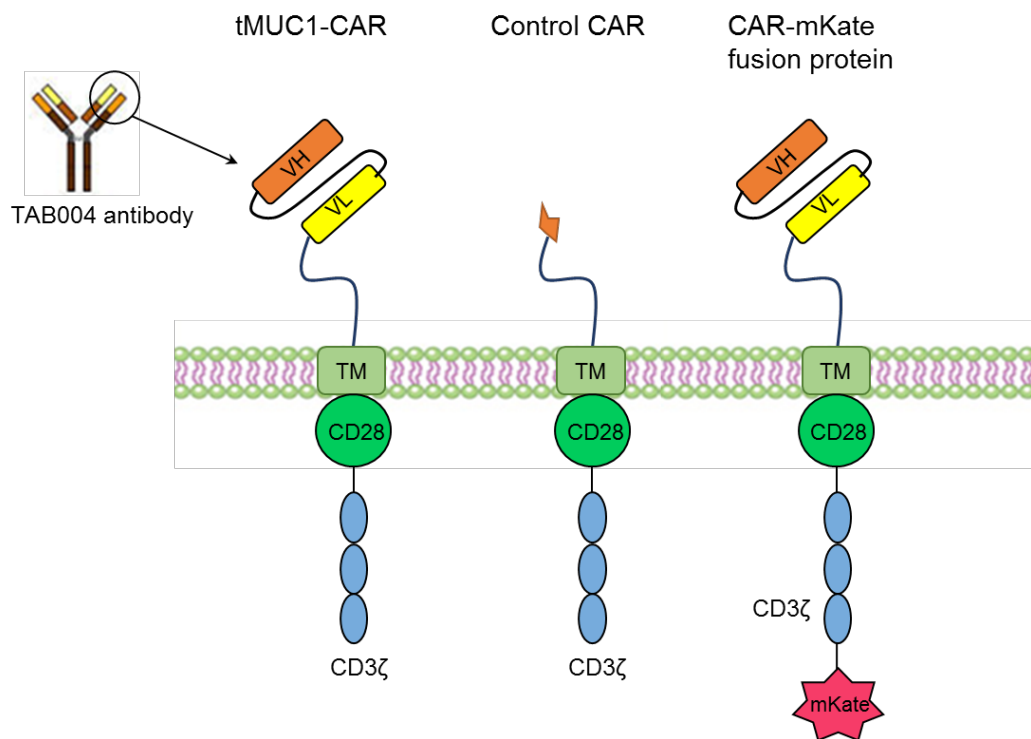


Figure 13. CAR structure on the engineered T cells membrane. The schematic of three different CAR constructs used in this study are shown. In the original construct (tMUC1-CAR), scFv of TAB004 antibody is linked to CD28 transmembrane (TM) domain followed by CD28 and CD3ζ intracellular domains. In the CTL-CAR construct, scFv of TAB was removed so that there is no antigen recognition site in the extracellular domain. In the CAR-mKate fusion construct, mKate2 gene was fused to the C-terminus of CAR flanking with a GA linker.

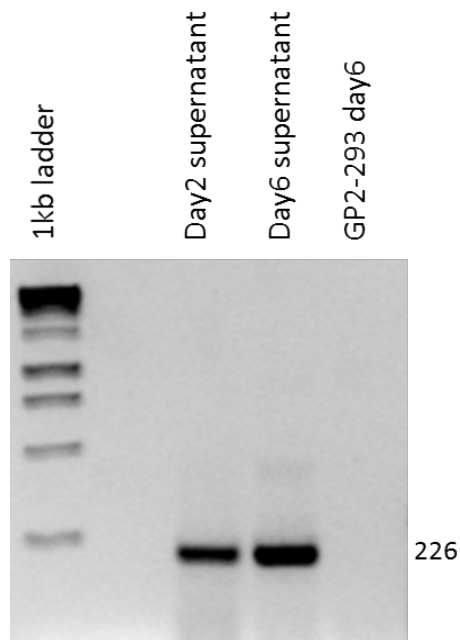


Figure 14. RT-PCR on mRNA isolated from CAR viral particles. Primers reading TAB004 scFv sequence in CAR DNA was used and the expected band size of 226bp is observed.

Next, human primary T cells were infected with the CAR viral supernatant and the CAR expression was monitored at 48 hrs onward. The representative dot-plot graphs show ~42% myc tag positive cells in both CD4+ and CD8+ human primary T cells by day 12 after infection (figure 15). CAR surface expression on T cells was visualized using DeltaVision microscopy. Bright field and florescent images of the entire population of CAR-mKate expressing cells are shown in figure 16 (top panel). The projection image (bottom left), and a single z stack image (bottom right) of the CAR T cell is shown in figure 16 (bottom panel). Cell nuclei were stained blue with live cell stain Hoechst. A distinct red ring indicates CAR expression on the cell surface and confirms even distribution of CAR across the cell membrane, with no significant irregular patch or co-localization (figure 16 bottom right).

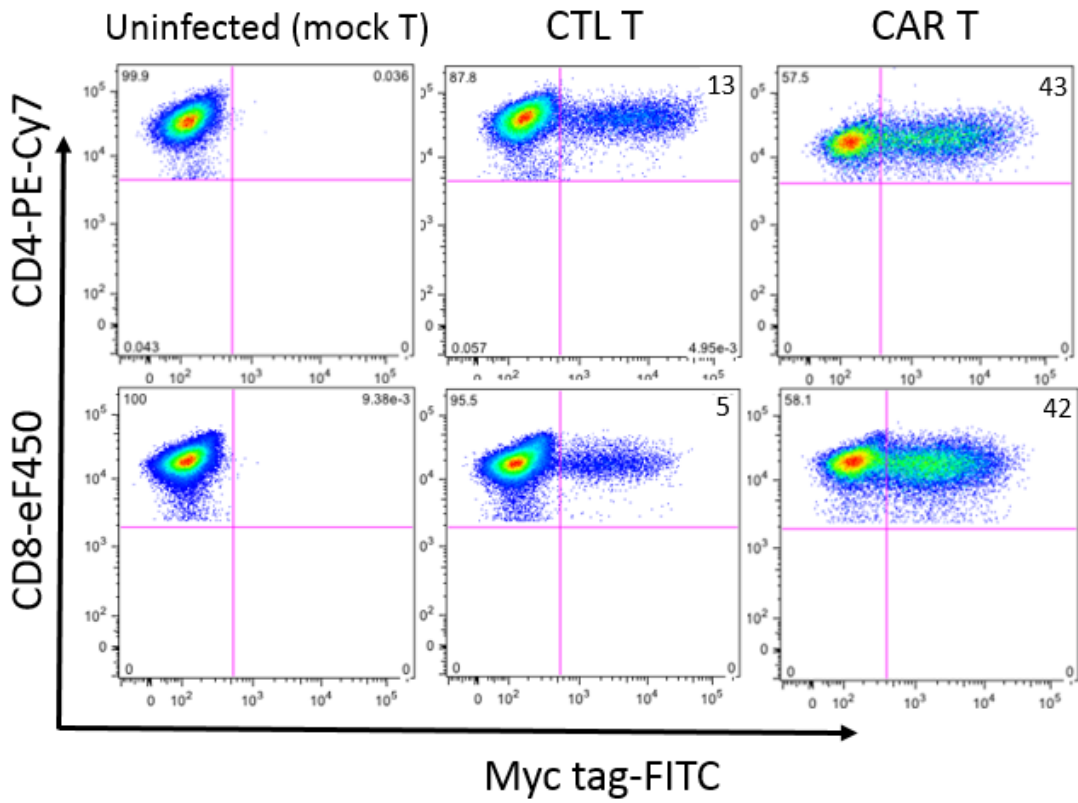


Figure 15. CAR expression on human primary T cells detected by flowcytometry. The representative dot-plot graphs resulted from flowcytometry data showing the CAR expression on human primary T cells. CTL-CAR and tMUC1-CAR expression was measured by flow cytometry using FITC-conjugated anti-myc tag antibody, in CD4+ and CD8+ primary T cells on day 12 after infection. On average 43% of human primary T cells (both CD4+ and CD8+) expressed tMUC1-CAR and up to 13% expressed CTL CAR on day 12 after infection.

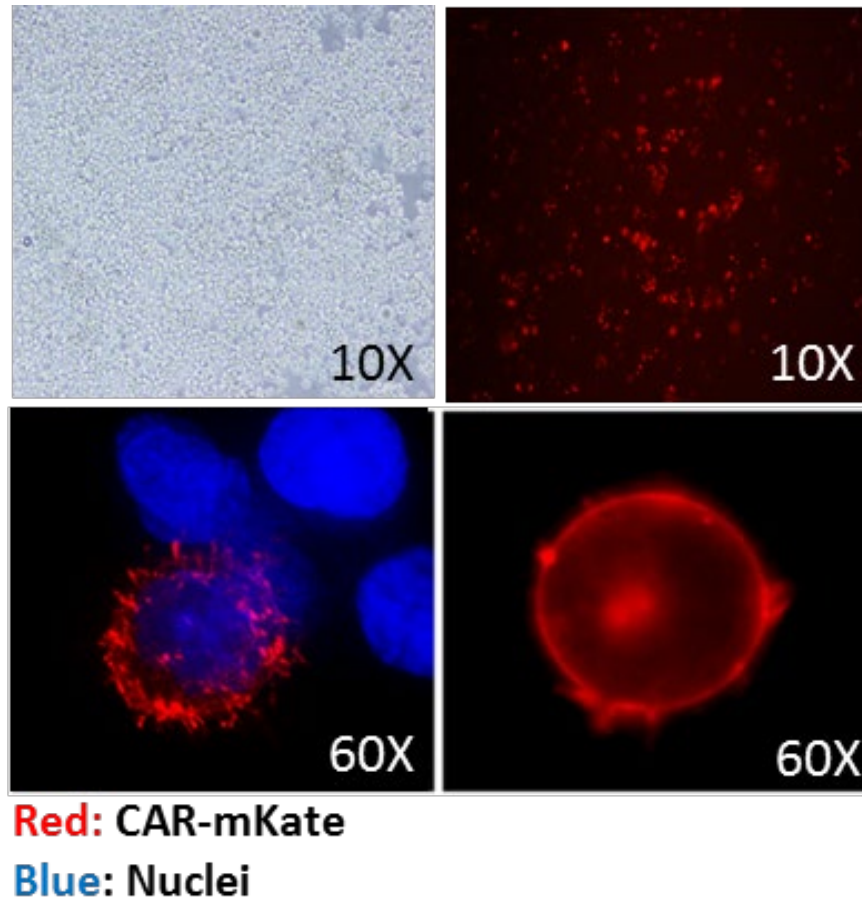


Figure 16. Fluorescent tagged-CAR (CAR-mKate) expression on T cells. Bright field (top left) and fluorescent image (top right) of live T cells expressing CAR-mKate plated in 35mm poly-D-lysine coated MatTek dish and imaged by DeltaVision workstation (Applied Precision). Red signal indicates CAR T cells. Projection image of a T cell expressing CAR-mKate (bottom left), and one Z image of the CAR-mKate T cell (bottom right) illustrating the ring-like structure around the cells formed by CAR-mKate expression, which indicates even distribution of CAR molecules on the T cell membrane. Nuclei were stained with Hoechst nuclei blue dye.

2.2.3 tMUC1-CAR T Cells Binding to Target PDA Cells

We have previously shown that TAB004 antibody can detect tMUC1 in >85% of malignant PDA tissues [66]. To test binding of tMUC1-CAR T cells to PDA cells, CAR-mKate engineered T cells were co-cultured with MUC1 expressing PDA cell line (HPAFII) for 4 hrs and imaged using

DeltaVision microscope. Strong binding to the target HPAFII cells is observed (figure 17); however, when CTL-mKate engineered T cells were co-cultured with the same target cells, no binding to target cells was observed (data not shown). A close up image at the red spots revealed an intensified red signal where CAR T cell binds HPAFII cells, verifying co-localization of CAR molecules at the site of contact. This localization suggests formation of an immunologic synapse between the CAR T cell and target cell which is required for cytolytic activity of the CD8⁺ CAR T cells (figure 17).

2.2.4 tMUC1-CAR T Cells Show Robust Cytotoxicity Against PDA Cells

A panel of human PDA cell lines were used that expressed varying levels of MUC1. BxPC3 cells overexpressing full-length MUC1 (BxPC3-MUC1) or vector alone (BxPC3-Neo) were included to further determine if CAR T cell cytotoxicity was dependent on antigen expression. Expression level of MUC1 gene and protein was assessed using RT-PCR and flowcytometry (figure 18A and B) respectively. Cells were categorized into three groups of low MUC1, moderate to high MUC1 and high MUC1 according to flowcytometry data (figure 18B). According to RT-PCR and flowcytometry data, most PDA cell lines express some level of MUC1. Jurkat cell line was used as negative control for MUC1 gene expression in RT-PCR. Human pancreatic normal epithelial cell line, HPDE (H6c7) was used as negative control in flowcytometry and cytotoxic assays. CTL T and uninfected T cells showed similar cytotoxic activity against target cells (figure S1A); therefore, uninfected T cells (designated mock T) were used as control for all cytotoxic assays.

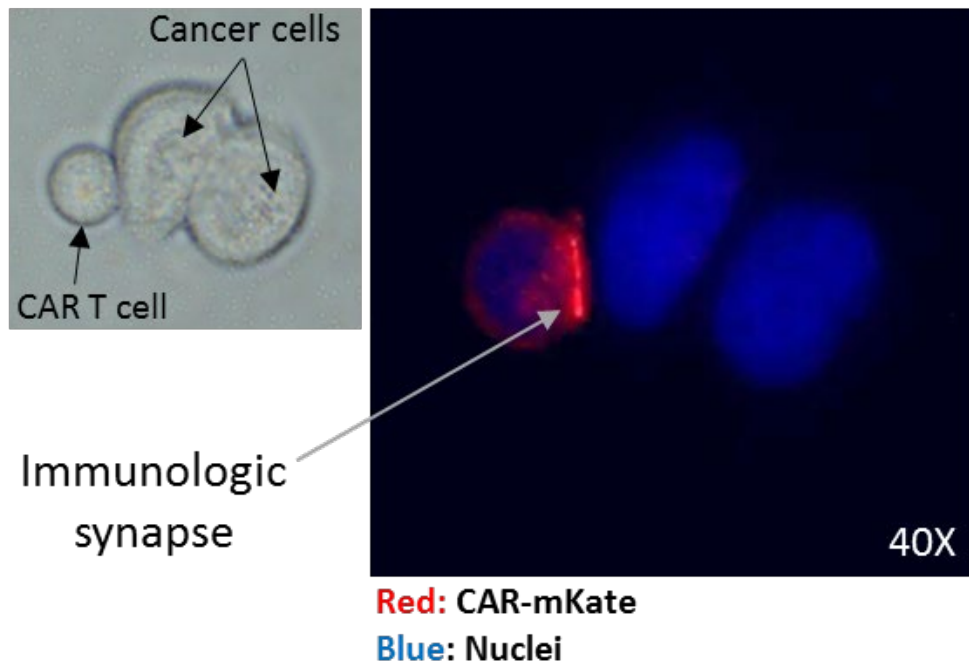
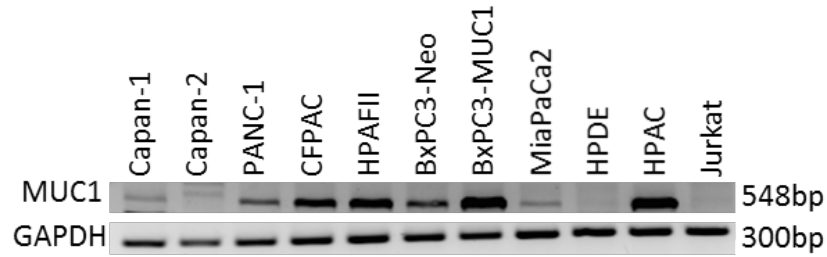


Figure 17. Light and fluorescent image of CAR-mKate T cells binding to MUC1 expressing cancer cell. HPAFII cells were incubated with CAR-mKate T cells for 4 hours, then T cell were removed, HPAFII cell was washed and imaged using DeltaVision microscope. The intense red signal observed between CAR T cell and HPAFII indicates co-localization and strong binding of CAR molecules, which suggests formation of immunological synapse. Nuclei were stained with Hoechst nuclei blue dye.

A



B

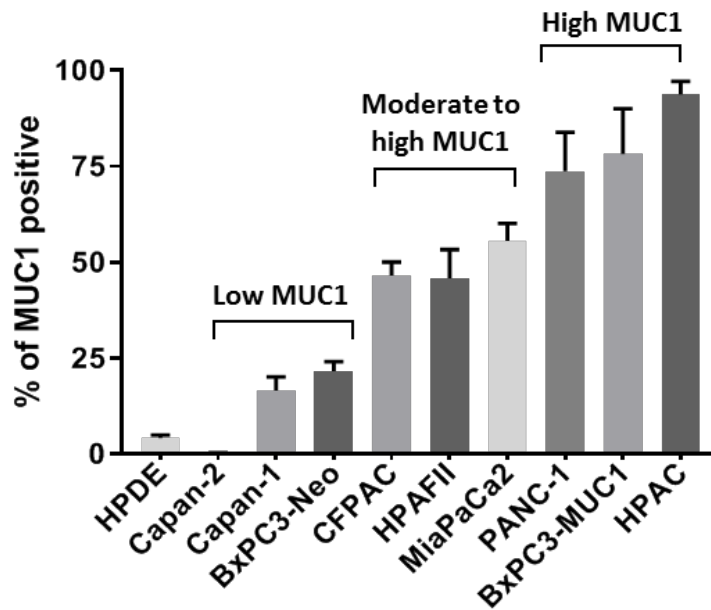


Figure 18. MUC1 level in PDA cells. A. Human MUC1 mRNA level in a panel of human PDA cells lines acquired by RT-PCR. Jurkat cell line was used as negative control for MUC1 gene expression in RT-PCR B. Surface MUC1 expression in a panel of PDA cell lines detected by TAB004antibody staining and flow cytometry. Most PDA cell lines express some level of MUC1. Human pancreatic normal epithelial cell line, HPDE was used as negative control in flowcytometry. PDA cells were categorized into three groups of low MUC1, moderate to high MUC1 and high MUC1 according to flowcytometry data. MUC1 expression was normalized to isotype control. Error bars, SEM.

PDA cell lines were incubated with CAR T or mock T cells for 24, 48 and 72 hrs at different Target : Effector (T:E) ratios and survival of target cells was measured using MTT assay. Percent survival was normalized to mock T cells and calculated as $100 - [(mock\ T\ OD - CAR\ T\ OD) / mock\ T\ OD \times 100]$. Figure 19A shows the percentage of surviving target cells 72 hrs post T cell treatment at T:E ratio of 1:10. Majority of the tested PDA cells were efficiently killed by CAR T cells especially the high MUC1 and moderate to high tMUC1-expressing cells (80-95% killing) except for HPAFII and CFPAC (~20% and 50% killing). Interestingly, one of the low tMUC1-expressing cell line, Capan-1 also responded well to CAR T cell cytotoxicity. The normal pancreatic cell line, HPDE, showed 100% survival post co-culture with CAR T cells.

The sensitivity of the PDA cells to CAR T cell killing cannot be accurately compared between the different cell lines, since each cell line has distinct genetic makeup, which endows them different intrinsic resistance levels. To investigate this, we used BxPC3-MUC1 and BxPC3-Neo cells, which are identical in all aspects except for their MUC1 level. As shown in figures 19A, B and C, BxPC3-MUC1 cells are significantly more sensitive to CAR T cell killing as compared to BxPC3-Neo cells. At a T:E ratio of 1:10 (figure 19A), ~100% of BxPC3-MUC1 cells are killed by CAR T cell treatment while ~50% of BxPC3-Neo cells are killed. This 50% killing with a high T:E ratio (1:10) in BxPC3-Neo cells was possibly because of the existing endogenous MUC1 expression in these cells (figure 18, 19A). However, the killing effect was completely negated when T:E ratio was lowered to 1:5 (figure 19B). The cell survival data was further confirmed using a different cell cytotoxicity assay (CytoTox 96® Non-Radioactive Cytotoxicity Assay). Percent cytotoxicity of CAR T cells/mock T cells show significant killing of BxPC3-MUC1 but not BxPC3-Neo cells (figure 19C). Taken together, results clearly suggest a critical correlation between antigen expression levels and efficacy of CAR T cells. Next, we evaluated whether the efficacy of CAR T cell killing is dose dependent. Indeed, increasing ratio of CAR T cells to target PDA cells resulted in dose dependent killing of the target cells (figure 19D). CAR T cells had no effect on normal

pancreatic epithelia cells (HPDE) at 1:5, 1:10 or 1:20 T:E ratio while the same CAR T cell effectively killed the high-MUC1 expressing PDA cell lines, at all T:E ratios (figure 19D).

2.2.5 tMUC1-CAR T Cells Do Not Harm Normal Cells

Lastly, we tested if tMUC1-CAR T cells kill other normal epithelial cells or fibroblasts. We performed the same cell survival assay using eight different primary cells as targets (granted from Coriell institute) at a 1:10 T:E ratio and 72 hrs incubation with CAR T cells. Three fibroblasts from three different tissue origins and 5 breast epithelial cells (from mammoplasty) derived from different healthy donors were tested. All normal cells showed 100% survival when exposed to CAR T cells for 72 hrs (figure 20). These data suggest that the tMUC1-CAR T cells are non-toxic toward normal cells while robustly killing most PDA cell lines. This is of utmost importance since CAR T cell toxicity in patients with epithelial tumors has raised major concerns.

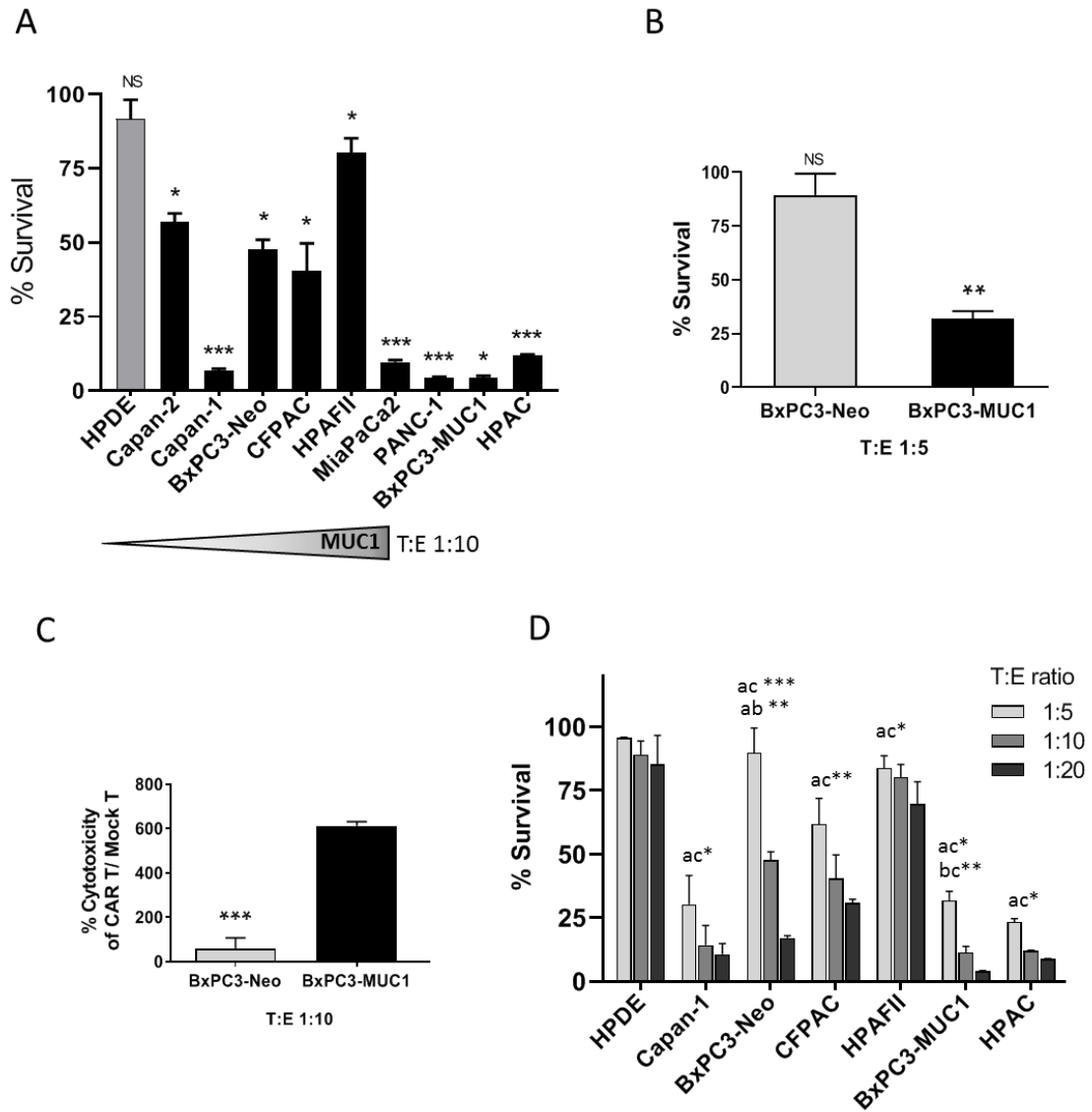


Figure 19. tMUC1-CAR T cells show robust cytotoxicity against PDA cells. A. Percentage survival of 9 PDA cell lines when treated with CAR T cells measured by MTT assay. Percentage survival of cancer cells treated with CAR T cell was normalized to the mock T cell (uninfected). Cancer cells are ordered from low to high MUC1 (left to right). HPDE cell was used as normal control cell line. T:E ratio of 1:10 and 72 hrs incubation was applied to all cell lines. All PDA cells show significant reduction in survival after treated with CAR T cells. Significance is determined between CAR T cell vs. mock T cell treated for each cancer cells. B. The percentage survival of BxPC3-Neo and BxPC3-MUC1 treated with CAR T cells for 72 hrs at T:E ratio of 1:5. BxPC3-Neo stays intact when treated with low dose of CAR T cells (T:E 1:5), while BxPC3-MUC1 is effectively killed. Significance is determined between CAR T cell vs. mock T cell treated for each cells. C.

Spontaneous killing of BxPC3-MUC1 cells by CAR T cells within 24 hrs measured by an LDH-based technique, Cytotox assay. CAR T cells show significantly higher level of cytotoxicity against BxPC3-MUC1 cells compared to BxPC3-Neo cells. Significance is determined between BxPC3-MUC1 and BxPC3-Neo, each normalized to mock T cell. D. The percentage survival of PDA cells and normal pancreatic epithelial cell line (HPDE) when treated with different dose of CAR T cells. Data shows that CAR T cell killing is dose dependent. By increasing the dose of CAR T cells, more killing was observed in PDA cells, while the survival of normal cell (HPDE) even at T:E of 1:20 remained unchanged. Significance is determined between different T:E ratio groups (a 1:5, b 1:10 and c 1:20). All data presented is normalized to mock T cell. Two-way ANOVA-Multiple comparisons and Student's t-test were performed for determining significance. Error bars, SEM. * $p < 0.05$, ** $p < 0.01$, *** $p < 0.001$.

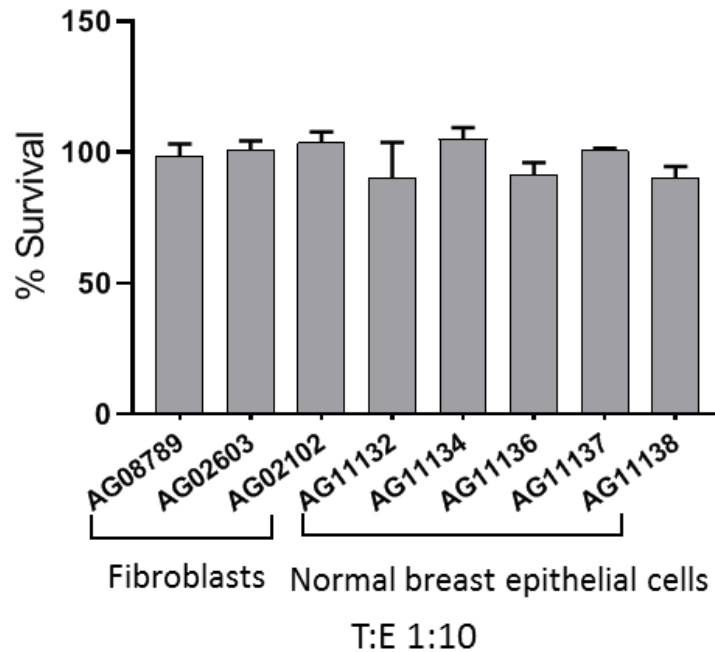


Figure 20. tMUC1-CAR T cells do not harm normal cells. The percentage survival of a panel of human normal primary cells including fibroblasts and breast epithelial cells obtained from healthy donors treated with CAR T cells for 72 hrs at T:E 1:10. There is no significant reduction in the survival level of normal primary cells when treated by CAR T cells. Significance is evaluated between CAR T cell vs. mock T cell treated for each normal cell. Two-way ANOVA-Multiple comparisons and Student's t-test were performed for determining significance. Error bars, SEM. * $p < 0.05$, ** $p < 0.01$, *** $p < 0.001$, **** $p < 0.0001$.

2.2.6 tMUC1-CAR T Cells Produce IFN- γ and Granzyme B upon Activation and Antigen Recognition

To determine the mechanism of T cell activation and function, T cells were co-cultured with target cells for 72 hrs and supernatants were tested for IFN- γ and granzyme B production by specific ELISAs (figure 21A, B). In addition, intracellular production of IFN- γ by T cells after co-culture was measured by flowcytometry (figure S1B). Results show that even before exposure to cancer cells, activated T cells produced some level of IFN- γ cytokine (intracellular and released); however, when exposed to cancer cells, IFN- γ secretion by CAR T cells significantly increased. As may be expected, ELISA data showed that higher MUC1 expressing PDA cells triggered higher levels of IFN- γ and granzyme B release by CAR T cells. CTL T and mock T cells released negligible amount of IFN- γ and granzyme B into the media even after exposure to target cells. Other controls including supernatants from a) cancer cells alone and b) Jurkat T cells, as well as c) media alone, showed undetectable amount of released IFN- γ and granzyme B by ELISA (figure 21A, B). Intracellular level of IFN γ (figure S1B) and granzyme B (data not shown) in CAR T cells post exposure to PDA cells showed similar results as the ELISA. We further tested levels of intracellular perforin in CAR T cells before and after exposure to target cells by flowcytometry and the results showed no difference between resistant and sensitive target cells (figure S1C).

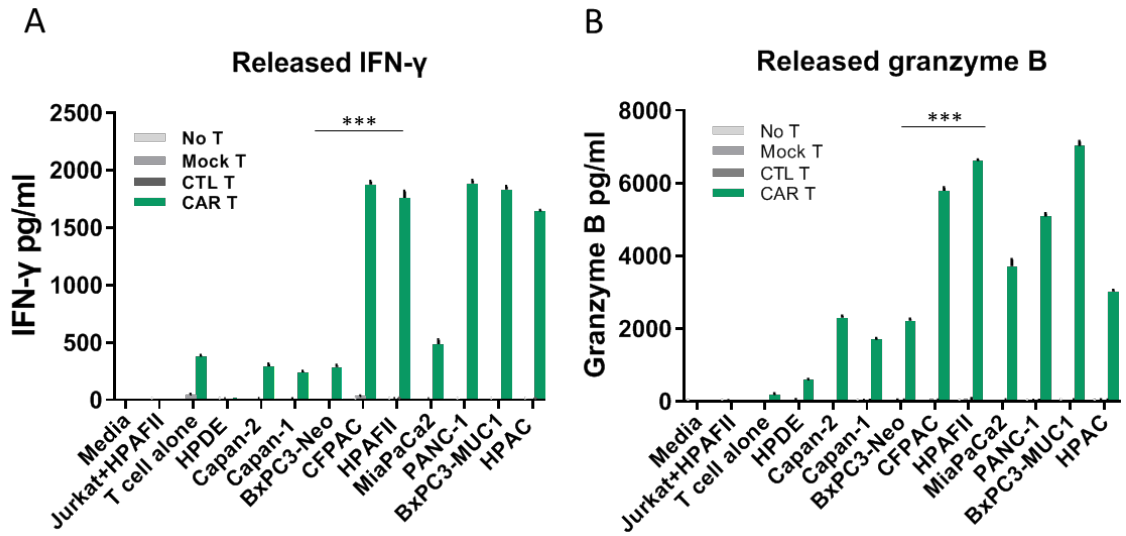


Figure 21. tMUC1-CAR-T cells produce IFN- γ and granzyme B upon activation and antigen recognition. The amount of released IFN- γ (A) and granzyme B (B) in the co-culture media of CAR T cells and cancer cells measured by sandwich ELISA. Controls include supernatant of 1) cancer cells alone, 2) Jurkat and HPAFII cells co-culture, 3) T cells alone as well as 4) media alone. The cancer cells are ordered based on their MUC1 level from left to right (low to high MUC1). tMUC1-CAR T cells exposed to cancer cells produce significant amount of IFN- γ and granzyme B, while CTL T and mock T cells exposed to cancer cells produce negligible amount of IFN- γ and granzyme B. CAR T cells exposed to normal epithelial cell line, HPDE, did not release noticeable amount of IFN- γ and granzyme B. Significance is determined by comparing CAR T vs. mock T groups for each cell line. Error bars, SEM. Student's t-test, *** P value < 0.0005 for CAR T cells vs. mock T cells.

2.3 Discussion

Recently, a MUC1 CAR T cell using the scFv from a different MUC1 antibody was shown to be efficacious against breast and pancreatic tumors [174] [146]. Our data corroborates that tumor-associated MUC1 remains a critical targetable antigen in PDA. This study differs from previously reported data in 2 major ways. 1) use of variable fragment from a highly specific tMUC1 Ab, TAB004, that does not recognize normal MUC1; and 2) testing the efficacy of the tMUC1-CAR T cell against a large panel of PDA cell lines and normal epithelial and fibroblastic cells.

CAR T cell therapy, though extremely successful in treating hematopoietic cancers, has not gained momentum in the treatment of solid tumors [95]. This is primarily because of limited selection of tumor specific antigen and a dearth of specific antibodies against them. CAR based on antibodies which recognize a shared tumor antigen such as ERBB2, have led to lethal outcomes [122]. Other MUC1 antibodies may be limited by their specificity, wherein they bind to tumor and normal MUC1. TAB004 has high specificity and binding to tMUC1 [65] and spares binding to normal MUC1. We present data that clearly shows the tMUC1-CAR T cells do not kill normal cells but effectively kill majority of tMUC1 expressing PDA cells. Recently, our group has published the effectiveness of tMUC1-CAR T cell efficacy against TNBC cells *in vitro* and *in vivo* [148]. This highlights the potency of tMUC1-CAR T cells as a potential therapy for multiple adenocarcinomas.

CHAPTER 3: *IN VIVO* EFFICACY OF TMUC1-CAR T CELLS

In this chapter, the efficacy of CAR T cells in controlling the pancreatic tumor growth in mouse model of PDA will be discussed. The procedure of establishing the PDA tumors in the pancreas as well as the treatment administrative rout will be explained. In addition, T cells infiltration into the tumor, and their persistence *in vivo* will be discussed.

3.1 Materials and Methods

3.1.1 Cell Culture

The MiaPaCa2-Luc cell line was generated by Lipofectamine transfection (Lipofectamine 3000, Invitrogen, #L3000015) of the MiaPaCa2 cell line with pGL4.50[luc2/CMV/Hygro] vector (Promega) followed by drug selection and screening for a month until a permanently transduced cell population was achieved. For drug selection, hygromycin B (50 mg/mL, Invitrogen/Life tech) was applied at a concentration of 500 ug/ml. The hygromycin B IC50 was determined by performing a kill curve experiment on MiaPaCa2 cells (data not shown).

3.1.2 Animal Study

12 female Non-obese diabetic (NOD)-SCID gamma (NOD.Cg-prkdcscidIl2rgtm1w1; NSGTM, Jackson Laboratory) mice were anesthetized. Using aseptic techniques, an incision was made in abdominal area off midline just above the pancreas. Then, pancreas was gently retracted and injected with 0.5×10^6 MiaPaCa2-Luc cancer cells. The abdominal incision was sutured and the skin layers were closed using surgical clips. Mice were monitored and their body weights were checked daily for a week. 7 days post-surgery, tumor presence was confirmed using *in vivo* imaging system (IVIS, PerkinElmer). On day 8 post-surgery, when average ROI for pancreatic tumors was 1.4×10^6 , mice were randomized into two groups (with even distribution of tumor size) based on

their baseline luminescence intensity. One group received intravenous (IV) injection of Mock T (n=6) and the other received tMUC1-CAR T cells (n=6) (10×10^6 per mouse). On day 68 post tumor injection, mice were sacrificed and tumors were harvested and weighed. Two mice (1 per group) died of irrelevant cause before the endpoints. All animal studies were approved by the Institutional Animal Care and Use Committee of the University of North Carolina at Charlotte. All the experimental procedures complied with institutional guidelines.

3.1.3 *In vivo* Imaging

Mice were imaged weekly by *in vivo* imaging system (IVIS) using chemo-luminescence, open filter setting in Living Image 4.3 software. Mice were injected intraperitoneally (i.p.) with luciferin (RediJect D-Luciferin, Perkin Elmer) at 150mg/kg body weight before imaging. Mice were imaged at 2, 5 and 8 minute after luciferin injections. Images were analyzed using Living Image 4.3 software.)

3.1.4 CAR T Cells Tracking

To assess T cell trafficking in mice after injection, mock or CAR T cells were labeled with Vivotrack-680 dye (PerkinElmer) according to the manufacturer's protocol. Six MiaPaCa2-Luc tumor-bearing NSG mice were injected with either 4×10^6 labeled CAR T or mock T cells through tail vein (n=3). Mice were sacrificed 24 hrs after injection and tumors were dissected and imaged by IVIS. Images were acquired using fluorescence Vivotrack-680 channel with excitation=676 and emission=696 nm, and analyzed using Living Image 4.3 software.

3.1.5 Immunohistochemistry (IHC)

Tumor tissues were fixed in 10% neutral-buffered formalin. Paraffin-embedded blocks were prepared by the Histology Core at the Carolina Medical Center and 4- μ m-thick sections were cut

for staining. IHC was performed as described previously [170, 175]. Briefly, the tumor sections were deparaffinized in xylene, rehydrated in a series of ethanol (100, 95 and 70%) followed by tap water and PBS, and then subjected to antigen retrieval in 99°C water bath for 40 min. The activity of endogenous peroxidases was blocked by 2% hydrogen peroxide for 15 min. The slides were washed twice in PBS and blocked with 50% FBS for 1 hr at room temperature and then incubated with primary antibody overnight at 4°C. Antibodies were prepared in 15% FBS in PBS diluent. For MUC1 staining horseradish peroxidase (HRP)-conjugated TAB004 was used at 1:375 dilution. For CD3 staining, anti-human CD3 antibody (abcam, ab16669) was used at 1:150 dilution. A HRP-conjugated secondary anti-rabbit antibody (Dako, P0448) was used for detecting CD3 antibody and incubated for 1 hr in room temperature. Subsequently, the tissues were washed twice in PBS and incubated with the substrate 3,3'-diaminobenzidine (Vector Laboratories, Burlington, CA) for 5 min, followed by counterstaining with Mayer's hematoxylin solution. The tissues were then dehydrated in a series of ethanol, immersed into xylene and mounted using Permount (Fisher Scientific). After two days, representative images were taken at ×10 magnification using light microscopy.

3.1.6 Statistical Analysis

All of the data were analyzed by Prism (version 8.0; GraphPad Software) and results presented as mean ± SEM. Data are representative of two or more independent experiments. The statistical analysis was done using Prism software and significance was determined using unpaired Student's t-test, two-way ANOVA, or Non-parametric Mann-Whitney U test where indicated (*, $p < 0.05$, **, $p < 0.01$, ***, $p < 0.001$). Significance of data was evaluated using Non-parametric Mann-Whitney U test.

3.2 Results

3.2.1 tMUC1-CAR T Cells Control Pancreatic Tumor Growth *in vivo*

To investigate the efficacy of CAR T cells in hampering tumor growth *in vivo*, orthotopic mouse model of human PDA was established by injecting 0.5×10^6 MiaPaCa2-Luc cells into the pancreas of NSG mice. Seven days post-surgery, mice were imaged using IVIS and tumor presence was confirmed. On day 8 post-surgery, mice were randomized into two groups based on their baseline luminescence intensity. One group received IV injection of mock T and the other received CAR T cells (10×10^6 per mouse) (figure 22A). Tumor growth was monitored using weekly IVIS imaging and the serial images are shown in figure 22B. Data clearly confirmed that CAR T cells controlled the tumor growth in mouse model of PDA compared to mock T treated group. On day 68 post-surgery, mice were sacrificed and tumors were harvested. Mock T cell-treated mice had significantly larger tumors than CAR T cell-treated mice (figure 22C). Many metastasis lesions were present on organs in the abdominal cavity of mock T cell-treated mice, whereas CAR T cell-treated mice had more confined tumors (data not shown). Tumor wet weights were measured and results showed significant difference between the CAR T and mock T cell treated groups (P value=0.0476, figure 22D).

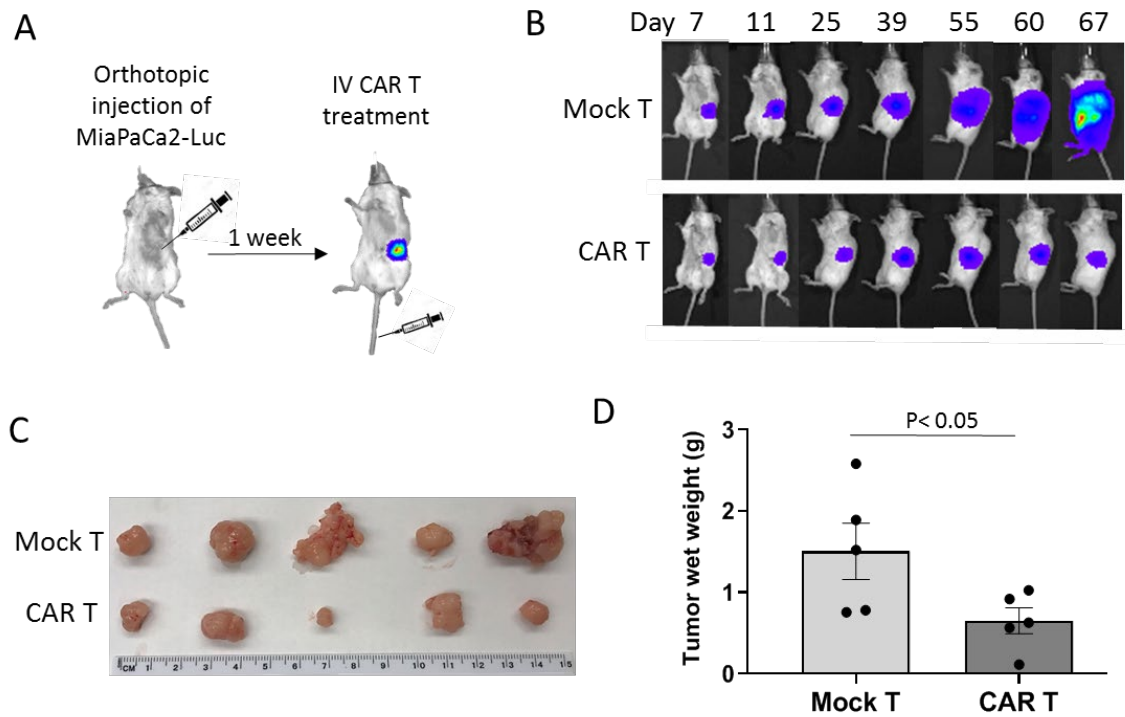


Figure 22. tMUC1-CAR T cells control pancreatic tumor growth in vivo. A. Establishing the mouse model of human PDA using orthotopic injection of MiaPaCa2-Luc cancer cells into the pancreas. 7 days post-surgery, tumor presence was confirmed using IVIS imaging. On day 8, mice were randomized into two groups and injected IV with 10×10^6 mock or CAR T cells. Images were taken 8 minute after luciferin injection using IVIS system. B. Serial IVIS images of MiaPaCa2-Luc implanted mice treated with mock or CAR T started on day 7 post tumor inoculation. One mouse per group is shown as representative of 6 mice. C. Images of the tumors harvested from mice treated with mock T or CAR T cells on day 68 post tumor inoculation. D. Tumor wet weights of the mice treated with mock T or CAR T cells on day 68 after tumor inoculation. Significance of data was evaluated using Non-parametric Mann-Whitney U test. P value=0.05 (n=5).

3.2.2 tMUC1-CAR T Cells Traffic to the Tumor Site

To see if CAR T cells can successfully traffic into the fibrotic pancreatic tumors, mock and CAR T cells were labeled with Vivotrack-680 dye and IV injected into six MiaPaCa2-Luc tumor-bearing NSG mice on day 52 post-surgery (n=3). Mice were sacrificed 24 hrs after (since Vivotrack-680 signal intensity peaks at 24 hrs), and tumors were dissected and imaged by IVIS

using Vivotrack-680 channel. There was strong signal emitted from CAR T cell-injected tumors compared to the control group, which suggests that CAR T cells were able to infiltrate into and localize in the pancreatic tumor mass as early as 24 hrs after infusion, while mock T cells were not directed to the tumor mass (figure 23).

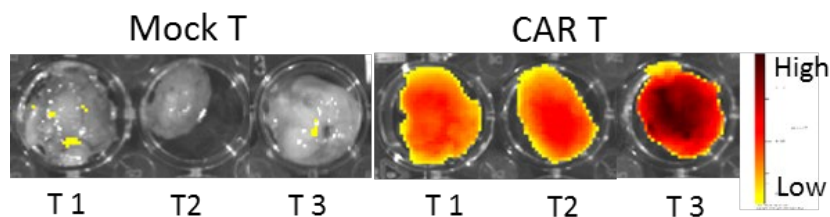


Figure 23. Visual representation of CAR T cells trafficking in the pancreatic tumors. To evaluate T cells trafficking into the fibrotic pancreatic tumor, six tumor-bearing mice (day 52 post-surgery) were injected IV with either 4×10^6 vivotrack-680 labeled-CAR T cells or mock T cells. After 24 hrs, mice were sacrificed and tumors were harvested and imaged using fluorescent channel on IVIS machine with excitation=676 and emission=696 nm. The fluorescent signal acquired from tumors of mice treated with CAR T cells was significantly higher than the ones treated with mock T cells, which indicates more CAR T cells are directed to the tumor site than mock T cells. T1-3, tumor 1-3.

3.2.3 Immunohistochemistry Analysis of Tumor Tissues

Tumor tissues were harvested at day 68 at endpoints and fixed in 10% neutral-buffered formalin. Paraffin-embedded blocks were prepared and 4 micron sections were cut for staining. IHC was performed as described previously. To evaluate CAR T cell infiltration and persistence in the tumor by day 68, tissues were stained with a human anti-CD3 antibody. Results showed no significant staining in either group. This may indicate that the T cell persistence in the tumor tissue was minimal by the time the tumors were dissected (figure 24). Although they infiltrated into the tumor initially within 24 hrs as shown in previous section, they did not persist in the tumor microenvironment.

To test for MUC1 expression in the tumors, tumor tissues were stained with TAB004 antibody and the result showed noticeably higher staining in mock T cell treated group compared to CAR T cell treated group (figure 24). Two possible mechanisms explain this result: 1) Elimination

of MUC1 positive cells by CAR T cells in the CAR T cell treated group leading to low staining. 2) Antigen loss, an immune evasion mechanism utilized by tumor cells in order to evade CAR T cells in CAR T cell treated group.

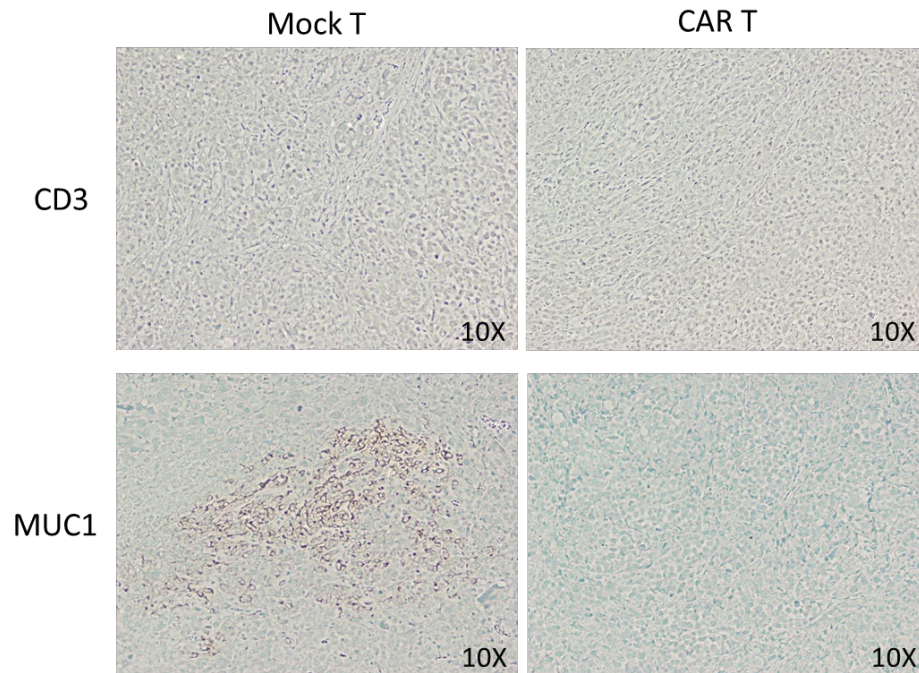


Figure 24. Immunohistochemistry staining of CD3 and MUC1 in tumor tissues harvested at day 68 post tumor inoculation. CD3 staining did not generate a clear positive staining. In the bottom row, the brown staining shows tMUC1 positivity, which was higher in mock T, treated group that CAR T.

3.3 Discussion

In this chapter, results related to the evaluation of the *in vivo* efficacy of MUC1-specific CAR T cells was presented. Initially we decided to establish a PDA xenograft model where assessment of tumor growth and response to treatment could be performed with IVIS imaging. This imaging system provides a quantitative, objective, non-invasive and high throughput method for monitoring tumor growth [176]. Additionally, it can detect microscopic tumors with accuracy and high sensitivity, even before the tumors are palpable using caliper measurements [177]. For this purpose, we engineered MiaPaCa2 cells to express firefly luciferase. PDA tumor establishment in

NSG mice orthotopically injected with MiaPaCa2-Luc cells was confirmed using IVIS imaging. All the mice had noticeable size of pancreas tumor 7 days post-surgery. However, over time, the signal emitting from the tumors was not correlating with the final size and weight of the tumor. The CAR T cell treated group has significantly smaller tumors than mock T cell treated group. We discovered the difference when we dissected the tumors at the endpoints. One reason could be that the PDA tumors in the pancreas are too deeply buried in the abdominal cavity for bioluminescence signal to penetrate through the tissues. Rotating the mice to the side didn't seem to help, since it only detected the signal from one side of the PDA tumor which is not a good indicative of the whole tumor. Therefore, we avoided presenting the IVIS data and only show the final tumor wet weights, which are more reliable. To address this issue, we suggest imaging the mice from the dorsal view instead of the ventral or lateral. Moreover, performing a longer mouse experiment may show more dramatic difference in the bioluminescence signal from different groups of mice.

Mice were monitored through the experiment and no sign of weight loss or ailment was observed. Organs such as lung, liver, spleen and kidney were harvested at endpoint and later examined for sign of toxicity. Luckily, there was no sign of treatment toxicity in the mice. Therefore, we can deduce that MUC1 CAR T cell therapy does not induce toxicity in NSG mice.

Imaging CAR T cells in vivo has been a challenge for many years. We have implemented a new method, which allows quick and easy labeling of T cells. Using Vivotrack 680 dye, any cell can be labeled in 1 hr and used for in vivo imaging. The signal will peak at 24 hrs and last for up to a week. We labeled tMUC1-CAR and mock T cells with Vivotrack 680 dye and injected them i.v. into the PDA tumor bearing mice. The IVIS machine was able to successfully pick up the signal in the dissected mice 24 hrs after T cells injection. Comparatively, more fluorescence was emitting from the tumors of mice injected with CAR T cells than the one with mock T cells. This data suggest that MUC1-CAR T can successfully traffic to the PDA tumor site whereas mock T cells are less directed.

To track the CAR T cells systemically, whole mouse body was imaged using IVIS. Unfortunately, a strong signal was not observed. After opening the mouse, IVIS imaging detected significant amount of signal from the entire abdominal cavity. Most organs were glowing especially liver. It is rational to see T cells travel everywhere within 24 hrs. However, they might clear out of organs after few days. To track T cells for a longer period, other staining methods should be considered or stably transferred CAR T cells with fluorescent tag must be utilized.

Although tMUC1 CAR T cells could significantly reduce the burden of PDA tumors, they were unable to eradicate the tumor completely. Several reasons are speculated for the lack of efficacy: 1) high burden of tumors at the time-point of CAR T cell injection, 2) Low persistence of CD3+ CAR T cells in the tumor (Figure 24), 3) tMUC1 antigen loss (Figure 24), and 4) CAR T cell exhaustion. Low overall response was not attributed to lack of T cells migration to the tumor site, as our *in vivo* tracking data confirmed that T cells could infiltrate into the tumors within 24 hrs.. To attempt to overcome the challenge of antigen loss, researchers have designed various strategies such as using bispecific CAR T cells, which contain two scFv from two different antibody. These CAR T cells, which target multiple antigens simultaneously, prevent antigen escape by malignant cells [130, 178].

CAR T cell exhaustion due to tonic signaling might contribute to the reduction of CAR T cells activity *in vivo*. Tonic signaling is defined as a constitutive or chronic activation of T cells in the absence of a ligand [179]. Physiologically, low-level continuous tonic signaling via interactions between the endogenous TCR and self-peptide loaded MHC molecules establishes a key mechanism to regulate T cell homeostasis [180]. In the contrary, tonic signaling mediated by T cell engrafted CAR can be dependent or independent of the relevant Ag and has major effects on CAR T cell based therapies. Although, in some instances, CAR tonic signaling may promote T cell expansion by providing stimulating signals [181]; tonic signaling mostly leads to terminal effector

T cell differentiation, exhaustion and/or enhanced activation-induced cell death, and therefore, restricts *in vivo* persistence and antitumor activity [182, 183].

To overcome the effects of tonic signaling, different strategies could be designed. In a previous study by Long et al. it has been shown that the detrimental effects of continuous signaling of CAR T-cells could be abrogated by replacing the CD28 co-stimulatory molecule of the CAR signaling domain with that of 4-1BB [182]. Another possible solution in order to improve T cell function *in vivo* is to use checkpoint inhibitors along with CAR T cells therapy. Two different types of experiments could be designed: 1) simultaneous treatment of PDA cancer xenograft mice with both CAR T cells and a checkpoint inhibitor, and 2) *in vitro* treatment of CAR T cells with a checkpoint inhibitor in order to reverse T cell exhaustion, prior to their administration in mice with established PDA tumors. In support of the second strategy, K. Moon et al. have shown that mesothelin-targeted CAR T cells exhaustion in mice due to suppressive tumor microenvironment could be restored by *ex vivo* treatment of CAR TILs with a PD-L1 inhibitor [184]. In our studies, using anti-PD1 antibody did not improve the efficacy of CAR T cell therapy *in vitro*. Other checkpoint pathways such as Tim-3 should be further investigated in order to find the right targeting candidate.

Other researchers have designed strategies in order to improve the anti-tumor activity of CAR T-cells. These include the targeted integration of the CAR transgene to the TRAC locus [185] and co-expression of a CAR with the IL-17R cytokine receptor and they could be combined with the MUC1- immunotherapeutic approach presented herein [186].

To avoid antigen loss, we will need to design bi-specific CAR constructs. Mesothelin and MUC1 may be the most commonly expressed target antigens in PDA. Another solution may be to inject CAR T cells more than once to address the concern of T cell persistence. However, we need to first determine at what time point post 1st injection, T cells are lost in the tumor microenvironment.

CHAPTER 4. PDA RESISTANCE TO CAR T CELL THERAPY

In this chapter, the resistance of PDA cells to the CAR T cell treatment and the involved mechanism will be investigated. We have studied the possible immunosuppression mechanisms performed by cancer cells to evade from immune cells and found that PD1/PDL1 interaction does not play an important role in our model. Also, shed MUC1 level did not show any relevance to the resistance level of PDA cells. However, CAR T cells proliferation seemed to be affected by resistant cancer cells. To pinpoint the particular factors conferring resistance, qPCR analysis was performed on 16 resistance related genes in three PDA cell lines before and after CAR T treatment. Our data suggests that IDO1, COX1 and COX2, ADAR1 and galectin-9 might be possible players in PDA resistance. Hence, combination therapies targeting these molecules along with CAR T cells was performed and resulted in improved treatment in some cases. In addition, CAR T cells compatibility with standard of care drugs for PDA was investigated. Low dose chemotherapy drugs such as gemcitabine, paclitaxel and 5-FU were applied on the PDA cells before CAR T cell treatment and the results showed enhanced efficacy. Here, we provide insights into some of the resistance mechanisms in PDA and suggest candidate molecules to target in order to reverse the immunosuppression of PDA cells to CAR T cell treatment.

4.1 Materials and Methods

4.1.1 Flow Cytometry

PD1-APC (eBioJ105) and PDL1-FITC (clone MIH2) antibodies were obtained from eBioscience. Dead cells were excluded by 7-AAD staining (BD Biosciences #555816). Data were acquired on BD LSR Fortessa flow cytometer (BD Biosciences) and analyzed using the FlowJo software (version 8.8.7, Tree Star Inc).

4.1.2 Apoptosis Assay

Mock and CAR T cells were stained with Annexin V/PI dyes according to the Dead Cell Apoptosis Kit protocol (Life Technology V13242) before and after co-culture with cancer cells for 24, 48, and 72 hrs. The percentage of positive cells for Annexin V, PI or both was assessed using flowcytometry.

4.1.3 Proliferation Assay

HPAFII, CFPAC and MiaPaCa2 cells were plated in 6well plate (500,000 cells/well). Next day, mock and CAR T cells were added to the cancer cells at 1:5 T:E ratio. Number of live T cells per well were calculated at 24, 48 and 72 hrs using trypan blue (0.4%, Thermo Fisher) staining and Countess II automated cell counter (Life Technologies, Carlsbad, USA).

4.1.4 RT-PCR, qPCR

RNA was extracted from cancer cells by RNeasy Plus Mini Kit (Qiagen #74134). RT-PCR was performed using AccessQuick™ RT-PCR system (Promega #A1700) and samples were ran on 1.2% agarose gel. The human MUC1 primers used were Forward TGC ATC AGG CTC AGC TTC A, Reverse GAA ATG GCA CAT CAC TCA G, and Tm 60 °C. qPCR primers were designed using the NCBI primer design tool and synthesized by MWG Eurofins (Louisville, USA). The primer sequences and their Tm are shown in table 1. Average Tm of F and R primers was used for each reaction. The relative expression levels of multiple genes such as MUC1, PD1, PDL1, LIF, VEGF, IDO1/2, COX1/2, ADAR1, TGFB, TGFBR1/II, PDGF, M6PR, Gal-9 and TRAIL were quantified in cancer cells before and after exposure to mock and CAR T cells using Applied Biosystems® 7500 fast Real-Time PCR machine and SYBR Green PowerUp Master Mix (Life Tech, A25742). Relative expression of each gene was calculated as $1 / (\text{gene CT} - \text{GAPDH CT})$.

Gene name	Primer sequence	T _m (°C)
LIF F	TGTCTTACAACACAGGCTCCA	60
LIF R	CACAACCTCCTGCCGCAA	61
VEGF-A F	ATCACCATGCAGATTATGCGG	59
VEGF-A R	CCCCTTTCCCTTTCCTCGAAC	61
IDO1 F	TGTCTGGCTGGAAAGGCAAC	61
IDO1 R	CTGAAAGACGCTGCTTTGGC	60
IDO2 F	CAGTTCCTGAAGGGTCACCG	60
IDO2 R	GATTCCTTGGCAGGACCTCTG	60
COX1 F	ACCAGGCATCAGAAACGGAG	60
COX1 R	GGAACTCATTTCCTTGGTGC	60
COX2 F	CAAATTGCTGGCAGGGTTGC	61
COX2 R	AGGGCTTCAGCATAAAGCGT	60
ADAR F	TTGGCGAGCTCGTGAGATAC	60
ADAR R	AAACGAACTTGGGCTCGTGA	60
TGF-B1 F	GGAAATTGAGGGCTTTCGCC	60
TGF-B1 R	AGTGAACCCTGCGTTGATGT	60
TGFB-R1 F	GTCGCAGAGGGAAGCGTTAC	61
TGFB-R1 R	AAGCAGAGCCCATCTGTCAC	60
TGFB-R2 F	ACGTTCAGAAGTCGGATGTGG	60
TGFB-R2 R	TCAGTGGATGGGCAGTCCTA	60
PDGF-B F	CCTGTCTCTCTGCTGCTACC	60
PDGF-B R	ATCTTCCTCTCCGGGGTCTC	60
PDL1 F	CTGAACGCATTTACTGTACCGG	60
PDL1 R	GACAATTAGTGCAGCCAGGTC	60
TRAIL F	CCCTTGACCAAATGTGAAC	58
TRAIL R	AGAAGACAAAGCCACCCCAA	59
Galectin9 F	TACCTGAGTCCAGCTGTCCC	61
Galectin9 R	AGCTGAGAACGGTCCCATTG	60
M6PR F	TGAAACTAGCTCTGGGACCG	59
M6PR R	AAGGGAACATCGTGTCTGG	60
MUC1 F	CAGTGCTTACAGTTGTTACGGG	60
MUC1 R	GCTGGGCACTGAACTTCTCT	60
GAPDH F	CCTGCACCACCAACTGCTTA	61
GAPDH R	GGCCATCCACAGTCTTCTGAG	60

Table 1. List of primers used in qPCR experiment with their melting temperature (T_m). Average T_m of F and R primers was used for each reaction. F, forward, R, reverse.

4.1.5 Combination Therapy with Drugs and Blocking Antibody

To assess the effect of drugs on CAR T cell cytotoxicity, cancer cells were plated at 5,000/well concentration in 96 well plates in triplicate. Next day, cells were treated with drugs (1-MT [Sigma, #452483], indomethacin [Sigma, #17378], gemcitabine hydrochloride [Sigma, #G6423], paclitaxel [Invitrogen, Taxol equivalent, #P3456] and 5-Fluorouracil [Sigma, F6627]) at indicated concentrations for 24 hrs. After 24 hrs drug was removed, cells were washed and further incubated with mock or CAR T cells at T:E ratio of 1:10 for 72 hrs. Thereafter, the percentage of surviving cancer cells were measured using the MTT assay. For Gal-9 and PD-1 blocking experiments, cancer cells were plated at 10,000 cells/well concentration in 96 well plates in triplicate. After 24 hrs, mock or CAR T cells were added at T:E ratio of 1:10. 0.1, 1, and 10 ug/ml of Gal-9 (clone 9M1-3, BioLegend) or PD-1 blocking antibody (clone EH12.2H7, BioLegend) was added to the media and incubated at 37 °C for 72 hrs. Survival was measured using the MTT assay.

4.1.6 Statistical Analysis

All of the data were analyzed by Prism (version 8.0; GraphPad Software) and results presented as mean \pm SEM. Data are representative of two or more independent experiments. The statistical significance was determined using unpaired Student's t-test or two-way ANOVA where indicated (*, $p < 0.05$, **, $p < 0.01$, ***, $p < 0.001$).

4.2 Results

4.2.1 Deciphering the Intrinsic Resistance Mechanism Utilized by PDA Cells to CAR T Cell Therapy: Role of IDO1 and Gal-9

To assess why some PDA cell lines are resistant to CAR T cell killing independent of their tMUC1 expression or the CAR T cell's ability to express perforin (figure S1C), or produce IFN- γ and granzyme B (figure 21 and S1B), we considered some common immune evasion tactics used by tumor cells. We selected two highly resistant cell lines; HPAFII and CFPAC (both express

similar levels of tMUC1, figure 18B). As control, we included a highly sensitive cell line, MiaPCa2 with similar tMUC1 level.

Impairing T cells function by cancer cells is reported as a common mechanism involved in tumor immune evasion. Main factors in T cells anti-tumor cytotoxicity include IFN γ , granzyme B and perforin secretion. Results show no correlation between the amount of released IFN γ and granzyme B and levels of intracellular perforin with the resistance of tumor cells (figures 21 and S1B, C).

Another common mechanism of immune evasion is associated with tumor-induced apoptosis of effector T cells. PDL1 expressed by cancer cells can interact with PD1 receptor on T cells and trigger T cell apoptosis. To test if HPAFII and CFPAC utilize this mechanism, mock and CAR T cells were exposed to resistant (HPAFII, CFPAC) or sensitive (MiaPaCa2) cells for 24, 48 and 72 hrs and the apoptosis was assessed by Annexin V/PI staining and flowcytometry. Data shows that apoptosis of mock and CAR T cells did not significantly alter after 24, 48 and 72 hrs exposure to resistant vs. sensitive PDA cells. T cell apoptosis level at 48 hrs time-point is shown in figure 25A. Level of PD1 expression by T cells before and after exposure to resistant or sensitive cells were measured by flowcytometry and the results are shown in figure S2A, B. There was no significant difference between level of PD1 expression by mock and CAR T cells before and after co-culture with resistant or sensitive cells at 24, 48 and 72 hrs. Most PDA cells used in this study express considerable amount of PDL1; however, the PDL1 level is not correlated with the resistance of PDA cells (figure S2A, B). To confirm the results, PD1 blocking with anti-PD1 antibody was performed in combination with CAR T cell therapy on the three cell lines. We detected no improvement in killing of the resistant PDA cell lines (HPAFII, CFPAC), while sensitive cell line (MiaPaCa2) killing was enhanced (figure S3). Data suggests that PD1/PDL1 interaction may not be the major factor driving CAR T cell resistance in HPAFII and CFPAC cells.

Because apoptosis of CAR T cells was not significantly different when co-cultured with resistant versus sensitive PDA cell lines, we enumerated cell numbers post co-culture. Proliferation of CAR T and mock T cells was evaluated before and after co-culture with resistant (HPAFII and CFPAC) and sensitive (MiaPaCa2) PDA cells at 24, 48, and 72 hours using a cell counter. Interestingly, CAR T cell proliferation was significantly hindered when co-cultured with HPAFII and CFPAC cells by 72 hrs, while growth of CAR T cells was enhanced when co-cultured with MiaPaCa2 cells. Mock T cell proliferation did not show the same trend (figure 25B).

Studies have shown that PDA cells shed MUC1 into the supernatant and that may impair T cells function. It is also reported that depletion of soluble MUC1 from the tumor supernatants reversed the inhibitory effects on T cells [187]. Thus, we assessed the amount of released MUC1 by PDA cells in the co-culture media using a specific ELISA (figure S2C). Results show that only HPAC cells release high levels of MUC1, while other PDA cells shed minimal levels of MUC1. Since HPAC cell line is highly sensitive to CAR T cell treatment, we negated the role of shed MUC1 as a mechanism for antigen loss and immune escape (figure S2C).

Thus, we moved to investigate the gene expression profile of HPAFII, CFPAC, and MiaPaCa2 cells. Sixteen genes linked to immune resistance (based on literature) were analyzed using qPCR technique. Figure 25C shows relative expression of each gene (normalized to GAPDH) in three cell lines before and after CAR T cell treatment. MUC1 mRNA expression in resistant vs. sensitive cells did not significantly change after CAR T cell treatment, indicating no antigen loss through gene downregulation, and therefore may not account for the immune evasion in the HPAFII and CFPAC PDA cells (figure 25C). Most of the genes were expressed at low levels in resistant cells except indoleamine 2, 3-dioxygenases-1 (IDO1), cyclooxygenase 1 and 2 (COX1/2), adenosine deaminases acting on RNA (ADAR1) and Gal-9. According to qPCR data, IDO1 gene expression in HPAFII cells was significantly increased (69-fold increase) after treatment with CAR T cells, while its level declined in MiaPaCa2 cells. COX1 and 2 expressions were slightly higher

in HPAFII and CFPAC, and their level increased after CAR T treatment. The expression of ADAR1 gene was higher in HPAFII cells compared to MiaPaCa2 before treatment, and expression of this gene was only increased in CFPAC after CAR T treatment. Gal-9 gene expression was also high in both resistant cells before and after CAR T cell therapy. These genes are appropriate candidates to further study as some of the important players in immune resistance of HPAFII and CFPAC cells. Hence, we combined CAR T cell treatment with inhibitors or blocking antibodies to the above-mentioned molecules.

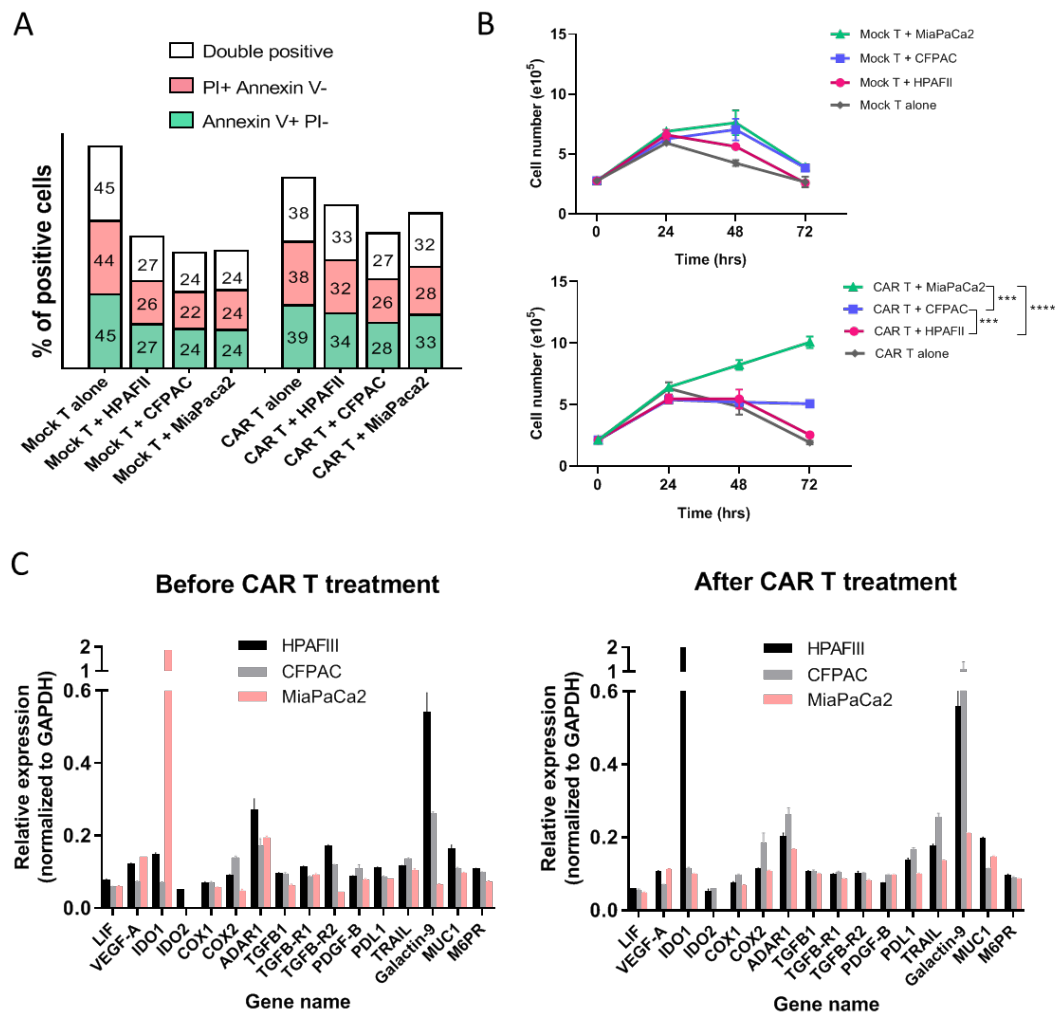


Figure 25. Deciphering the resistance mechanism utilized by PDA cells against CAR T cell therapy. A. Apoptosis of CAR T cells before and after exposure to HPAFII, CFPAC and MiaPaCa2 cells. Mock and CAR T cells were co-cultured with PDA cells and their apoptosis level was measured

by Annexin V/PI staining at 24, 48 and 72 hrs post co-culture. A shows percentage of positive Annexin V, PI or both in T cells after 48 hrs co-culture. There is no significant difference between apoptosis level of mock and CAR T cells when exposed to resistant vs. sensitive PDA cells. B. Mock and CAR T cells proliferation over time after exposure to HPAFII, CFPAC and MiaPaCa2 cells. T cells were enumerated using an automated cell counter. MiaPaCa2 cells enhanced proliferation of CAR T cells after 48 and 72 hrs, whereas CFPAC and HPAFII cells hindered CAR T cells proliferation. Mock T cells did not show the same trend. Significance of data was evaluated using Two Way ANOVA (Multiple Comparison). Error bars, SEM. *** $p < 0.001$, **** $p < 0.0001$. C. q-PCR data showing relative expression level of 16 genes in HPAFII, CFPAC and MiaPaCa2 cells before and after exposure to CAR T cells. CTs are normalized to GAPDH in each sample and higher number in Y-axis represents higher expression of the gene. IDO1, COX1/2, ADAR1 and galectin-9 genes were overexpressed in resistant PDA cells after exposure to CAR T cells. Error bars, SEM.

4.2.2 Battling the Resistance of PDA Cells with Combination Therapy

4.2.2.1 Targeting Resistance Related Genes with Small Molecule Inhibitors

IDO1 was one of the candidate genes involved in immune resistance. IDO1 function can be inhibited by 1-Methyl-D-tryptophan (1-MT) drug. Three cell lines were treated with 1-MT drug at three different concentrations for 1 day followed by 3 days of mock or CAR T cell treatment. CAR T cells plus drug killing was normalized to mock T cell plus drug, and the asterisk shows significant difference between the CAR T cells plus drug (combination therapy) and CAR T cells alone. Results showed a significant reduction in survival of HPAFII and CFPAC cells by combination of CAR T cells and 1-MT therapy in a dose dependent manner compared to CAR T alone or 1-MT alone therapy, while MiaPaCa2 cells showed no significant difference in survival (figure 26). Combination of CAR T cells and 1-MT did not improve the treatment efficacy for MiaPaCa2 cells. However, 1MT alone reduced the MiaPaCa2 cells survival by 50%. It may be due to elevated level of IDO1 in MiaPaCa2 before the therapy and its reduction after the therapy. Data suggests that IDO1 may be one of the major factors causing immune resistance in HPAFII and CFPAC cells and

targeting IDO1 along with CAR T cell therapy may enhance the treatment efficacy in resistant PDA cells.

Several studies have shown the importance of COX1 and COX2 in causing resistance of cancer cells to immune therapy [188] [189]. Therefore, celecoxib (specific COX-2 inhibitor) and indomethacin (COX1 and 2 inhibitor) were used in combination with CAR T cells. Both HPAFII and CFPAC cells showed reduction in survival when treated with indomethacin and CAR T cells, while MiaPaCa2 cells showed no difference in survival (figure 26). Celecoxib did not change the efficacy of CAR T cells (Data not shown).

Next candidate gene for resistance was ADAR1. qPCR data showed an elevation in ADAR1 gene expression level in resistant cells compared to MiaPaCa2. PDA cells were treated with EHNA drug (ADAR1 inhibitor) for 24 hrs before adding CAR T cells, and cell survival was measured at 72 hrs post co-culture. Combination therapy with EHNA drug did not result in significant reduction in the survival of the target cells (data is not shown). Hence, we inferred that ADAR1 might not play an important role in immune resistance of HPAFII and CFPAC cells.

4.2.2.2 Targeting Resistance Related Genes with Blocking Antibody

Gal-9 was another gene that showed increased expression in the resistant cells. Gal-9 is a tandem-repeat galectin interacting with Tim3 receptor on T cells [190]. To neutralize the effects of Gal-9, a blocking Ab, 9M1-3 (Biolegend) was used in combination with CAR T cells and the results are shown in figure 27. HPAFII and CFPAC cells are efficiently targeted by CAR T cells when Gal-9 checkpoint inhibitor is added to the co-culture media compared to CAR T cell or 9M1-3 treatment alone. In contrast, survival of MiaPaCa2 cells was not affected by the combination. Data suggests Gal-9 –Tim3 interaction may play an important role in immune evasion by resistant PDA cells.

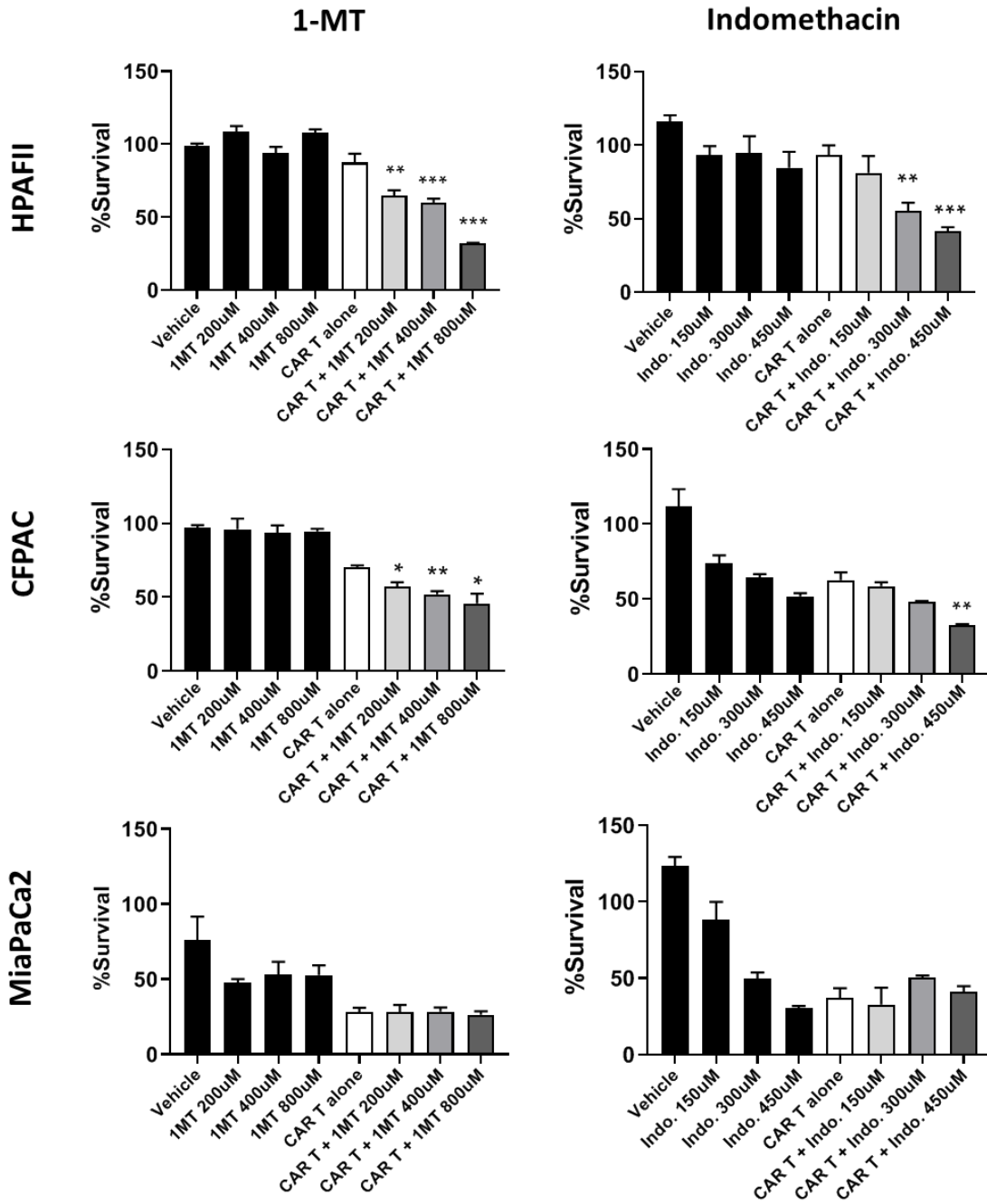


Figure 26. Targeting resistance related genes with small molecule inhibitors. HPAFII, CFPAC and MiaPaCa2 cells were pre-treated with IDO1 inhibitor (1-MT) or COX1/2 inhibitor (indomethacin) for 24 hrs, then drugs were removed and PDA cells were co-cultured with mock or CAR T cells for 72 hrs at T:E ratio of 1:10. Percentage survival was measured using MTT assay and normalized to mock T. HPAFII and CFPAC killing by CAR T cells was significantly improved when pre-treated with 1-MT and indomethacin; while MiaPaCa2 cell did not respond to the combinational

treatment. Student's t-test comparing CAR T + drug group to CAR T alone group. * $p < 0.05$, ** $p < 0.01$, ***, $p < 0.001$.

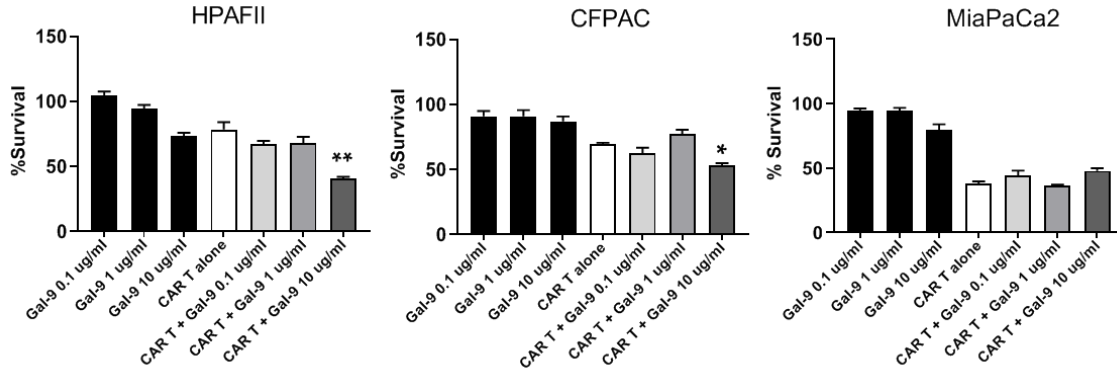


Figure 27. Targeting resistance related genes with anti-Gal-9 blocking antibody. Percentage survival of HPAFII, CFPAC and MiaPaCa2 cells after treatment with CAR T alone, Gal-9 blocking antibody alone, and combination of CAR T cell and Gal-9 blocking Ab. Anti-Gal-9 antibody was added at 3 different concentrations to the co-culture media of PDA cells and mock or CAR T cells (T:E 1:10). Percentage survival was obtained using MTT assay and data was normalized to mock T. HPAFII and CFPAC survival were reduced with combination of CAR T and anti-Gal-9 blocking Ab; while MiaPaCa2 did not respond to the combination therapy. Student's t-test comparing CAR T + anti-Gal-9 antibody group to CAR T alone group. * $p < 0.05$, ** $p < 0.01$.

4.2.2.3 tMUC1-CAR T Cells Work Synergistically with Common Chemotherapy Drugs to Kill Resistant PDA Cells

Another approach to break resistance of target cells to CAR T cells is pre-sensitizing them with common chemotherapy drugs. Three widely used drugs for PDA include gemcitabine (GEM), 5-Fluorouracil (5FU) and paclitaxel (PTX). GEM is analog of deoxy-cytidine, inhibits DNA synthesis, PTX suppresses microtubule detachments from centrosome, and 5-FU inhibits Thymidine synthase. We treated PDA cells with the drugs for 24 hrs prior to CAR T cell treatment. After 72 hrs of CAR T treatment, target cell viability was measured using MTT assay. Results demonstrate significantly enhanced sensitivity of HPAFII cells to CAR T cell treatment when pre-

exposed to low-dose chemotherapy drugs (figure 28, top row). All three drugs improved killing of HPAFII cells with CAR T cells, while only 5-FU showed the same effect on CFPAC cells. GEM and PTX did not assist the CFPAC sensitivity to CAR T cells (figure 28, bottom row). Data suggests that pre-sensitizing the resistant PDA cells with low dose of appropriate chemotherapeutic drug may enhance the efficacy of CAR T cell treatment.

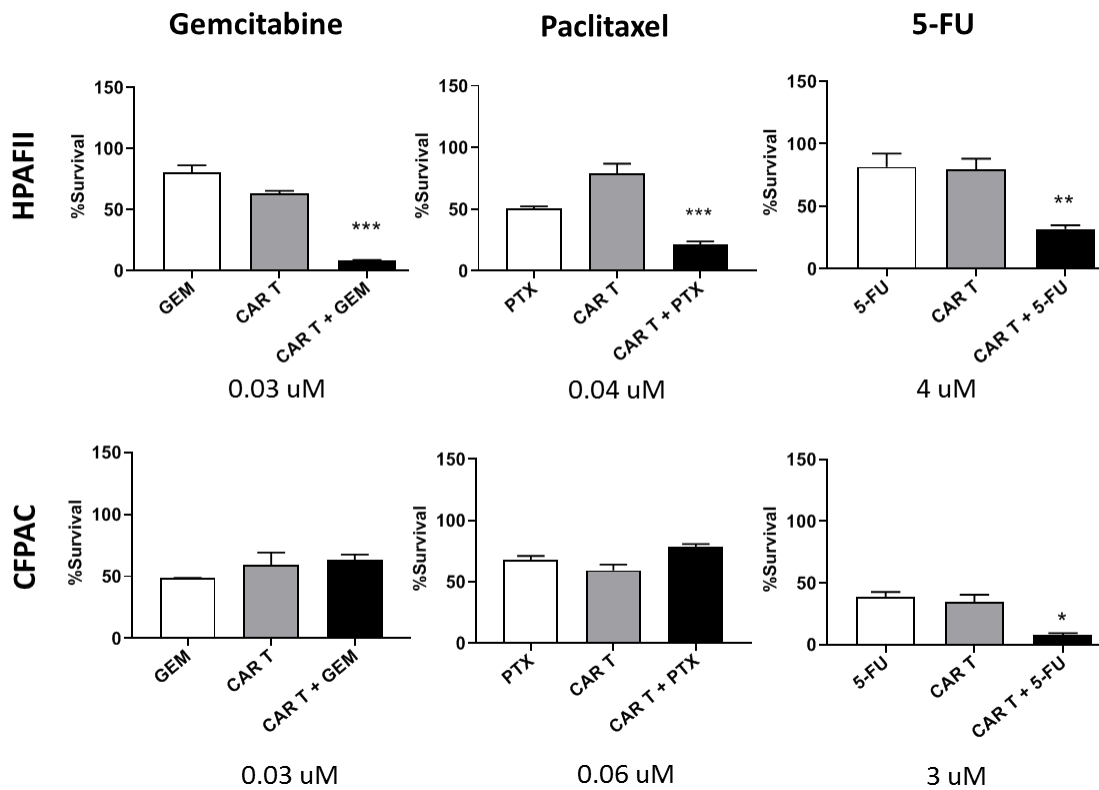


Figure 28. tMUC1-CAR T cells work synergistically with common chemotherapy drugs to kill resistant PDA cells. Percentage survival of two resistant PDA cells, HPAFII and CFPAC, treated with combination of CAR T and chemo drugs. HPAFII and CFPAC were exposed to gemcitabine, paclitaxel or 5-FU for 24 hrs at indicated concentrations, then co-cultured with mock or CAR T cells at T:E ratio of 1:10. Survival level was measured using MTT assay and data was normalized to mock T. Student's t-test comparing CAR T + drug to CAR T alone group, * $p < 0.05$, ** $P > 0.0021$, *** $P < 0.0004$.

4.3 Discussion

We present preclinical data showing efficacy of a novel TAB004-derived CAR T cell targeting tMUC1 against a panel of human PDA cell lines. Data demonstrates that some PDA cells remain highly resistant to CAR T cell therapy. Thus, we determined the genes that may be involved in the immune resistance. Data clearly implicate IDO1, Gal-9 and to a lesser extent, COX genes as mechanisms of CAR T cell resistance. To our knowledge, this is the first study to show that blocking the function of IDO1 or Gal-9 can enhance CAR T cells therapy against PDA cells. We also report that pre-treating the resistant HPAFII cells with standard drugs such as PTX, GEM, and 5FU enhanced CAR T cell efficacy. However, for CFPAC cells, only pre-treatment with 5FU enhanced CAR T cell efficacy. Data suggest that not all PDA cells are alike and biomarkers such as IDO1 and Gal-9 may be useful tools to determine response to CAR T cell therapy.

Despite many PDA cells being efficiently destroyed by CAR T cells, few PDA lines were highly resistant. This was not surprising. Human PDA is known to be immunologically cold and refractory to the treatments. Thus, deciphering mechanisms involved in PDA immune-resistance is of cardinal importance. Majority of combination therapy to date have focused on targeting the PD1/PDL1 axis using blocking antibodies [159], but in our study with HPAFII and CFPAC cells, we saw no evidence supporting enhanced CAR T cell efficacy when combined with anti-PD1 antibody [148]. A study by Koyama et al [191] has shown that failure of PD1 monotherapy blockade or PD1 adaptive resistance in lung adenocarcinoma is associated with upregulation of alternative immune checkpoint molecules particularly Tim-3. This may explain why PD1 blockade in our model did not improve HPAFII and CFPAC killing, dissimilar to MiaPaCa2 cells. Tim-3 upregulation in HPAFII and CFPAC cells with elevated levels of its ligand, Gal-9, may potentially deteriorate CAR T cells function.

Multiple factors can dictate the resistance of a tumor cells to a treatment. High-throughput screening is required and yet it may result in inconclusive data. In this study, we focused on key

proteins and genes known to be associated with immune tolerance. Sixteen genes were analyzed using qPCR. Among those, IDO1, an enzyme that catabolizes tryptophan to kynurenine acid thereby provides metabolic advantage to cancer cells against T cells, was found to be of utmost importance [192, 193]. IDO1 contributes to peripheral immune tolerance and evasion of tumors by downregulating T cell metabolism. Several studies have confirmed that IDO1 and the downstream tryptophan catabolites inhibit T cell proliferation, thereby suppressing T cell function [194-197]. The effect of tumor IDO on CD19-CAR T cell activity in a B cell lymphoma model has been previously shown. They reported that IDO overexpression in xenograph lymphoma could inhibit CAR T cells function by diminishing their proliferation, cytotoxicity, and cytokine secretion *in vitro* in response to CD19 recognition. Using two IDO inhibitors, fludarabine and cyclophosphamide, CAR T cell function was restored [198]. Here we showed that elevated intrinsic IDO activity plays a critical role in immune suppression of CAR T cells against solid tumor. As shown in our study, CAR T cell proliferation was stunted when co-cultured with resistant PDA cell line (figure 25B). This reduction in proliferation could be due to elevated IDO1 activity in cancer cells and the release of tryptophan catabolites in the co-culture media. Accordingly, neutralizing the effect of IDO1 by 1-MT drug resulted in improved lysis of HPAFII and CFPAC cells by CAR T cells. It must be noted that 1-MT did not improve CAR T cell's cytotoxic activity against MiaPaCa2 cells; however, 1MT alone did reduce MiaPaCa2 cell survival by 50%. These results may have occurred due to the presence of high level of IDO1 in MiaPaCa2 prior to treatment with CAR T cells (Figure 25C) which reduced dramatically after the CAR T cell treatment (Figure 25D). According to a previous study, IDO1 promote cancer cells proliferation independent of its ability to limit T-cell-mediated immune surveillance. This is performed through activation of β -catenin signaling and transcription of its target genes (cyclin D1 and Axin2) by IDO1 metabolites, which promote cancer cell proliferation and increased tumor growth [199]. Accordingly, in our study, 1MT prior to CAR T cell therapy could neutralize the effect of IDO1 on MiaPaCa2 cell

growth; however due to unknown mechanisms, IDO1 gene expression was decreased after CAR T cells therapy which nullified the effect of 1MT when combined with CAR T cells.

Another gene with distinct overexpression in resistant cells was Gal-9. Gal-9 is a tandem-repeat type galectin that like other galectins modulate multiple biological functions such as cell adhesion and aggregation. Although the role of Gal-9 in immunity is controversial [200], many studies confirmed that Gal-9 negatively regulates T cells via interaction with Tim-3 receptor [190, 201, 202]. Tim-3 is a negative regulatory immune checkpoint expressed on T cell which is known to inhibit the immune responses of TH1 cells and plays an important role in immune exhaustion of T cells [203]. Studies have shown that interaction between Gal-9 and Tim-3 triggers cell death in effector Th1 cells [204] and in Tim-3⁺CD8⁺ Tumor infiltrating lymphocytes [205]. However, not all Gal-9-Tim-3 interactions result in cell death, as Gal-9 was found to increase Tim-3-mediated IFN- γ production in an NK cell line [206]. We have evaluated the level of Tim-3 expression on CAR T cells when exposed to resistant and sensitive target cells, but no significant difference was detected (data not shown). However, we found that targeting Gal-9 with a blocking antibody reduced tolerance of resistant HPAFII and CFPAC to tMUC1-CAR T cell therapy. Hence, Gal-9 immunosuppressive role may be mediated through other less known mechanisms.

ADAR1 was noticeably overexpressed in HPAFII and CFPAC cells. ADAR1 regulates the biogenesis of members of the miR-222 family and thereby ICAM1 expression, which ultimately leads to immune resistance [207]. Loss of function of ADAR1 in tumor cells strongly sensitizes tumors to immunotherapy and overcomes resistance to PD1 checkpoint blockade [208]. Surprisingly, in this study, blocking ADAR1 function with EHNA drug did not result in breaking resistance of HPAFII and CFPAC cells to CAR T cells treatment.

Finally, COX1/2 are enzymes catalyzing the synthesis of prostaglandin E2 (PGE2), a major player in inflammation, angiogenesis, and immunosuppression in cancer [209, 210]. COX2 is often overexpressed in cancer cells and is associated with progressive tumor growth, as well as resistance

of cancer cells to conventional chemotherapy, immunotherapy, and radiotherapy [209]. COX1/2 inhibitors have been used in combination with anti-cancer agents and immunotherapy against cancers [211]. COX1 and COX2 were slightly higher in the resistant vs. sensitive PDA cells. Indeed, indomethacin significantly improved CAR T cell efficacy when HPAFII cells were pre-treated with the drug. To our surprise, celecoxib had no such effect. This may indicate COX1 and 2 together play a more important role in HPAFII resistance to CAR T cells than COX2 by itself. This data is in line with other immunotherapy strategies such as checkpoint blockades combined with COX2 inhibitors [188]. Further studies are needed in order to explain the molecular events governing the success or failure of these combination therapies.

Since tMUC1-CAR T cell is new, we wished to confirm other published studies that combined CAR T cell treatment with standard of care chemotherapy drugs. Chemo and radiotherapy have primarily been used to make tumors leaky or to deplete lymphocytes to make new niches for CAR T cells prior to adoptive cell transfer. Results showed improved tumor regression and enhanced survival in metastatic melanoma [212, 213]. Moreover, chemotherapeutic drugs may be used to remove immunosuppressive T regulatory cells [214]. Data from this study clearly corroborate previous findings. Pre-treating resistant HPAFII cells with suboptimal dose of GEM, PTX or 5FU significantly enhanced CAR T cell cytotoxicity. To our surprise, PTX and GEM did not have the same effect on the CFPAC. In CFPAC, only 5FU was effective in enhancing CAR T cell treatment. Thus, we strongly believe that every tumor is different and responds differently to drugs and immunotherapy. These results provide a promising strategy for the potentiation of CAR T therapy in treating refractory PDA tumors.

CHAPTER 5: SUPPLEMENTAL DATA

In this chapter the supplemental data will be presented. First, the characteristic of T cells *in vitro* including their cytotoxicity against cancer cells are shown. Uninfected, CTL- and CAR T cells show similar cytotoxicity against MUC1 expressing PDA cells. In addition, to test The amount of intracellular IFN- γ and granzyme B was studied. Also, PD1 and PDL1 surface expression on T cells and cancer cells respectively will be evaluated.

Interaction of CAR T cells with BxPC3-MUC1 and BxPC3-Neo cells were recorded overnight using GE DeltaVision OMX-SR microscope and the videos were created using the ImageJ program. BxPC3-MUC1 cells were attacked and killed by CAR T cells in 7/9 spots, while only 2/9 spots showed killing in BxPC3-Neo plate. Red staining is indicative of dead cells that have absorbed propidium iodide (PI) dye present in the media. Videos are available as supplementary data: Video. Provided as separate file.

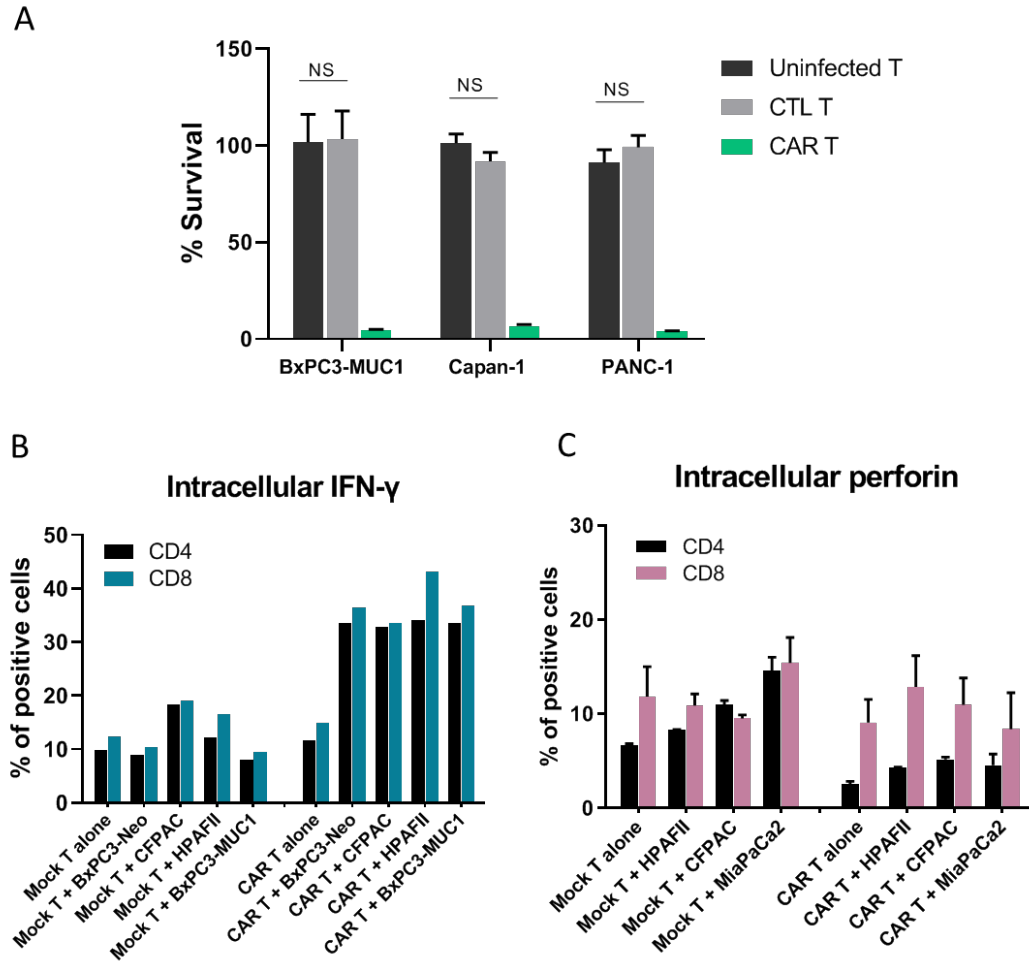


Figure S1. *In vitro* characterization of T cells. A. Similar activity of uninfected T and CTL T cells. Uninfected, CTL or CAR T cells were exposed to indicated PDA cell lines for 72 hrs at T:E 1:10, and survival level of PDA cells were measured using MTT assay. Data was normalized to media alone. Uninfected and CTL T show similar killing ability against PDA cells. Student's t-test, NS $P > 0.05$. B, C. Intracellular level of IFN- γ (B) and perforin (C) in mock and CAR T cells before and after exposure to PDA cells for 24 hrs at T:E 1:10. Percentage of CD4⁺ and CD8⁺ CAR T cells that are positive for IFN- γ and perforin was measured by flowcytometry. Data suggests CAR T cells exposed to HPAFII and CFPAC resistant cells are not functionally impaired regarding the production of IFN- γ and perforin internally. Each graph is representative of three independent experiments.

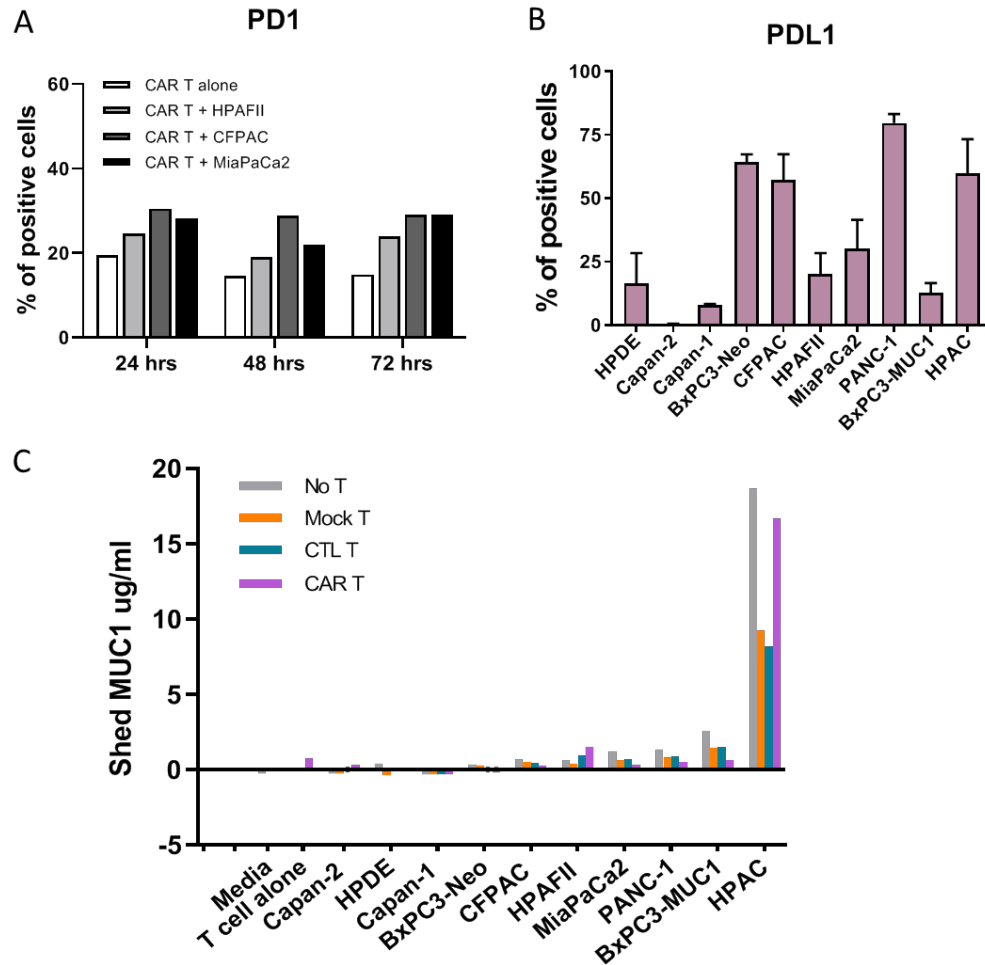


Figure S2. Immune resistance related mechanisms. A. PD1 expression on CAR T cells before and after exposure to HPAFII, CFPAC and MiaPaCa2 cells for 24, 48 and 72hrs. Percentage of positive cells was measured using flowcytometry. CAR T cells exposed to PDA cells express higher level of PD1 compared to unexposed CAR T cells, however there was no significant difference in PD1 expression of CAR T cells when co-cultured with resistant (HPAFII and CFPAC) vs. sensitive cells (MiaPaCa2). This graph represents three independent experiments. B. PDL1 expression in a panel of PDA cells measured using flowcytometry. There was no correlation between the PDL1 and resistance level in PDA cells. Error bars, SEM. C. Level of shed MUC1 in the 72 hrs co-culture supernatant of PDA cells and T cells measured by ELISA. High MUC1 expressing cells released higher amount of MUC1 compared to low MUC1 expressing cells. However, this amount is negligible (<4ug/ml). HPAC exceptionally released significant amount of MUC1 (~18ug/ml) into the media before and after exposure to CAR T cells (72 hrs). Data suggests shed MUC1 does not contribute to the immune resistance of HPAFII and CFPAC. Each bar represents average of three replicates.

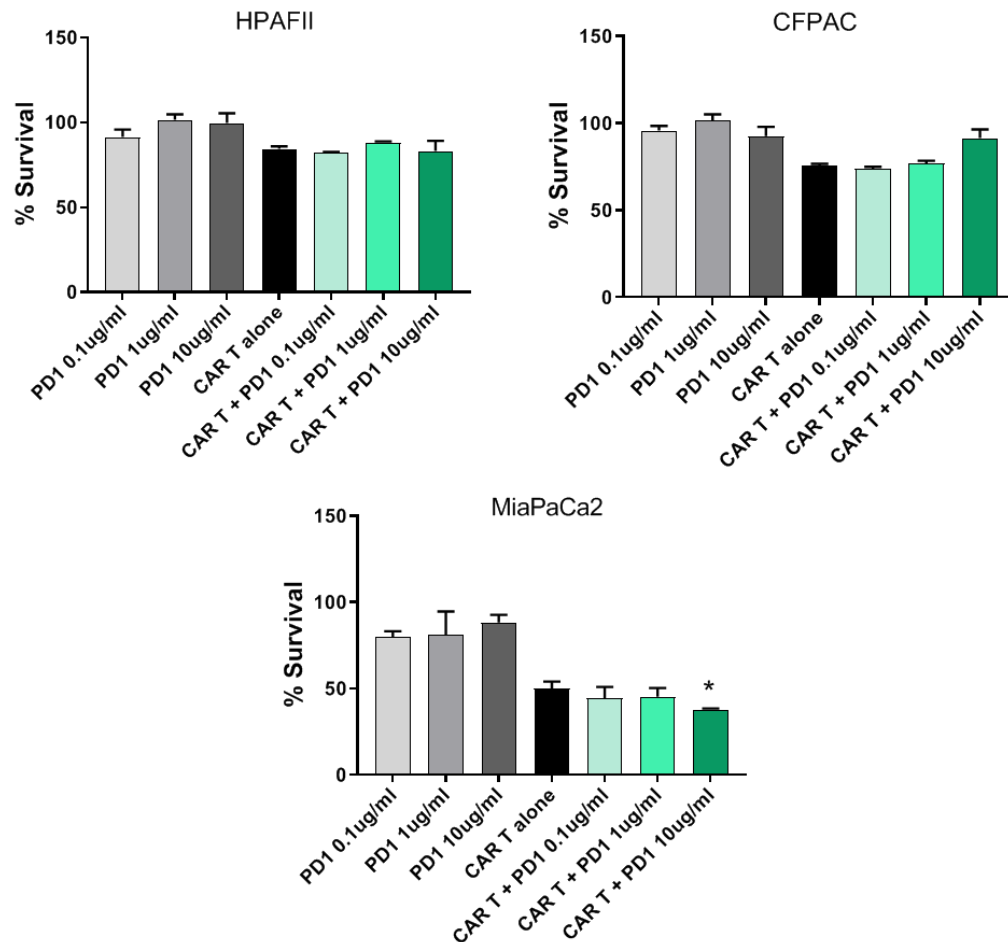


Figure S3. CAR T cell therapy in combination with anti-PD1 blocking antibody. Percentage survival of HPAFII, CFPAC and MiaPaCa2 PDA cells treated with PD1 blocking antibody alone, T cells alone, and combination, at 3 different concentrations of Ab. PDA cells were co-cultured with mock or CAR T cells, +/- anti-PD1 blocking antibody for 72 hrs at T:E 1:10, and their survival level was measured using MTT assay. Percentage survival was normalized to mock T cells. Resistant cells killing by CAR T cells was not improved by adding anti-PD1 blocking Ab; while MiaPaCa2 cells killing was improved by the combination therapy. Unpaired Student's t-test, comparing CAR T + PD1 group to CAR T alone group, * P=0.0404.

CHAPTER 6: CONCLUSIONS AND FUTURE DIRECTION

6.1 Conclusions and Future Direction

In this PhD thesis, we present data that indicates the tMUC1-CAR T cells do not kill normal cells but effectively kill majority of tMUC1 expressing PDA cells. Additionally, our results provide promise for the use of tMUC1-CAR T cells against treatment-refractory PDA in combination with inhibitors against IDO1, COX1/2 and Gal-9 or in combination with low-dose standard chemotherapy drugs. Recently, our group has published the effectiveness of tMUC1-CAR T cell efficacy against TNBC cells *in vitro* and *in vivo* [148]. This highlights the potency of tMUC1-CAR T cells as a potential therapy for multiple adenocarcinomas.

In this study, unlike previous works on CAR T cell therapy, we used variable fragment from a highly specific tMUC1 Ab, TAB004, that does not recognize normal MUC1. We also tested the efficacy of the tMUC1-CAR T cell against a large panel of PDA cell lines and normal epithelial and fibroblastic cells. Moreover, we deciphered the potential intrinsic immune tolerance mechanisms utilized by PDA cells to resist CAR T cell therapy. Furthermore, this is the first study indicating the role of IDO1 and Gal-9 in conferring resistance in PDA cells to CAR T cell treatment and that ADAR1 and COX pathway were less critical in conferring resistance.

Based on the *in vivo* orthotopic model of MiaPaCa2 tumors, tMUC1-CAR T cell was effective in reducing tumor burden but was unable to eradicate the tumor. We attribute the inefficacy to high tumor burden at time of CAR T cell injection, tMUC1 antigen loss, long-term CAR T cell persistence within the microenvironment, and exhaustion of CAR T cells. As addressed in Chapter 3, several strategies to overcome these challenges must be the next steps. In addition to the strategies discussed in chapter 3, replacing the CD28 co-stimulatory molecule of the CAR signaling domain with that of 4-1BB [182] may also be a strategy that our lab may pursue. Use of checkpoint inhibitors such as blocking PD1/PDL1 signaling is a highly regarded and used strategy.

However, according to our data, using anti-PD1 antibody did not improve the efficacy of CAR T cell therapy in our study. Other checkpoint pathways such as Tim-3 should be further investigated in order to find the right targeting candidate. Other researchers have designed different strategies in order to augment the anti-tumor activity of CAR T-cells. These include the targeted integration of the CAR transgene to the TRAC locus [185] and co-expression of a CAR with the IL-17R cytokine receptor, and they could be combined with the MUC1-immunotherapeutic approach presented herein [186]. Moreover, other treatment strategies such as multiple injections of CAR T cells and using an immunocompetent model of PDA can be investigated. Testing CAR T cells function in human MUC1 transgenic mouse model of spontaneous PDA, is currently under way by our group. Thorough examination of the role of IDO1 in tumor resistance and deciphering its mechanism of action by generating an IDO1 knock in/out model is ongoing.

Another concern related to a MUC1 targeting immunotherapeutic approach is the potential ability of the infused CAR T cells to bind circulating (tumor-derived) MUC1. This could prevent the CAR T cells from engaging MUC1 in the tumor site. However, it has been previously shown that radiolabeled MUC1 antibodies effectively trafficked into the tumor site in patients with MUC1-expressing malignancies, such as ovarian, breast and gastrointestinal cancer [215]. In our recent unpublished data, we calculated that only 3-8% of the total tMUC1 present in tumor cells get released in circulation. Therefore, we do not believe that circulating tMUC1 is an issue when designing tMUC1 targeted immunotherapies.

In summary, tMUC1-CAR T cells presented significant anti-tumor activity *in vitro* and *in vivo* setting. An important finding of this PhD project was that targeting IDO1, COX1/2 and Gal-9 in combination with tMUC1-CAR T cells therapy significantly improved the treatment efficacy against refractory PDA tumor cells. In addition, low-dose standard chemotherapy drugs could synergistically enhance tMUC1-CAR T cells function in killing resistant PDA cells. The results presented in this PhD project highlight one of the major obstacles in immunotherapy of solid

tumors, which is immune resistance of one resistant lineage of cancer cells leading to lack of response to the treatment, overgrowth and subsequent recurrence.

From our data (figures 26 and 28), we envision that using CAR T cells in combination with an IDO inhibitor or a sub-optimal dose of chemotherapy will improve efficacy and persistence of CAR T cells in vivo.

Cancer rates throughout the world are increasing at an alarming rate. Yet, we have not seen a significant change in the standard of care treatment options. It is time to bring cancer research to the 21st century through the exploration of novel therapies including immunotherapy. We have already witnessed the potential benefits of immunotherapy, with the use of antibodies and T cell therapies, in treating multiple cancers. We are at the forefront of an era in cancer research and treatment where we no longer have to rely solely on surgery, radiotherapy, and chemotherapy. The time for immunotherapy is here, and the potential is bright.

6.2 Appendix

6.2.1 DNA Sequences of CAR Constructs

6.2.1.1 TMUC1-CAR

ggatccGGATTAGTCCAATTTGTTAAAGACAGGATATCAGTGGTCCAGGCTCTAGTTTTGACTCA
ACAATATCACCAGCTGAAGCCTATAGAGTACGAGCCATAGATAAAAATAAAAGATTTTATTTAG
TCTCCAGAAAAAGGGGGGAATGAAAGACCCACCTGTAGGTTTGGCAAGCTAGCTTAAGTAA
CGCCATTTTGAAGGCATGGAAAAATACATAACTGAGAATAGAGAAGTTCAGATCAAGGTCA
GGAACAGATGGAACAGCTGAATATGGGCCAAACAGGATATCTGTGGTAAGCAGTTCCTGCCC
CGGCTCAGGGCCAAGAACAGATGGAACAGCTGAATATGGGCCAAACAGGATATCTGTGGTAA
GCAGTTCCTGCCCCGGCTCAGGGCCAAGAACAGATGGTCCCCAGATGCGGTCCAGCCCTCAGC
AGTTTCTAGAGAACCATCAGATGTTTCCAGGGTGCCCCAAGGACCTGAAATGACCCTGTGCCT
TATTTGAACTAACCAATCAGTTCGCTTCTCGCTTCTGTTTCGCGCGCTTCTGCTCCCCGAGCTCA
ATAAAAGAGCCCACAACCCCTCACTCGGGGCGCCAGTCTCCGATTGACTGAGTCGCCCCGGT
ACCCGTGTATCCAATAAACCCCTCTTGCAGTTGCATCCGACTTGTGGTCTCGCTGTTCTTGGGA
GGGTCTCCTCTGAGTGATTGACTACCCGTCAGCGGGGGTCTTTCACACATGCAGCATGTATCA
AAATTAATTTGGTTTTTTTTTCTTAAGTATTTACATTAATGGCCATAGTACTTAAAGTTACATT
GGCTTCCTTGAATAAACATGGAGTATTCAGAATGTGTCATAAATATTTCTAATTTTAAAGATA
GTATCTCCATTGGCTTTCTACTTTTTCTTTATTTTTTTTTTGTCTCTGTCTTCCATTTGTTGTTG
TGTTGTTTGTGTTGTTGTTGTTGTTGTTGTTGTTGTTGTTGTTGTTGTTGTTGTTGTTGTTGTTG
TCAAGCTAGACTATTAGCTACTCTGTAACCCAGGGTGACCTTGAAGTCATGGGTAGCCTGCTG
TTTTAGCCTTCCCACATCTAAGATTACAGGTATGAGCTATCATTTTTGGTATATTGATTGATTG
ATTGATTGATGTGTGTGTGTGTGATTGTGTTTGTGTGTGTGACTGTGAAAATGTGTGTATGGGT
GTGTGTGAATGTGTGTATGTATGTGTGTGTGTGAGTGTGTGTGTGTGTGTGTGTGTGTGTGT
GTGTGACTGTGTCTATGTGTATGACTGTGTGTGTGTGTGTGTGTGTGTGTGTGTGTGTGTGTGT
GTGTGTGTTGTGAAAAAATATTCTATGGTAGTGAGAGCCAACGCTCCGGCTCAGGTGTCAGGT
TGGTTTTTGAGACAGAGTCTTTCACTTAGCTTGGAATTCactggccgtcgtttacaacgtcgtgactgggaaaacct
ggcgttacccaactaatgccttgcagcacatcccccttccagctggcgtaatagcgaagagcccgcaccgatgcaccttccaacagttgcgag
cctgaatggcgaatggcgcctgatgcggtatfttctcttacgcatctgtgcggtatftcacaccgcatatggtgcaactctcagtacaatctgctctgatccgc
atagtttaagccagccccgacaccgccaacaccgctgacgcgccctgacggcctgtctgctcccgcacccttacagacaagctgtgaccgtctcc
gggagctgcatgtgtagaggtttaccgctacccgaaacgcgcgatgacgaaaggcctcgtgatacgcctatftttataggtaatgtcatgataataa
tggttcttagacgtcaggtggcactttcgggaaatgtgcgcggaaccctatftggtatfttttaataacattcaaatatgtatccgctcatgagacaataa
cctgataaatgctcaataatattgaaaaggagatgatgattcaacattccgtgctgcccttattccctttttggcgcatttgccttctgttttgcac
ccagaacgctggtgaaagtataatgatgagatcagttgggtgacagagtggttacatcgaactggatctcaacagcggtaagatccttgagagttt
cgccccgaagaacgtttccaatgatgacacttttaagtctgctatgtggcgcggtattatcccgtattgacgccgggcaagagcaactcggcgcgca
tacactattctcagaatgactggtgagtactaccagtcacagaaaagcatctacggatgcatgacagtaagagaattatgcagtgctgccataacctg
agtataacactgcccgaacttacttctgacaacgacggaggaccgaaggagcgaaccgctttttgcaacaacatgggggatcatgtaactcgcctgac
gttgggaaccggagctgaatgaagccataccaacgacgagcgtgacaccagatgctgtagcaatggcaacaacgttgcgcaaacattaactggcg
aactacttacttagcttcccggcaacaattaatagactggatggaggcgataaagttgcaggaccacttctgcgctcggcccttccggctgctggttatt
gctgataaatctggagccgtgagcgtgggtctcgcggtatcattgcagcactggggccagatggttaagccctcccgtatcgtatctacacgacggg
gagtcaggcaactatggatgaacgaaatagacagatcgtgagataggtgectcactgattaagcattggttaactgtcagaccaagtttactcatatactt
agattgattfaaaccttcttttaattaaaaggatctaggtgaagatccttttgataatctcatgacaaaaatcccctaacgtgagtttcttccactgagcgtca
gaccccgtagaaaagatcaaaagatcttctgagatcctttttctgcgcgtaatctgctgctgcaaaacaaaaaacaccgctaccagcgggtgtttgttg
ccggatcaagactaccaactcttttccgaaggtaactggctcagcagagcgcagataccaataactgtccttctagtgtagccgtagttaggccaccact
caagaactctgtagcaccgctacatactcgtctgtaactctgttaccagtggtgctgctccagtgccgataagtcgtgtctaccgggtggactcaaga
cgatagttaccgataaggcgcagcggctggcgtgaacgggggtcgtgcacacagcccagcttgagcgaacgacctacaccgaactgagatacct
acagcgtgagcattgagaaagcgcacgctcccgaaggagaaagcggacaggtatccgtaagcggcagggctggaacaggagagcgcacgag
ggagcttccaggggaaacgctggtatcttatagtcctgtcgggttccaccctctgactgagcgtcgtttttgtgatgctcgcagggggcggagc
ctatgaaaaacgccagcaacgcggccttttacggcttctgctgcttttctcactgcttatccctgattctgtgataaccgt

attaccgctttgagtgagctgataccgctcgcgcagccgaacgaccgagcgcagcagtgagcgcgaggaagcggagagcggccaatacgc
aaccgctcctccccgcggtggccgattcattaatgcagctggcagcacaggttcccactggaagcgggagtgagcgaacgcaattaatgtgagt
tagctcactcattagcaccggccttacattatgctcggctcgtatggtgtggaattgtgagcggataacaattcacacaggaaacagctatgac
catgattacgccAAGCTTTGCTCTTAGGAGTTTCTAATACATCCCAAACCTCAAATATATAAAGCATT
TGACTTGTCTATGCCCTAGGGGGCGGGGGAAGCTAAGCCAGCTTTTTTTAAACATTTAAAAT
GTTAATTCCATTTTAAATGCACAGATGTTTTTATTTCATAAGGGTTTCAATGTGCATGAATGCT
GCAATATTCCTGTTACCAAAGCTAGTATAAATAAAAATAGATAAACGTGGAAATTACTTAGAG
TTTCTGTCATTAACGTTTCCTTCCTCAGTTGACAACATAAATGCGCTGCTGAGCAAGCCAGTTT
GCATCTGTCAGGATCAATTTCCCATTTATGCCAGTCATATTAATTACTAGTCAATTAGTTGATTT
TTATTTTTGACATATACATGTGAATGAAAGACCCACCTGTAGGTTTGGCAAGCTAGCTTAAG
TAACGCCATTTTGAAGGCATGGA AAAAATACATAACTGAGAATAGAAAAGTTTCAGATCAAGG
TCAGGAACAGATGGAACAGCTGAATATGGGCCAAACAGGATATCTGTGGTAAGCAGTTTCTG
CCCCGGCTCAGGGCCAAGAACAGATGGAACAGCTGAATATGGGCCAAACAGGATATCTGTGG
TAAGCAGTTCTGCCCGGCTCAGGGCCAAGAACAGATGGTCCCCAGATGCGGTCCAGCCCTC
AGCAGTTTCTAGAGAACCATCAGATGTTTTCCAGGGTGCCCAAGGACCTGAAATGACCCCTG
CCTTATTTGAACTAACCAATCAGTTCGTTCTCGCTTCTGTTCTCGCGCTTATGCTCCCCGAGC
TCAATAAAAGAGCCCAACACCCCTCACTCGGGCGCCAGTCTCCGATTGACTGAGTCGCCCCG
GGTACCCGTGTATCCAATAAACCCCTCTGTCAGTTGCATCCGACTTGTGGTCTCGCTGTTCTTG
GGAGGGTCTCCTCTGAGTGATTGACTACCCGTCAGCGGGGTCTTTCAATTTGGGGGCTCGTCC
GGGATCGGGAGACCCCTGCCAGGGACCACCGACCCACCACCGGGAGGTAAGCTGGCCAGCA
ACTTATCTGTGTCTGTCCGATTGTCTAGTGTCTATGACTGATTTTATGCGCCTGCGTCCGTTACT
AGTTAGCTAACTAGCTCTGTATCTGGCGGACCCGTGGTGGAACTGACGAGTTCCGGAACACCCG
GCCGCAACCCTGGGAGACGTCCAGGGACTTCGGGGGCGCTTTTTGTGGCCCGACCTGAGTCC
TAAAATCCCGATCGTTTAGGACTCTTTGGTGCACCCCTTAGAGGAGGGATATGTGGTTCTG
GTAGGAGACGAGAACCTAAAACAGTTCCCGCCTCCGTCTGAATTTTTGCTTTCCGTTTGGGAC
CGAAGCCGCGCCGCGCTTGTCTGCTGCAGCATCGTTCTGTGTTGTCTCTGTCTGACTGTGT
TTCTGTATTTGTCTGAAAATATGGGCCCGGGCTAGactgttaccactCCCTAAGTTTACCTTAGGTC
ACTGGAAGATGTGAGCGGATCGCTACAACCAGTCGGTAGATGTCAAGAAGAGACGTTGG
GTTACCTTCTGCTCTGCAGAATGGCCAACCTTTAACGTCCGATGGCCGCGAGACGGCACCTTT
AACCGAGACCTCATCACCCAGGTTAAGATCAAGGTCTTTTACCTGGCCCGCATGGACACCCA
GACCAGGTcccTACATCGTGACCTGGGAAGCCTTGGCTTTTGACCCCTCCCTGGGTCAAGCC
CTTTGTACACCCTAAGCCTCCGCCTCCTTCTCCATCCGCCCGTCTCTCCCCCTTGAACCTC
CTCGTTGACCCCGCCTCGATCCTCCCTTTATCCAGCCCTCACTCCTTCTTAGGCGCCCCCAT
ATGGCCATATGAGATCTTATATGGGGCACCCCGCCCTTGTAACCTTCCCTGACCCTGACAT
GACAAGAGTTACTAACAGCCCTCTCTCCAAGCTCACTTACAGGCTCTCTACTTAGTCCAGCA
CGAAGTCTGGAGACCTCTGGCGGCAGCCTACCAAGAACAACCTGGACCGACCGGTGGTACCTC
ACCTTACCGAGTCGGCGACACAGTGTGGGTCCGCCGACACCAGACTAAGAACCTAGAACCT
CGCTGGAAGGACCTTACACAGTCTGCTGACCACCCCAACCGCCCTCAAAGTAGACGGCAG
GCAGCTTGATACACGCCGCCACGTGAAGGCTGCCGACCCCGGGGTGGACCATCCTCTAG
ACTGCcATGGCCCTGCCCGTGACCGCCCTGCTTCTGCCCCTGGCCCTTCTGCTCCACGCCGCCA
GACCCGAGGTGCAGCTGCAGCAGAGCGGAGGCGAGAGGCCACCCCTGGCGCCAGCGTGAA
GATGAGCTGCAAGACCAGCGGCTACACCTTACCAACTACTGGATGCACTGGGTGAAGCAGA
GACCCGGCCAGGGCCTGGAGTGGATCGGCTACATCAACCCTAGCTCCGGCTACACCCAGTAC
AACCAGAAGTTCAAGGACAAGGCCACCTGACCGCCGACAAGAGCTCCAGCACCGCCTACAT
CCAGCTGAGCTCCCTGACCAGCGAGGACTCCGCCGTGACTATTGCAGCACCTACTACGGCGA
CTACCTGTTCCCTACTGGGGCCAGGGCACCTGGTGACCGTGAGCGCCGGCGGAGGCGGAA
GCGGAGGCGGCGGATCCGGAGGAGGCGGCAGCGACGTGCTGATGACCCAGACCCCTCTGAGC
CTGCCCGTGAGCCTGGGCGACCAGGCCAGCATCAGCTGCAGAAGCTCCCAGGACATCGTGTA
CGGCAACGGAAACACCTACCTGGAGTGGTACCTCCAGAAGCCCGGCCAGAGCCCCAAGCTGC
TGATCTACAAGGTGAGCAACAGATTACGCGCGTGCCCGACAGATTACGCGGCTCCGGAAGC
GGAACCGACTTACCCCTGAAGATCAGCAGAGTGGAGGCCGAGGACCTGGGCGTGTACTATTG
CTTCCAGGGCAGCCACGTGCCCTACACCTTCGGCGGAGGCCACCAAGCTGGAGATCAAGAGAG
CGGCCGCTATCGAGGTGGAGCAGAAGCTGATCAGCGAGGAGGACCTGCTAGACAATGAGAAG
AGCAATGGAACCATTATCCATGTGAAAGGGAAACACCTTTGTCCAAGTCCCCTATTTCCCGGA
CCTTCTAAGCCCTTTTGGGTGCTGGTGGTGGTGGTGGAGTCTGGCTTGCTATAGCTTGCTAG

TAACAGTGGCCTTTATTATTTTCTGGGTGAGGAGTAAGAGGAGCAGGCTCCTGCACAGTGACT
ACATGAACATGACTCCCCGCCGCCCGGGCCACCCGCAAGCATTACCAGCCCTATGCCCCAC
CACGCGACTTCGCAGCCTATCGCTCCAGAGTGAAGTTCAGCAGGAGCGCAGACGCCCCCGCG
TACCAGCAGGGCCAGAACCAGCTCTATAACGAGCTCAATCTAGGACGAAGAGAGGAGTACGA
TGTTTTGGACAAGAGACGTGGCCGGGACCCTGAGATGGGGGGAAAGCCGAGAAGGAAGAAC
CCTCAGGAAGGCCTGTACAATGAACTGCAGAAAGATAAGATGGCGGAGGCCTACAGTGAGAT
TGGGATGAAAGGCGAGCGCCGGAGGGGCAAGGGGCACGATGGCCTTTACCAGGGTCTCAGTA
CAGCCACCAAGGACACCTACGACGCCCTTACATGCAGGCCCTGCCCCCTCGCTAACAGCCAC
TCGAG

6.2.1.2 CTL-CAR

AGGTATGAGCTATCATTTTTGGTATATTGATTGATTGATTGATTGATGTGTGTGTGTGATTG
TGTTTGTGTGTGTGACTGTGAAAATGTGTGTATGGGTGTGTGTGAATGTGTGTATGTATGTGTG
TGTGTGAGTGTGTGTGTGTGTGTGTGCATGTGTGTGTGTGTGACTGTGTCTATGTGTATGACTG
TGAAAAAATATTCTATG
GTAGTGAGAGCCAACGCTCCGGCTCAGGTGTCAGGTTGGTTTTTGAGACAGAGTCTTTCACTT
AGCTTGAATTCACTGGCCGTCGTTTTACAACGTCGTGACTGGGAAAACCCTGGCGTTACCCA
ACTTAATCGCCTTGCAGCACATCCCCCTTTCGCCAGCTGGCGTAATAGCGAAGAGGCCCGCAC
CGATCGCCCTTCCCAACAGTTGCGCAGCCTGAATGGCGAATGGCGCCTGATGCGGTATTTTCT
CCTTACGCATCTGTGCGGTATTTACACCCGCATATGGTGCCTCTCAGTACAATCTGCTCTGAT
GCCGCATAGTTAAGCCAGCCCCGACACCCGCCAACACCCGCTGACGCGCCCTGACGGGCTTGT
CTGCTCCCGCATCCGCTTACAGACAAGCTGTGACCGTCTCCGGGAGCTGCATGTGTCAGAGG
TTTTACCGTCATCACCGAAACGCGGATGACGAAAGGGCCTCGTGATACGCTATTTTTATA
GGTTAATGTCATGATAATAATGGTTTCTTAGACGTCAGGTGGCACTTTTCGGGGAAATGTGCG
CGGAACCCCTATTTGTTTATTTTTCTAAATACATTCAAATATGTATCCGCTCATGAGACAATAA
CCCTGATAAATGCTTCAATAATATTGAAAAAGGAAGAGTATGAGTATTCAACATTTCCGTGTC
GCCCTTATCCCTTTTTTTCGGGCATTTTGCCTTCTGTTTTTGCTCACCCAGAAACGCTGGTGAA
AGTAAAAGATGCTGAAGATCAGTTGGGTGCACGAGTGGGTTACATCGAACTGGATCTCAACA
GCGGTAAGATCCTTGAGAGTTTTTCGCCCCGAAGAACGTTTTTCCAATGATGAGCACTTTTAAAG
TTCTGCTATGTGGCGCGGTATTATCCCGTATTGACGCCGGGCAAGAGCAACTCGGTGCGCCGA
TACACTATTCTCAGAATGACTTGGTTGAGTACTACCAGTACAGAAAAGCATCTTACGGATG
GCATGACAGTAAGAGAATTATGCAGTGTGCCATAACCATGAGTGATAACAACTGCGGCCAAC
TACTTCTGACAACGATCGGAGGACCGAAGGAGCTAACCGTTTTTTGCACAACATGGGGGAT
CATGTAACCTCGCCTTGATCGTTGGGAACCGGAGCTGAATGAAGCCATAACCAACGACGAGCG
TGACACCACGTGCCTGTAGCAATGGCAACAACGTTGCGCAAACCTATTAAGTGGCGAACTACT
TACTCTAGCTTCCCGGCAACAATTAATAGACTGGATGGAGGCGGATAAAGTTGCAGGACCACT
TCTGCGCTCGGCCCTTCCGGCTGGCTGGTTTATTGCTGATAAATCTGGAGCCGGTGAGCGTGG
GTCTCGCGGTATCATTGCAGCACTGGGGCCAGATGGTAAGCCCTCCCGTATCGTAGTTATCTA
CACGACGGGGAGTCAAGCAACTATGGATGAACGAAATAGACAGATCGCTGAGATAGGTGCCT
CACTGATTAAGCATTGGTAACTGTCAGACCAAGTTTACTCATATATACTTTAGATTGATTTAA
ACTTCATTTTTAATTTAAAAGGATCTAGGTGAAGATCCTTTTTTGATAATCTCATGACCAAAATC
CCTAACGTGAGTTTTTCGTTCCACTGAGCGTCAGACCCCGTAGAAAAGATCAAAGGATCTTCT
TGAGATCCTTTTTTCTGCGCGTAATCTGCTGCTTGCAAACAAAAAAACCACCGCTACCAGCG
GTGTTTTGTTTCCGGATCAAGAGCTACCAACTCTTTTTCCGAAGGTAAGTGGCTTACAGCAGA
GCGCAGATAACCAATACTGTCCTTCTAGTGTAGCCGTAGTTAGGCCACCACTTCAAGAACTCT
GTAGCACCGCCTACATACTCGCTCTGCTAATCCTGTTACCAGTGGCTGCTGCCAGTGGCGAT
AAGTCGTGTCTTACCGGGTTGACTCAAGACGATAGTTACCGGATAAGGCGCAGCGGTGCGG
CTGAACGGGGGGTTCGTGCACACAGCCAGCTTGGAGCGAACGACCTACACCGAACTGAGAT
ACCTACAGCGTGAGCATTGAGAAAGCGCCACGCTTCCCGAAGGGAGAAAGGCGGACAGGTAT
CCGGTAAGCGGCAGGGTCGGAACAGGAGAGCGCACGAGGGAGCTTCCAGGGGGAAACGCCT
GGTATCTTTATAGTCTGTGCGGTTTTGCCACCTCTGACTTGAGCGTCGATTTTTGTGATGCTC
GTCAGGGGGGCGGAGCCTATGAAAAACGCCAGCAACGCGGCCTTTTTACGGTTCCTGGCCTT

TTGCTGGCCTTTTGTCTACATGTTCTTTCCTGCGTTATCCCCTGATTCTGTGGATAACCGTATTA
CCGCCTTTGAGTGAGCTGATACCGCTCGCCGACCCGAACGACCGAGCGCAGCGAGTCAGTG
AGCGAGGAAGCGGAAGAGCGCCAATACGCAAACCGCTCTCCCCGCGGTTGGCCGATTCA
TTAATGCAGCTGGCACGACAGGTTTCCCAGCTGGAAAGCGGGCAGTGAGCGCAACGCAATTA
ATGTGAGTTAGCTACTCATTAGGCACCCAGGCTTACACTTTATGCTTCCGGCTCGTATGTT
GTGTGGAATTGTGAGCGGATAACAATTTACACAGGAAACAGCTATGACCATGATTACGCCA
AGCTTTGCTCTTAGGAGTTTCTAATACATCCCAAACCTCAAATATATAAAGCATTGACTTGT
CTATGCCCTAGGGGGCGGGGGAAGCTAAGCCAGCTTTTTTTAAACATTTAAAATGTTAATTCC
ATTTTAAATGCACAGATGTTTTTATTTTATAAGGGTTTCAATGTGCATGAATGCTGCAATATTC
CTGTTACCAAAGCTAGTATAAATAAAAAATAGATAAACGTGGAAATTACTTAGAGTTTCTGTCA
TTAACGTTTCTTCTCAGTTGACAACATAAATGCGCTGCTGAGCAAGCCAGTTTGCATCTGTC
AGGATCAATTTCCATTATGCCAGTCATATTAATTACTAGTCAATTAGTTGATTTTTATTTTTG
ACATATACATGTGAATGAAAGACCCACCTGTAGGTTTGGCAAGCTAGCTTAAGTAACGCCAT
TTTGCAAGGCATGGAAAAATACATAACTGAGAATAGAAAAGTTCAGATCAAGGTCAGGAACA
GATGGAAACAGCTGAATATGGGCCAAACAGGATATCTGTGGTAAGCAGTTCCTGCCCGGCTC
AGGGCCAAGAACAGATGGAAACAGCTGAATATGGGCCAAACAGGATATCTGTGTAAGCAGT
CCTGCCCGGCTCAGGGCCAAGAACAGATGGTCCCCAGATGCGGTCCAGCCCTCAGCAGTTT
TAGAGAACCATCAGATGTTTCCAGGGTGCCCCAAGGACCTGAAATGACCCTGTGCCTTATTTG
AACTAACCAATCAGTTCGCTTCTCGCTTCTGTTTCGCGCTTATGCTCCCCGAGCTCAATAAAA
GAGCCCAACCCCTCACTCGGGGCGCCAGTCCCTCCGATTGACTGAGTCGCCCGGGTACCCGT
GTATCCAATAAACCCCTCTTGCAGTTGCATCCGACTTGTGGTCTCGCTGTTCCCTTGGGAGGGTCT
CCTCTGAGTGATTGACTACCCGTGAGCGGGGGTCTTTCATTTGGGGGCTCGTCCGGGATCGGG
AGACCCCTGCCAGGGACACCGACCCACCACCGGGAGGTAAGCTGGCCAGCAACTTATCTG
TGTCTGCCGATTGTCTAGTGTCTATGACTGATTTTATGCGCCTGCGTCCGTTACTAGTTAGCTA
ACTAGCTCTGTATCTGGCGGACCCGTGGTGGAACTGACGAGTTCGGAACACCCGGCCGCAACC
CTGGGAGACGTCCCAGGGACTTCGGGGGCCGTTTTTGTGGCCGACCTGAGTCTAAAATCCC
GATCGTTTAGGACTCTTTGGTGCACCCCTTAGAGGAGGGATATGTGGTCTGGTAGGAGAC
GAGAACCTAAAACAGTTCGCCCTCCGTCTGAATTTTTGCTTTCGGTTTGGGACCGAAGCCGC
GCCGCGCTTGTCTGCTGCAGCATCGTCTGTGTTGTCTGTCTGACTGTGTTTCTGTATT
GTCTGAAAATATGGGCCCGGGCTAGACTGTTACCACTCCCTAAGTTTGACCTTAGGTCACTG
GAAAGATGTCGAGCGGATCGCTCACAACCAGTCCGTAGATGTCAAGAAGAGACGTTGGGTTA
CCTTCTGCTCTGCAGAATGGCCAACCTTTAACGTCCGATGGCCGCGAGACGGCACCTTTAACC
GAGACCTCATCACCCAGGTTAAGATCAAGGTCTTTTACCTGGCCCGCATGGACACCCAGACC
AGGTCCCCTACATCGTGACCTGGGAAGCCTTGGCTTTTACCCCTCCCTGGGTCAAGCCCTT
TGTACACCCTAAGCCTCCGCTCCTCTTCTCCATCCGCCCGTCTCTCCCCCTTGAACCTCCT
GTTCCAGCCCGCTCGATCCTCCCTTATCCAGCCCTCACTCCTTCTCTAGGCGCCCCATATG
GCCATATGAGATCTTATATGGGGCACCCCGCCCTTGTAACTTCCCTGACCTGACATGAC
AAGAGTTACTAACAGCCCCTCTCTCAAGCTCACTTACAGGCTCTCTACTTAGTCCAGCACGA
AGTCTGGAGACCTCTGGCGGCAGCCTACCAAGAACAACCTGGACCGACCGGTGGTACCTCAC
CTTACCAGTTCGGCGACACAGTGTGGTCCGCCGACACCAAGACTAAGAACCTAGAACCTCGC
TGGAAAGGACCTTACACAGTCTGCTGACCACCCCAACCGCCCTCAAAGTAGACGGCATCGCA
GCTTGGATACACGCCGCCACGTGAAGGCTGCCGACCCCGGGGTGGACCATCTCTAGACTG
CCatggcctgcccgtgaccgacctgctcttggccttggccttctgctccacgccgagaccgaggtgcagctgcagcagagcggaggcaggg
cggaggcaccagctggagatcaagagagcggccgctatcgaggtggagcagaagctgatcagcgaggagacctgctagacaatgagaagcaat
ggaaccattatccatgtgaaagggaacaccttgtccaagtcccctatttcccgaccttctaagccctttgggtgctggtggtggtgagctcctgct
tgctatagcttgctagtaacagtgcccttattatfttgggtgaggagtaagaggagcaggtcctgcacagtgactacatgaacatgactccccgccgccc
eggccccaccgcaagcattaccagccctatgccccaccagcgacttgcagcctatcctccagagtgaagttcagcaggagcgcagacgccccg
cgtaccagcagggccagaaccaactctataacgagctcaatctaggacgaagagaggagtacgatgtttggacaagagacgtggccgggacctgaga
tggggggaaagccgagaaggaagaacctcaggaaggcctgtacaatgaactgcagaagataagatggcgaggcctacagtgagattggatgaa
aggcgagcggcggaggggcaaggggcacgatggccttaccaggtctcagtagcaccaccaaggacacctacgacgaccttccatgagccctg
ccccctgctaaCAGCCACTCGAGGGATCCGGATTAGTCCAATTTGTTAAAGACAGGATATCAGTGG
TCCAGGCTCTAGTTTTGACTCAACAATATCACCAGCTGAAGCCTATAGAGTACGAGCCATAGA
TAAAATAAAAGATTTTATTTAGTCTCCAGAAAAAGGGGGGAATGAAAGACCCACCTGTAGG
TTTGGCAAGCTAGCTTAAGTAACGCCATTTTGAAGGCATGGAAAAATACATAACTGAGAATA
GAGAAGTTCAGATCAAGGTCAGGAACAGATGGAACAGCTGAATATGGGCCAAACAGGATATC

CCTCGATCCTCCCTTTATCCAGCCCTCACTCCTTCTCTAGGCGCCCCATATGGCCATATGAGA
TCTTATATGGGGCACCCCGCCCTTGTAACTTCCCTGACCCTGACATGACAAGAGTTACTA
ACAGCCCCTCTCTCCAAGCTCACTTACAGGCTCTCTACTTAGTCCAGCACGAAGTCTGGAGAC
CTCTGGCGGCAGCCTACCAAGAACAACCTGGACCGACCGGTGGTACCTCACCTTACCGAGTCG
GCGACACAGTGTGGGTCCGCCGACACCAGACTAAGAACCTAGAACCTCGCTGGAAAGGACCT
TACACAGTCTGCTGACCACCCCAACGCCCTCAAAGTAGACGGCATCGCAGCTTGGATACAC
GCCGCCACGTGAAGGCTGCCGACCCCGGGGTGGACCATCTCTAGACTGCCATGGCCCTGC
CCGTGACCGCCCTGCTCTTGCCCTGGCCCTTCTGCTCCACGCCGCCAGACCCGAGGTGCAGC
TGCAGCAGAGCGGAGGCGAGAGAGCCACCCCTGGCGCCAGCGTGAAGATGAGCTGCAAGAC
CAGCGGTACACCTTACCAACTACTGGATGCACTGGGTGAAGCAGAGACCCGGCCAGGGCC
TGGAGTGGATCGGCTACATCAACCCTAGCTCCGGCTACACCCAGTACAACCAGAAGTTCAAG
GACAAGGCCACCCTGACCGCCGACAAGAGCTCCAGCACCGCTACATCCAGCTGAGCTCCCT
GACCAGCGAGGACTCCGCCGTGACTATTGCAGCACCTACTACGGCGACTACCTGTTCCCTA
CTGGGGCAGGGCACCCCTGGTACCCTGAGCGCCGGCGGAGGCGGAAGCGGAGGCGGCGGA
TCCGAGAGGCGGCAGCGACGTGCTGACTGACCCAGACCCCTCTGAGCTGCCCTGAGCCCT
GGCGACCGCCAGCCAGCATCAGCTGCAGAAGCTCCAGGACATCGTGTACGGCAACGGAACA
CCTACCTGGAGTGGTACCTCCAGAAGCCCGGCCAGAGCCCAAGCTGCTGATCTACAAGGTG
AGCAACAGATTACGCGCGTGCCCGACAGATTACGCGGCTCCGGAAGCGGAACCGACTTCAC
CCTGAAGATCAGCAGAGTGGAGGCCGAGGACCTGGGCGTGTACTATTGCTTCCAGGGCAGCC
ACGTGCCCTACACCTTCGGCGGAGGCACCAAGCTGGAGATCAAGAGAGCGGCCGCCATCGAG
GTGGAGCAGAAGCTGATCAGCGAGGAGGACCTGCTGGACAACGAGAAGAGCAACGGCACCA
TCATCCACGTGAAGGGCAAGCACCTGTGCCCCAGCCCCCTGTTCCCCGGCCCCAGCAAGCCCT
TCTGGGTGCTGGTGGTGGTGGGCGGCGTGTGCTGACAGCCTGCTGGTACCCTGGCCCT
TCATCATCTTCTGGGTGCGGAGCAAGCGGAGCCGGCTGCTGCACAGCGACTACATGAACATG
ACCCCGCGGCGCCTGGGCCACCCGCAAGCATTACCAGCCCTATGCCCCACCACGCGACTTC
GCAGCCTATCGCTCCAGAGTGAAGTTCAGCAGGAGCGCAGACGCCCCGCGTACCAGCAGGG
CCAGAACCAGCTCTATAACGAGCTCAATCTAGGACGAAGAGAGGAGTACGATGTTTTGGACA
AGAGACGTGGCCGGACCCTGAGATGGGGGAAAGCCGAGAAGGAAGAACCCTCAGGAAGG
CCTGTACAATGAACTGCAGAAAGATAAGATGGCGGAGGCCTACAGTGAAGTGGGATGAAAG
GCGAGCGCCGGAGGGGCAAGGGGCACGATGGCCTTACCAGGGTCTCAGTACAGCCACCAAG
GACACCTACGACGCCCTTCACATGCAGGCCCTGCCCCCTCGCGCCCCGAGGCGCAGCAGCGGG
AGCAGGAGGAGCAGGTGCAATGGTGAAGCGAGCTGATTAAGGAGAACATGCACATGAAGCTGT
ACATGGAGGGCACCGTGAACAACCACCACTTCAAGTGCACATCCGAGGGCGAAGGCAAGCCC
TACGAGGGCACCCAGACCATGAGAATCAAGGCGGTGAGGGCGGCCCTCTCCCTTCGCCTTC
GACATCCTGGCTACCAGCTTCATGTACGGCAGCAAAACCTTCATCAACCACCCAGGGC
CCCGACTTCTTTAAGCAGTCTTCCCCGAGGGCTTACATGGGAGAGAGTACCACATACGAA
GACGGGGGCGTGTGACCGCTACCCAGGACACCAGCCTCCAGGACGGCTGCCTCATCTACAA
CGTCAAGATCAGAGGGGTGAACCTCCCATCCAACGGCCCTGTGATGCAGAAGAAAACACTCG
GCTGGGAGGCCTCCACCGAGACCCTGTACCCCGTACGCGCGCCTGGAAGGCAGAGCCGAC
ATGGCCCTGAAGCTCGTGGGCGGGGCCACCTGATCTGCAACTTGAAGACCACATACAGATC
CAAGAAACCCGCTAAGAACCTCAAGATGCCCGCGTCTACTATGTGGACAGAAGACTGGAAA
GAATCAAGGAGGCCGACAAAGAGACCTACGTCGAGCAGCAGAGGTGGCTGTGGCCAGATAC
TGCGACCTCCCTAGCAAACTGGGGCACAGATGAGGGATCCGGATTAGTCCAATTTGTTAAAGA
CAGGATATCAGTGGTCCAGGCTCTAGTTTTGACTCAACAATATCACCAGCTGAAGCCTATAGA
GTACGAGCCATAGATAAAAATAAAAGATTTTTATTTAGTCTCCAGAAAAAGGGGGGAATGAAAG
ACCCACCTGTAGGTTTGGCAAGCTAGCTTAAAGTAACGCCATTTTGCAAGGCATGGAAAAATA
CATAACTGAGAATAGAGAAGTTCAGATCAAGGTCAGGAACAGATGGAACAGCTGAATATGGG
CCAAACAGGATATCTGTGGTAAGCAGTTCCTGCCCCGGCTCAGGGCCAAGAACAGATGGAAC
AGCTGAATATGGGCCAAACAGGATATCTGTGGTAAGCAGTTCCTGCCCCGGCTCAGGGCCAA
GAACAGATGGTCCCCAGATGCGGTCCAGCCCTCAGCAGTTTCTAGAGAACCATCAGATGTTTC
CAGGGTGCCCCAAGGACCTGAAATGACCCTGTGCCTTATTTGAACTAACCAATCAGTTCGCTT
CTCGCTTCTGTTTCGCGCGCTTCTGCTCCCCGAGCTCAATAAAAGAGCCACAACCCCTCACTCG
GGGCGCCAGTCTCCGATTGACTGAGTCGCCCGGTACCCGTGTATCCAATAAACCCCTCTTGC
AGTTGCATCCGACTTGTGGTCTCGCTGTTCTTGGGAGGGTCTCCTCTGAGTGATTGACTACCC
GTCAGCGGGGTCTTTCACACATGCAGCATGTATCAAAATTAATTTGGTTTTTTTTCTTAAGTA

6.3 References

1. Gittes, G.K., *Developmental biology of the pancreas: A comprehensive review*. Developmental Biology, 2009. **326**(1): p. 4-35.
2. Puri, S., Alexandra E. Folias, and M. Hebrok, *Plasticity and Dedifferentiation within the Pancreas: Development, Homeostasis, and Disease*. Cell Stem Cell, 2015. **16**(1): p. 18-31.
3. Williams, J.A., *Regulation of acinar cell function in the pancreas*. Current opinion in gastroenterology, 2010. **26**(5): p. 478-483.
4. Hellman, B.O., *Actual Distribution of the Number and Volume of the Islets of Langerhans in Different Size Classes in Non-diabetic Humans of Varying Ages*. Nature, 1959. **184**(4697): p. 1498-1499.
5. Mastracci, T.L. and L. Sussel, *The Endocrine Pancreas: insights into development, differentiation and diabetes*. Wiley interdisciplinary reviews. Membrane transport and signaling, 2012. **1**(5): p. 609-628.
6. Gromada, J., I. Franklin, and C.B. Wollheim, *Alpha-cells of the endocrine pancreas: 35 years of research but the enigma remains*. Endocr Rev, 2007. **28**(1): p. 84-116.
7. Cnop, M., et al., *Mechanisms of Pancreatic β -Cell Death in Type 1 and Type 2 Diabetes*. Diabetes, 2005. **54**(suppl 2): p. S97.
8. Ludvigsen, E., *Somatostatin receptor expression and biological functions in endocrine pancreatic cells: review based on a doctoral thesis*. Ups J Med Sci, 2007. **112**(1): p. 1-20.
9. Müller, T.D., et al., *Ghrelin*. Molecular metabolism, 2015. **4**(6): p. 437-460.
10. Da Silva Xavier, G., *The Cells of the Islets of Langerhans*. J Clin Med, 2018. **7**(3).
11. philschatz, *Anatomy and physiology. Chapter 23*. Vol. Chapter 23.
12. Kindler, H.L., *A Glimmer of Hope for Pancreatic Cancer*. New England Journal of Medicine, 2018. **379**(25): p. 2463-2464.
13. Siegel, R.L., K.D. Miller, and A. Jemal, *Cancer statistics, 2016*. CA: A Cancer Journal for Clinicians, 2016. **66**(1): p. 7-30.
14. Rahib, L., et al., *Projecting Cancer Incidence and Deaths to 2030: The Unexpected Burden of Thyroid, Liver, and Pancreas Cancers in the United States*. Cancer Research, 2014.
15. Kamisawa, T., et al., *Pancreatic cancer*. The Lancet, 2016. **388**(10039): p. 73-85.
16. Sharma, C., et al., *Advances in diagnosis, treatment and palliation of pancreatic carcinoma: 1990-2010*. World journal of gastroenterology, 2011. **17**(7): p. 867-897.
17. DiMagno, E.P., *Pancreatic cancer: clinical presentation, pitfalls and early clues*. Ann Oncol, 1999. **10 Suppl 4**: p. 140-2.
18. Griffin, J.F., K.E. Poruk, and C.L. Wolfgang, *Pancreatic cancer surgery: past, present, and future*. Chinese journal of cancer research = Chung-kuo yen cheng yen chiu, 2015. **27**(4): p. 332-348.
19. Paulson, A.S., et al., *Therapeutic advances in pancreatic cancer*. Gastroenterology, 2013. **144**(6): p. 1316-26.
20. Chiaravalli, M., M. Reni, and E.M. O'Reilly, *Pancreatic ductal adenocarcinoma: State-of-the-art 2017 and new therapeutic strategies*. Cancer Treat Rev, 2017. **60**: p. 32-43.
21. Conroy, T., et al., *FOLFIRINOX versus Gemcitabine for Metastatic Pancreatic Cancer*. New England Journal of Medicine, 2011. **364**(19): p. 1817-1825.
22. Marthey, L., et al., *FOLFIRINOX for locally advanced pancreatic adenocarcinoma: results of an AGEO multicenter prospective observational cohort*. Ann Surg Oncol, 2015. **22**(1): p. 295-301.
23. Koido, S., et al., *Current Immunotherapeutic Approaches in Pancreatic Cancer*. Clinical and Developmental Immunology, 2011. **2011**: p. 15.
24. Plate, J.M., *Advances in therapeutic vaccines for pancreatic cancer*. Discov Med, 2012. **14**(75): p. 89-94.
25. Yu, Y. and J. Cui, *Present and future of cancer immunotherapy: A tumor microenvironmental perspective*. Oncology letters, 2018. **16**(4): p. 4105-4113.
26. Brigger, I., C. Dubernet, and P. Couvreur, *Nanoparticles in cancer therapy and diagnosis*. Advanced Drug Delivery Reviews, 2012. **64**: p. 24-36.

27. Adamska, A., A. Domenichini, and M. Falasca, *Pancreatic Ductal Adenocarcinoma: Current and Evolving Therapies*. International journal of molecular sciences, 2017. **18**(7): p. 1338.
28. Delpu, Y., et al., *Genetic and epigenetic alterations in pancreatic carcinogenesis*. Curr Genomics, 2011. **12**(1): p. 15-24.
29. Garrido-Laguna, I. and M. Hidalgo, *Pancreatic cancer: from state-of-the-art treatments to promising novel therapies*. Nature Reviews Clinical Oncology, 2015. **12**: p. 319.
30. Vincent, A., et al., *Pancreatic cancer*. The Lancet, 2011. **378**(9791): p. 607-620.
31. Maitra, A. and R.H. Hruban, *Pancreatic Cancer*. Annual Review of Pathology: Mechanisms of Disease, 2008. **3**(1): p. 157-188.
32. Zeitouni, D., et al., *KRAS Mutant Pancreatic Cancer: No Lone Path to an Effective Treatment*. Cancers, 2016. **8**(4): p. 45.
33. Bardeesy, N. and R.A. DePinho, *Pancreatic cancer biology and genetics*. Nature Reviews Cancer, 2002. **2**(12): p. 897.
34. Yonezawa, S., et al., *Precursor lesions of pancreatic cancer*. Gut and liver, 2008. **2**(3): p. 137-154.
35. Bournet, B., et al., *Targeting KRAS for diagnosis, prognosis, and treatment of pancreatic cancer: Hopes and realities*. European Journal of Cancer, 2016. **54**: p. 75-83.
36. Bailey, P., et al., *Genomic analyses identify molecular subtypes of pancreatic cancer*. Nature, 2016. **531**: p. 47.
37. Xu, Z., et al., *Pancreatic cancer and its stroma: a conspiracy theory*. World journal of gastroenterology, 2014. **20**(32): p. 11216-11229.
38. Feig, C., et al., *The Pancreas Cancer Microenvironment*. Clinical Cancer Research, 2012. **18**(16): p. 4266.
39. Morris, J.P.t., S.C. Wang, and M. Hebrok, *KRAS, Hedgehog, Wnt and the twisted developmental biology of pancreatic ductal adenocarcinoma*. Nat Rev Cancer, 2010. **10**(10): p. 683-95.
40. Cheever, M.A., et al., *The prioritization of cancer antigens: a national cancer institute pilot project for the acceleration of translational research*. Clin Cancer Res, 2009. **15**(17): p. 5323-37.
41. Nath, S. and P. Mukherjee, *MUC1: a multifaceted oncoprotein with a key role in cancer progression*. Trends in Molecular Medicine. **20**(6): p. 332-342.
42. Nath, S. and P. Mukherjee, *MUC1: a multifaceted oncoprotein with a key role in cancer progression*. Trends Mol Med, 2014. **20**(6): p. 332-42.
43. Hollingsworth, M.A. and B.J. Swanson, *Mucins in cancer: protection and control of the cell surface*. Nat Rev Cancer, 2004. **4**(1): p. 45-60.
44. Gendler, S.J., *MUC1, the renaissance molecule*. J Mammary Gland Biol Neoplasia, 2001. **6**(3): p. 339-53.
45. Apostolopoulos, V. and I.F. McKenzie, *Cellular mucins: targets for immunotherapy*. Crit Rev Immunol, 1994. **14**(3-4): p. 293-309.
46. Kufe, D.W., *Mucins in cancer: function, prognosis and therapy*. Nature reviews. Cancer, 2009. **9**(12): p. 874-885.
47. Merlo, G.R., et al., *Frequent alteration of the DF3 tumor-associated antigen gene in primary human breast carcinomas*. Cancer Res, 1989. **49**(24 Pt 1): p. 6966-71.
48. Levitin, F., et al., *The MUC1 SEA module is a self-cleaving domain*. J Biol Chem, 2005. **280**(39): p. 33374-86.
49. Kufe, D.W., *Functional targeting of the MUC1 oncogene in human cancers*. Cancer Biol Ther, 2009. **8**(13): p. 1197-203.
50. Zhou, R., et al., *A novel association of neuropilin-1 and MUC1 in pancreatic ductal adenocarcinoma: role in induction of VEGF signaling and angiogenesis*. Oncogene, 2016.
51. Li, Y., et al., *The Epidermal Growth Factor Receptor Regulates Interaction of the Human DF3/MUC1 Carcinoma Antigen with c-Src and β -Catenin*. Journal of Biological Chemistry, 2001. **276**(38): p. 35239-35242.
52. Li, Y., et al., *The c-Src Tyrosine Kinase Regulates Signaling of the Human DF3/MUC1 Carcinoma-associated Antigen with GSK3 β and β -Catenin*. Journal of Biological Chemistry, 2001. **276**(9): p. 6061-6064.
53. Sahraei, M., et al., *MUC1 Regulates PDGFA Expression During Pancreatic Cancer Progression*. Oncogene, 2012. **31**(47): p. 4935-4945.

54. Singh, P.K. and M.A. Hollingsworth, *Cell surface-associated mucins in signal transduction*. Trends in Cell Biology, 2006. **16**(9): p. 467-476.
55. Thompson, E.J., et al., *Tyrosines in the MUC1 cytoplasmic tail modulate oncogenic signaling pathways*. Cancer Research, 2005. **65**(9 Supplement): p. 222-222.
56. Kaur, S., et al., *Mucins in pancreatic cancer and its microenvironment*. Nature reviews. Gastroenterology & hepatology, 2013. **10**(10): p. 607-620.
57. Nath, S., et al., *MUC1 induces drug resistance in pancreatic cancer cells via upregulation of multidrug resistance genes*. Oncogenesis, 2013. **2**: p. e51.
58. Roy, L.D., et al., *MUC1 enhances invasiveness of pancreatic cancer cells by inducing epithelial to mesenchymal transition*. Oncogene, 2011. **30**(12): p. 1449-59.
59. Tinder, T.L., et al., *MUC1 enhances tumor progression and contributes toward immunosuppression in a mouse model of spontaneous pancreatic adenocarcinoma*. J Immunol, 2008. **181**(5): p. 3116-25.
60. Levi, E., et al., *MUC1 and MUC2 in pancreatic neoplasia*. Journal of Clinical Pathology, 2004. **57**(5): p. 456-462.
61. Chhieng, D.C., et al., *MUC1 and MUC2 expression in pancreatic ductal carcinoma obtained by fine-needle aspiration*. Cancer, 2003. **99**(6): p. 365-71.
62. Schroeder, J.A., et al., *MUC1 overexpression results in mammary gland tumorigenesis and prolonged alveolar differentiation*. Oncogene, 2004. **23**(34): p. 5739-47.
63. Roy, L.D., et al., *A tumor specific antibody to aid breast cancer screening in women with dense breast tissue*. Genes & Cancer, 2017. **8**(3-4): p. 536-549.
64. Parham, D.M., W. Slidders, and A.J. Robertson, *Quantitation of human milk fat globule (HMFG1) expression in breast carcinoma and its association with survival*. J Clin Pathol, 1988. **41**(8): p. 875-9.
65. Curry, J.M., et al., *The use of a novel MUC1 antibody to identify cancer stem cells and circulating MUC1 in mice and patients with pancreatic cancer*. J Surg Oncol, 2013. **107**(7): p. 713-22.
66. Zhou, R., et al., *A novel association of neuropilin-1 and MUC1 in pancreatic ductal adenocarcinoma: role in induction of VEGF signaling and angiogenesis*. Oncogene, 2016: p. Epub ahead of print.
67. Moore, L.J., et al., *Antibody-Guided In Vivo Imaging for Early Detection of Mammary Gland Tumors*. Transl Oncol, 2016. **9**(4): p. 295-305.
68. OncoTAB, *OncoTAB*. Available at: <https://www.oncotab.com/about/>.
69. Marincola, F.M., et al., *Loss of HLA haplotype and B locus down-regulation in melanoma cell lines*. J Immunol, 1994. **153**(3): p. 1225-37.
70. Hanahan, D. and R.A. Weinberg, *Hallmarks of cancer: the next generation*. Cell, 2011. **144**(5): p. 646-74.
71. Mantovani, A., et al., *Macrophage polarization: tumor-associated macrophages as a paradigm for polarized M2 mononuclear phagocytes*. Trends Immunol, 2002. **23**(11): p. 549-55.
72. Zou, W., *Regulatory T cells, tumour immunity and immunotherapy*. Nat Rev Immunol, 2006. **6**(4): p. 295-307.
73. Bunt, S.K., et al., *Inflammation enhances myeloid-derived suppressor cell cross-talk by signaling through Toll-like receptor 4*. J Leukoc Biol, 2009. **85**(6): p. 996-1004.
74. Pickup, M., S. Novitskiy, and H.L. Moses, *The roles of TGFbeta in the tumour microenvironment*. Nat Rev Cancer, 2013. **13**(11): p. 788-99.
75. Robert, C., et al., *Ipilimumab plus dacarbazine for previously untreated metastatic melanoma*. N Engl J Med, 2011. **364**(26): p. 2517-26.
76. Hodi, F.S., et al., *Improved survival with ipilimumab in patients with metastatic melanoma*. N Engl J Med, 2010. **363**(8): p. 711-23.
77. *U.S Food and Drug Administration. FDA approves Yervoy to reduce the risk of melanoma returning after surgery*. 7th July 2019]; Available from: <https://www.fda.gov/NewsEvents/Newsroom/PressAnnouncements/ucm469944.htm>.
78. *Keytruda (pembrolizumab) FDA Approval History - Drugs.com*. 7th July 2019]; Available from: <https://www.drugs.com/history/keytruda.html>.
79. *Opdivo (nivolumab) FDA Approval History - Drugs.com*. 7th July 2019]; Available from: <https://www.drugs.com/history/opdivo.html>.

80. U.S Food and Drug Administration. *FDA approves first cancer treatment for any solid tumor with a specific genetic feature*. 2017 7th July 2019]; Available from: <https://www.fda.gov/newsevents/newsroom/pressannouncements/ucm560167.htm>.
81. Rosenberg, S.A., et al., *Use of tumor-infiltrating lymphocytes and interleukin-2 in the immunotherapy of patients with metastatic melanoma. A preliminary report*. N Engl J Med, 1988. **319**(25): p. 1676-80.
82. *List results of engineered TCRs - ClinicalTrials.gov*. 7th July 2019]; Available from: <https://clinicaltrials.gov/ct2/results?cond=&term=engineered+TCRs&cntry1=&state1=%20&recrs=>
83. *Adaptimmune. Press Release : Investors : Adaptimmune*. 7th July 2019]; Available from: [http://ir.adaptimmune.com/phoenix.zhtml?c=253991&p=irol-](http://ir.adaptimmune.com/phoenix.zhtml?c=253991&p=irol-newsArticle&ID=2175118) newsArticle&ID=2175118.
84. Johnson, L.A., et al., *Gene therapy with human and mouse T-cell receptors mediates cancer regression and targets normal tissues expressing cognate antigen*. Blood, 2009. **114**(3): p. 535-46.
85. Morgan, R.A., et al., *Cancer regression and neurological toxicity following anti-MAGE-A3 TCR gene therapy*. J Immunother, 2013. **36**(2): p. 133-51.
86. Kalos, M., et al., *Chimeric Antigen Receptor Modified T Cells Directed Against CD19 (CTL019 cells) Have Long-Term Persistence and Induce Durable Responses In Relapsed, Refractory CLL*. Blood, 2013. **122**(21): p. 4162.
87. Srivastava, S. and S.R. Riddell, *Engineering CAR-T cells: Design concepts*. Trends in Immunology, 2015. **36**(8): p. 494-502.
88. Kalos, M., et al., *T Cells with Chimeric Antigen Receptors Have Potent Antitumor Effects and Can Establish Memory in Patients with Advanced Leukemia*. Science Translational Medicine, 2011. **3**(95): p. 95ra73.
89. Kochenderfer, J.N., et al., *B-cell depletion and remissions of malignancy along with cytokine-associated toxicity in a clinical trial of anti-CD19 chimeric-antigen-receptor-transduced T cells*. Blood, 2012. **119**.
90. Porter, D.L., et al., *Randomized, Phase II Dose Optimization Study of Chimeric Antigen Receptor Modified T Cells Directed Against CD19 (CTL019) in Patients with Relapsed, Refractory CLL*. Blood, 2014. **124**(21): p. 1982.
91. Dudley, M.E., et al., *Effective Treatment Of Chemotherapy-Refractory Diffuse Large B-Cell Lymphoma With Autologous T Cells Genetically-Engineered To Express An Anti-CD19 Chimeric Antigen Receptor*. Blood, 2013. **122**(21): p. 168.
92. Maude, S.L., et al., *Chimeric Antigen Receptor T Cells for Sustained Remissions in Leukemia*. New England Journal of Medicine, 2014. **371**(16): p. 1507-1517.
93. Gross, G., T. Waks, and Z. Eshhar, *Expression of immunoglobulin-T-cell receptor chimeric molecules as functional receptors with antibody-type specificity*. Proceedings of the National Academy of Sciences of the United States of America, 1989. **86**(24): p. 10024-10028.
94. Rosenberg, S.A., et al., *Treatment of Patients With Metastatic Melanoma With Autologous Tumor-Infiltrating Lymphocytes and Interleukin 2*. Journal of the National Cancer Institute, 1994. **86**(15): p. 1159-1166.
95. Yazdanifar, M., R. Zhou, and P. Mukherjee, *Emerging immunotherapeutics in adenocarcinomas: A focus on CAR-T cells*. Current Trends in Immunology, 2016. **17**: p. 95 - 115.
96. Eshhar, Z. and G. Gross, *Chimeric T cell receptor which incorporates the anti-tumour specificity of a monoclonal antibody with the cytolytic activity of T cells: a model system for immunotherapeutical approach*. The British journal of cancer. Supplement, 1990. **10**: p. 27-29.
97. Guest, R.D., et al., *The role of extracellular spacer regions in the optimal design of chimeric immune receptors: evaluation of four different scFvs and antigens*. J Immunother, 2005. **28**(3): p. 203-11.
98. Gong, M.C., et al., *Cancer patient T cells genetically targeted to prostate-specific membrane antigen specifically lyse prostate cancer cells and release cytokines in response to prostate-specific membrane antigen*. Neoplasia, 1999. **1**(2): p. 123-7.
99. Maher, J., et al., *Human T-lymphocyte cytotoxicity and proliferation directed by a single chimeric TCRzeta/CD28 receptor*. Nat Biotechnol, 2002. **20**(1): p. 70-5.

100. Zhao, Y., et al., *A herceptin-based chimeric antigen receptor with modified signaling domains leads to enhanced survival of transduced T lymphocytes and antitumor activity*. J Immunol, 2009. **183**(9): p. 5563-74.
101. U.S Food & Drug Administration. *Approved Drugs - FDA approves tisagenlecleucel for B-cell ALL and tocilizumab for cytokine release syndrome*. 2017 09/07/2017]; Available from: <https://www.fda.gov/drugs/resources-information-approved-drugs/fda-approves-tisagenlecleucel-b-cell-all-and-tocilizumab-cytokine-release-syndrome>.
102. Chmielewski, M. and H. Abken, *TRUCKs: the fourth generation of CARs*. Expert Opinion on Biological Therapy, 2015. **15**(8): p. 1145-1154.
103. Di Stasi, A., et al., *Inducible Apoptosis as a Safety Switch for Adoptive Cell Therapy*. New England Journal of Medicine, 2011. **365**(18): p. 1673-1683.
104. Chmielewski, M., et al., *IL-12 Release by Engineered T Cells Expressing Chimeric Antigen Receptors Can Effectively Muster an Antigen-Independent Macrophage Response on Tumor Cells That Have Shut Down Tumor Antigen Expression*. Cancer Research, 2011. **71**(17): p. 5697.
105. Carroll, R.G., et al., *Distinct Effects of IL-18 on the Engraftment and Function of Human Effector CD8+ T Cells and Regulatory T Cells*. PLOS ONE, 2008. **3**(9): p. e3289.
106. Hu, B., et al., *Augmentation of Antitumor Immunity by Human and Mouse CAR T Cells Secreting IL-18*. Cell Rep, 2017. **20**(13): p. 3025-3033.
107. Chmielewski, M. and H. Abken, *CAR T Cells Releasing IL-18 Convert to T-Bet(high) FoxO1(low) Effectors that Exhibit Augmented Activity against Advanced Solid Tumors*. Cell Rep, 2017. **21**(11): p. 3205-3219.
108. Jackson, H.J., S. Rafiq, and R.J. Brentjens, *Driving CAR T-cells forward*. Nature Reviews Clinical Oncology, 2016. **13**: p. 370.
109. Wang, X. and I. Rivière, *Clinical manufacturing of CAR T cells: foundation of a promising therapy*. Molecular Therapy — Oncolytics, 2016. **3**: p. 16015.
110. U.S Food & Drug Administration. *KYMRIAH Prescribing information*.
111. Beatty, G.L., et al., *Mesothelin-specific chimeric antigen receptor mRNA-engineered T cells induce anti-tumor activity in solid malignancies*. Cancer Immunol Res, 2014. **2**(2): p. 112-20.
112. Di Stasi, A., et al., *T lymphocytes coexpressing CCR4 and a chimeric antigen receptor targeting CD30 have improved homing and antitumor activity in a Hodgkin tumor model*. Blood, 2009. **113**(25): p. 6392-402.
113. Newick, K., E. Moon, and S.M. Albelda, *Chimeric antigen receptor T-cell therapy for solid tumors*. Molecular Therapy — Oncolytics, 2016. **3**: p. 16006.
114. Frigault, M.J. and M.V. Maus, *Chimeric antigen receptor-modified T cells strike back*. Int Immunol, 2016. **28**(7): p. 355-63.
115. Ikeda, H., et al., *Characterization of an antigen that is recognized on a melanoma showing partial HLA loss by CTL expressing an NK inhibitory receptor*. Immunity, 1997. **6**(2): p. 199-208.
116. Silvestri, I., et al., *A Perspective of Immunotherapy for Prostate Cancer*. Cancers (Basel), 2016. **8**(7): p. E64
117. Bonifant, C.L., et al., *Toxicity and management in CAR T-cell therapy*. Molecular Therapy — Oncolytics, 2016. **3**: p. 16011.
118. Ramos, C.A., B. Savoldo, and G. Dotti, *CD19-CAR trials*. Cancer J, 2014. **20**(2): p. 112-8.
119. Lee, D.W., et al., *Current concepts in the diagnosis and management of cytokine release syndrome*. Blood, 2014. **124**(2): p. 188-95.
120. Barrett, D.M., S.A. Grupp, and C.H. June, *Chimeric Antigen Receptor- and TCR-Modified T Cells Enter Main Street and Wall Street*. J Immunol, 2015. **195**(3): p. 755-61.
121. Sadelain, M., *CAR therapy: the CD19 paradigm*. J. Clin. Invest. , 2015. **125**(9): p. 3392-3400.
122. Morgan, R.A., et al., *Case Report of a Serious Adverse Event Following the Administration of T Cells Transduced With a Chimeric Antigen Receptor Recognizing ERBB2*. Molecular Therapy, 2010. **18**(4): p. 843-851.
123. Ahmed, N., et al., *Human Epidermal Growth Factor Receptor 2 (HER2) -Specific Chimeric Antigen Receptor-Modified T Cells for the Immunotherapy of HER2-Positive Sarcoma*. J Clin Oncol, 2015. **33**(15): p. 1688-96.

124. Davila, M.L., et al., *Efficacy and toxicity management of 19-28z CAR T cell therapy in B cell acute lymphoblastic leukemia*. *Sci Transl Med*, 2014. **6**(224): p. 224ra25.
125. Lee, D.W., et al., *T cells expressing CD19 chimeric antigen receptors for acute lymphoblastic leukaemia in children and young adults: a phase 1 dose-escalation trial*. *Lancet*, 2015. **385**(9967): p. 517-28.
126. Poirot, L., et al., *Multiplex Genome-Edited T-cell Manufacturing Platform for "Off-the-Shelf" Adoptive T-cell Immunotherapies*. *Cancer Res*, 2015. **75**(18): p. 3853-64.
127. Almásbak, H., T. Aarvak, and M.C. Vemuri, *CAR T Cell Therapy: A Game Changer in Cancer Treatment*. *Journal of Immunology Research*, 2016. **2016**: p. 5474602.
128. Ma, J.S., et al., *Versatile strategy for controlling the specificity and activity of engineered T cells*. *Proc Natl Acad Sci U S A*, 2016. **113**(4): p. E450-8.
129. Lanitis, E., et al., *Chimeric antigen receptor T Cells with dissociated signaling domains exhibit focused antitumor activity with reduced potential for toxicity in vivo*. *Cancer Immunol Res*, 2013. **1**(1): p. 43-53.
130. Wilkie, S., et al., *Dual targeting of ErbB2 and MUC1 in breast cancer using chimeric antigen receptors engineered to provide complementary signaling*. *J Clin Immunol*, 2012. **32**(5): p. 1059-70.
131. Kloss, C.C., et al., *Combinatorial antigen recognition with balanced signaling promotes selective tumor eradication by engineered T cells*. *Nat Biotech*, 2013. **31**(1): p. 71-75.
132. Jones, B.S., et al., *Improving the safety of cell therapy products by suicide gene transfer*. *Frontiers in Pharmacology*, 2014. **5**: p. 254.
133. Wang, X., et al., *A transgene-encoded cell surface polypeptide for selection, in vivo tracking, and ablation of engineered cells*. *Blood*, 2011. **118**(5): p. 1255-63.
134. Fedorov, V.D., M. Themeli, and M. Sadelain, *PD-1- and CTLA-4-based inhibitory chimeric antigen receptors (iCARs) divert off-target immunotherapy responses*. *Sci Transl Med*, 2013. **5**(215): p. 215ra172.
135. Gross, G. and Z. Eshhar, *Therapeutic Potential of T Cell Chimeric Antigen Receptors (CARs) in Cancer Treatment: Counteracting Off-Tumor Toxicities for Safe CAR T Cell Therapy*. *Annu Rev Pharmacol Toxicol*, 2016. **56**: p. 59-83.
136. Rodgers, D.T., et al., *Switch-mediated activation and retargeting of CAR-T cells for B-cell malignancies*. *Proc Natl Acad Sci U S A*, 2016. **113**(4): p. E459-68.
137. Juillerat, A., et al., *Design of chimeric antigen receptors with integrated controllable transient functions*. *Scientific Reports*, 2016. **6**: p. 18950.
138. Klebanoff, C.A., S.A. Rosenberg, and N.P. Restifo, *Prospects for gene-engineered T cell immunotherapy for solid cancers*. *Nat Med*, 2016. **22**(1): p. 26-36.
139. Barrett, D.M., et al., *Treatment of Advanced Leukemia in Mice with mRNA Engineered T Cells*. *Human Gene Therapy*, 2011. **22**(12): p. 1575-1586.
140. Brudno, J.N. and J.N. Kochenderfer, *Toxicities of chimeric antigen receptor T cells: recognition and management*. *Blood*, 2016. **127**(26): p. 3321-3330.
141. Roulois, D., M. Gregoire, and J.F. Fonteneau, *MUC1-specific cytotoxic T lymphocytes in cancer therapy: induction and challenge*. *Biomed Res Int*, 2013. **2013**: p. 871936.
142. Kondo, H., et al., *Adoptive immunotherapy for pancreatic cancer using MUC1 peptide-pulsed dendritic cells and activated T lymphocytes*. *Anticancer Res*, 2008. **28**(1b): p. 379-87.
143. Maher, J. and S. Wilkie, *CAR Mechanics: Driving T Cells into the MUC of Cancer*. *Cancer Research*, 2009. **69**(11): p. 4559.
144. Whilding, L.M., et al., *Targeting of Aberrant alphavbeta6 Integrin Expression in Solid Tumors Using Chimeric Antigen Receptor-Engineered T Cells*. *Mol Ther*, 2017. **25**(1): p. 259-273.
145. Posey, A.D., Jr., H. Clausen, and C.H. June, *Distinguishing Truncated and Normal MUC1 Glycoform Targeting from Tn-MUC1-Specific CAR T Cells: Specificity Is the Key to Safety*. *Immunity*, 2016. **45**(5): p. 947-948.
146. Posey, A.D., Jr., et al., *Engineered CAR T Cells Targeting the Cancer-Associated Tn-Glycoform of the Membrane Mucin MUC1 Control Adenocarcinoma*. *Immunity*, 2016. **44**(6): p. 1444-54.
147. You, F., et al., *Phase 1 clinical trial demonstrated that MUC1 positive metastatic seminal vesicle cancer can be effectively eradicated by modified Anti-MUC1 chimeric antigen receptor transduced T cells*. *Sci China Life Sci*, 2016. **59**(4): p. 386-97.

148. Zhou, R., et al., *CAR T Cells Targeting the Tumor MUC1 Glycoprotein Reduce Triple-Negative Breast Cancer Growth*. Front. Immunol., 2019.
149. PersonGen BioTherapeutics (Suzhou) Co., L. *CAR-T Cell Immunotherapy in MUC1 Positive Solid Tumor - Full Text View - ClinicalTrials.gov*. 7th July 2019]; Available from: <https://clinicaltrials.gov/ct2/show/NCT02617134?term=muc1+chimeric+antigen+receptors&rank=2>.
150. Taylor-Papadimitriou, J., et al., *MUC1 and cancer*. Biochim Biophys Acta, 1999. **1455**(2-3): p. 301-13.
151. Anurathapan, U., et al., *Kinetics of Tumor Destruction by Chimeric Antigen Receptor-modified T Cells*. Mol Ther, 2014. **22**(3): p. 623-633.
152. Yazdanifar, M., et al., *Overcoming Immunological Resistance Enhances the Efficacy of a Novel anti-tMUC1 CAR T Cell Treatment Against Pancreatic Ductal Adenocarcinoma*. bioRxiv, 2019: p. 642934.
153. Morello, A., M. Sadelain, and P.S. Adusumilli, *Mesothelin-Targeted CARs: Driving T cells to Solid Tumors*. Cancer discovery, 2016. **6**(2): p. 133-146.
154. Hudecek, M., et al., *Receptor affinity and extracellular domain modifications affect tumor recognition by ROR1-specific chimeric antigen receptor T cells*. Clin Cancer Res, 2013. **19**(12): p. 3153-64.
155. Berger, C., et al., *Safety of targeting ROR1 in primates with chimeric antigen receptor-modified T cells*. Cancer Immunol Res, 2015. **3**(2): p. 206-16.
156. Ribas, A., *Adaptive Immune Resistance: How Cancer Protects from Immune Attack*. Cancer Discovery, 2015. **5**(9): p. 915.
157. Callahan, M.K., M.A. Postow, and J.D. Wolchok, *CTLA-4 and PD-1 Pathway Blockade: Combinations in the Clinic*. Front Oncol, 2014. **4**: p. 385.
158. Cherkassky, L., et al., *Human CAR T cells with cell-intrinsic PD-1 checkpoint blockade resist tumor-mediated inhibition*. J Clin Invest, 2016. **126**(8): p. 3130-44.
159. John, L.B., et al., *Anti-PD-1 antibody therapy potently enhances the eradication of established tumors by gene-modified T cells*. Clin Cancer Res, 2013. **19**(20): p. 5636-46.
160. van der Most, R.G., B.W. Robinson, and R.A. Lake, *Combining immunotherapy with chemotherapy to treat cancer*. Discov Med, 2005. **5**(27): p. 265-70.
161. Ding, Z.-C. and G. Zhou, *Cytotoxic Chemotherapy and CD4+ Effector T Cells: An Emerging Alliance for Durable Antitumor Effects*. Clinical and Developmental Immunology, 2012. **2012**: p. 12.
162. Vanneman, M. and G. Dranoff, *Combining immunotherapy and targeted therapies in cancer treatment*. Nat Rev Cancer, 2012. **12**(4): p. 237-51.
163. Nefedova, Y., et al., *Activation of dendritic cells via inhibition of Jak2/STAT3 signaling*. Journal of immunology (Baltimore, Md. : 1950), 2005. **175**(7): p. 4338-4346.
164. Nefedova, Y., et al., *Regulation of dendritic cell differentiation and antitumor immune response in cancer by pharmacologic-selective inhibition of the janus-activated kinase 2/signal transducers and activators of transcription 3 pathway*. Cancer Res, 2005. **65**(20): p. 9525-35.
165. Kirkwood, J.M., et al., *Immunotherapy of cancer in 2012*. CA Cancer J Clin, 2012. **62**(5): p. 309-35.
166. Cancer.Gov, *Stat Facts : Pancreatic Cancer*: <https://seer.cancer.gov/statfacts/html/pancreas.html>. 2016.
167. Jackson, H.J., S. Rafiq, and R.J. Brentjens, *Driving CAR T-cells forward*. Nat Rev Clin Oncol, 2016. **13**(6): p. 370-83.
168. Mukherjee, P., *Tumor specific antibodies and uses therefor*. Google Patents, 2013. **US 8518405 B2, August 27th 2013**
169. Curry, J.M., et al., *The use of a novel MUC1 antibody to identify cancer stem cells and circulating MUC1 in mice and patients with pancreatic cancer*. J Surg Oncol, 2013.
170. Zhou, R., et al., *A novel association of neuropilin-1 and MUC1 in pancreatic ductal adenocarcinoma: role in induction of VEGF signaling and angiogenesis*. Oncogene, 2016. **35**(43): p. 5608-5618.
171. Hollingsworth, M.A., et al., *Expression of MUC1, MUC2, MUC3 and MUC4 mucin mRNAs in human pancreatic and intestinal tumor cell lines*. Int J Cancer, 1994. **57**(2): p. 198-203.

172. Delitto, D., S.M. Wallet, and S.J. Hughes, *Targeting tumor tolerance: A new hope for pancreatic cancer therapy?* Pharmacol Ther, 2016. **166**: p. 9-29.
173. Waterhouse, N.J., et al., *Cytotoxic T lymphocyte-induced killing in the absence of granzymes A and B is unique and distinct from both apoptosis and perforin-dependent lysis.* J Cell Biol, 2006. **173**(1): p. 133-44.
174. Wilkie, S., et al., *Retargeting of human T cells to tumor-associated MUC1: the evolution of a chimeric antigen receptor.* J Immunol, 2008. **180**(7): p. 4901-9.
175. Roy, L.D., et al., *A tumor specific antibody to aid breast cancer screening in women with dense breast tissue.* Genes Cancer, 2017. **8**(3-4): p. 536-549.
176. Close, D.M., et al., *In vivo bioluminescent imaging (BLI): noninvasive visualization and interrogation of biological processes in living animals.* Sensors (Basel), 2011. **11**(1): p. 180-206.
177. Kim, J.-B., et al., *Non-invasive detection of a small number of bioluminescent cancer cells in vivo.* PloS one, 2010. **5**(2): p. e9364-e9364.
178. Zah, E., et al., *T Cells Expressing CD19/CD20 Bispecific Chimeric Antigen Receptors Prevent Antigen Escape by Malignant B Cells.* Cancer Immunology Research, 2016. **4**(6): p. 498.
179. Ajina, A. and J. Maher, *Strategies to Address Chimeric Antigen Receptor Tonic Signaling.* Mol Cancer Ther, 2018. **17**(9): p. 1795-1815.
180. Garbi, N., et al., *Tonic T cell signalling and T cell tolerance as opposite effects of self-recognition on dendritic cells.* Curr Opin Immunol, 2010. **22**(5): p. 601-8.
181. Klenerman, P. and A. Oxenius, *T cell responses to cytomegalovirus.* Nat Rev Immunol, 2016. **16**(6): p. 367-77.
182. Long, A.H., et al., *4-1BB costimulation ameliorates T cell exhaustion induced by tonic signaling of chimeric antigen receptors.* Nat Med, 2015. **21**(6): p. 581-590.
183. Frigault, M.J., et al., *Identification of chimeric antigen receptors that mediate constitutive or inducible proliferation of T cells.* Cancer Immunol Res, 2015. **3**(4): p. 356-67.
184. Moon, E.K., et al., *Multifactorial T-cell hypofunction that is reversible can limit the efficacy of chimeric antigen receptor-transduced human T cells in solid tumors.* Clin Cancer Res, 2014. **20**(16): p. 4262-73.
185. Eyquem, J., et al., *Targeting a CAR to the TRAC locus with CRISPR/Cas9 enhances tumour rejection.* Nature, 2017. **543**(7643): p. 113-117.
186. Shum, T., et al., *Constitutive Signaling from an Engineered IL7 Receptor Promotes Durable Tumor Elimination by Tumor-Redirected T Cells.* Cancer Discov, 2017. **7**(11): p. 1238-1247.
187. Chan, A.K., et al., *Soluble MUC1 secreted by human epithelial cancer cells mediates immune suppression by blocking T-cell activation.* Int J Cancer, 1999. **82**(5): p. 721-6.
188. Zelenay, S., et al., *Cyclooxygenase-Dependent Tumor Growth through Evasion of Immunity.* Cell, 2015. **162**(6): p. 1257-70.
189. Mukherjee, P., et al., *Progression of Pancreatic Adenocarcinoma Is Significantly Impeded with a Combination of Vaccine and COX-2 Inhibition.* Journal of immunology (Baltimore, Md. : 1950), 2009. **182**(1): p. 216-224.
190. Fujihara, S., et al., *Galectin-9 in cancer therapy.* Recent Pat Endocr Metab Immune Drug Discov, 2013. **7**(2): p. 130-7.
191. Koyama, S., et al., *Adaptive resistance to therapeutic PD-1 blockade is associated with upregulation of alternative immune checkpoints.* Nature communications, 2016. **7**: p. 10501-10501.
192. van Baren, N. and B.J. Van den Eynde, *Tryptophan-degrading enzymes in tumoral immune resistance.* Front Immunol, 2015. **6**: p. 34.
193. Pilotte, L., et al., *Reversal of tumoral immune resistance by inhibition of tryptophan 2,3-dioxygenase.* Proc Natl Acad Sci U S A, 2012. **109**(7): p. 2497-502.
194. Frumento, G., et al., *Tryptophan-derived catabolites are responsible for inhibition of T and natural killer cell proliferation induced by indoleamine 2,3-dioxygenase.* The Journal of experimental medicine, 2002. **196**(4): p. 459-468.
195. Hwu, P., et al., *Indoleamine 2,3-dioxygenase production by human dendritic cells results in the inhibition of T cell proliferation.* J Immunol, 2000. **164**(7): p. 3596-9.

196. Terness, P., et al., *Inhibition of allogeneic T cell proliferation by indoleamine 2,3-dioxygenase-expressing dendritic cells: mediation of suppression by tryptophan metabolites*. J Exp Med, 2002. **196**(4): p. 447-57.
197. Munn, D.H., et al., *Inhibition of T cell proliferation by macrophage tryptophan catabolism*. J Exp Med, 1999. **189**(9): p. 1363-72.
198. Ninomiya, S., et al., *Tumor indoleamine 2,3-dioxygenase (IDO) inhibits CD19-CAR T cells and is downregulated by lymphodepleting drugs*. Blood, 2015. **125**(25): p. 3905-3916.
199. Thaker, A.I., et al., *IDO1 metabolites activate beta-catenin signaling to promote cancer cell proliferation and colon tumorigenesis in mice*. Gastroenterology, 2013. **145**(2): p. 416-25.e1-4.
200. Nagahara, K., et al., *Galectin-9 Increases Tim-3+ Dendritic Cells and CD8+ T Cells and Enhances Antitumor Immunity via Galectin-9-Tim-3 Interactions*. The Journal of Immunology, 2008. **181**(11): p. 7660.
201. Golden-Mason, L., et al., *Galectin-9 Functionally Impairs Natural Killer Cells in Humans and Mice*. Journal of Virology, 2013. **87**(9): p. 4835.
202. Goncalves Silva, I., et al., *The Tim-3-galectin-9 Secretory Pathway is Involved in the Immune Escape of Human Acute Myeloid Leukemia Cells*. EBioMedicine, 2017. **22**: p. 44-57.
203. He, Y., et al., *TIM-3, a promising target for cancer immunotherapy*. OncoTargets and therapy, 2018. **11**: p. 7005-7009.
204. Zhu, C., et al., *The Tim-3 ligand galectin-9 negatively regulates T helper type 1 immunity*. Nat Immunol, 2005. **6**(12): p. 1245-52.
205. Kang, C.-W., et al., *Apoptosis of tumor infiltrating effector TIM-3+CD8+ T cells in colon cancer*. Scientific reports, 2015. **5**: p. 15659-15659.
206. Gleason, M.K., et al., *Tim-3 is an inducible human natural killer cell receptor that enhances interferon gamma production in response to galectin-9*. Blood, 2012. **119**(13): p. 3064-3072.
207. Galore-Haskel, G., et al., *A novel immune resistance mechanism of melanoma cells controlled by the ADAR1 enzyme*. Oncotarget, 2015. **6**(30): p. 28999-9015.
208. Ishizuka, J.J., et al., *Loss of ADAR1 in tumours overcomes resistance to immune checkpoint blockade*. Nature, 2019. **565**(7737): p. 43-48.
209. Pang, L.Y., E.A. Hurst, and D.J. Argyle, *Cyclooxygenase-2: A Role in Cancer Stem Cell Survival and Repopulation of Cancer Cells during Therapy*. Stem cells international, 2016. **2016**: p. 2048731-2048731.
210. Kalinski, P., *Regulation of Immune Responses by Prostaglandin E₂*. The Journal of Immunology, 2012. **188**(1): p. 21.
211. Sobolewski, C., et al., *The Role of Cyclooxygenase-2 in Cell Proliferation and Cell Death in Human Malignancies*. International Journal of Cell Biology, 2010. **2010**.
212. Koike, N., S. Pilon-Thomas, and J.J. Mule, *Nonmyeloablative chemotherapy followed by T-cell adoptive transfer and dendritic cell-based vaccination results in rejection of established melanoma*. J Immunother, 2008. **31**(4): p. 402-12.
213. Dudley, M.E., et al., *Adoptive cell transfer therapy following non-myeloablative but lymphodepleting chemotherapy for the treatment of patients with refractory metastatic melanoma*. J Clin Oncol, 2005. **23**(10): p. 2346-57.
214. Wang, L., et al., *Chimeric antigen receptor T cell therapy and other therapeutics for malignancies: Combination and opportunity*. Int Immunopharmacol, 2019. **70**: p. 498-503.
215. Epenetos, A.A., et al., *Targeting of iodine-123-labelled tumour-associated monoclonal antibodies to ovarian, breast, and gastrointestinal tumours*. Lancet, 1982. **2**(8306): p. 999-1005.